Mineral matter in density separated coal fractions and their transformation during laboratory combustion studies

R Rautenbach

orcid.org 0000-0001-9525-7906

Thesis accepted in fulfilment of the requirements for the degree *Doctor of Philosophy in Chemistry* at the North-West University

Promoter:	Prof CA Strydom
Co-promoter:	Prof JR Bunt
Assistant Promoter:	Dr RH Matjie

Graduation July 2020

21667373

PREFACE

Format of the thesis

According to the academic rules of the North-West University, a thesis may be submitted in the format of published research articles. The format of this thesis is following these specifications and the three research articles are presented as one unit that includes a Literature Chapter as well as a Conclusions Chapter where the main conclusions drawn throughout the study are summarised.

The number and reference styles

The format of the published or submitted articles adhere to the guidelines provided by the relevant journal, however, the general outline of these manuscripts was adapted to achieve uniformity in the thesis. Minor typographical changes were made and the graphs were enlarged, however, the original content was not changed.

DECLARATION

I, Rudelle Rautenbach, hereby declare that this thesis entitled: ***"Mineral matter in density separated coal fractions and their transformation during laboratory combustion studies"***, submitted in fulfilment of the requirements for the degree *Doctor of Philosophy in Chemistry at the North-West University* is my own work and has not previously been submitted to any other institution in whole or in part. Written consent from authors had been obtained for publications where co-authors have been involved.

07/05/2020

Rudelle Rautenbach **Date**

STATEMENT FROM CO-AUTHORS

To whom it may concern,

The listed co-authors hereby give consent that Rudelle Rautenbach may submit the following manuscripts as part of her thesis entitled: **"Mineral matter in density separated coal fractions and their transformation during laboratory combustion studies",** submitted for the degree *Doctor of Philosophy in Chemistry*, at the North-West University.

Signed on the 7th of May 2020.

R. Rautenbach

C. A. Strydom

J. R. Bunt

R. H. Matjie

Q. P. Campbell

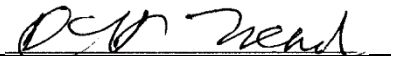

D. French

ACKNOWLEDGEMENTS

"A TREE GIVES GLORY TO GOD BY BEING A TREE". – THOMAS MERTON

I would like to extend my gratitude towards the following people for their assistance, guidance, prayers, and motivation throughout this journey.

- All the glory to our Heavenly Father, because I can do all things through Christ who strengthens me (Philippians 4:13).
- A special word of thanks to my promotors, Prof Christien Strydom and Prof John Bunt, for their wisdom, guidance and patience during this study.
- Dr Henry Matjie, for his time and efforts. Thank you for always assisting when needed and for walking this journey with me.
- The late Prof Colin R Ward, for his valuable insights and assistance.
- Dr David French, for his guidance.
- Chris van Alphen, Shinelka Singh, for their assistance with QEMSCAN analysis.
- Xolisa Goso (Mintek) for his help with the ashing of the coal samples, Vincent Dube (SABS) for the assistance with the float-sink density separation.
- Belinda Venter (NWU) and Ben Ashton (Sasol) for their assistance in the XRD, XRF, and HT-XRD experiments.
- Prof Nikki Wagner and Dr Christian Reinke for the EMP and Petrography results.
- Sasol and the NRF for funding.
- My colleagues from the Coal research group at the NWU for their motivations and suggestion throughout the study.
- My loving family for their continuous motivation and support.
- Kalla, my husband, for his patience, inspiration, guidance and encouragement from the beginning – thank you for always believing in me!

ABSTRACT

Mineral matter in coal is the primary cause of ash-related problems (fouling and slagging) during the combustion of coal. It is crucial to incorporate the behaviour of mineral matter under combustion conditions into ash-deposition prediction methods. The novelty of this approach is that the current ash-deposition prediction methods disregard the heterogeneous nature of ash properties, which are the results of the complexity of mineral matter transformations at elevated temperatures.

The first objective of this study was to comprehensively characterise and describe the included and excluded mineral matter transformational behaviour at elevated temperatures in order to comprehend the processes and operational problems which could occur during coal utilisation.

The combination of density separation through the float-sink method followed by reflux classification eliminated the liberated minerals successfully and produced maceral-rich float fractions (98% maceral content). Three South African feed coal samples for the combustion process were beneficiated to produce carbon-rich and mineral-rich fractions. The main differences between the feed coals were related to the mode of occurrence of mineral matter

The mineralogical, petrographical, and chemical properties of these feed coals and their density separated fractions were investigated using XRD, XRF, QEMSCAN, electron microprobe, and petrography analyses. By integrating these different analytical techniques, more comprehensive determination of the concentrations of mineral matter responsible for industrial ash related problems were possible.

Low-temperature ash (LTA) samples of feed coals and the density separated fractions were subjected to high-temperature X-ray diffraction (HT-XRD) to identify the mineral reactions occurred at elevated temperatures under oxidising conditions. Included minerals were predominantly present in the float fractions (<1.5 g/cm^3), while the excluded mineral particles were mainly concentrated in the sink fraction (>1.9 g/cm^3). QEMSCAN results indicate that the mineral associations in carbominerites and included minerals in Feeds A, B and C and sinks B and C are responsible for the melt formation during HT-XRD experiments. HT-XRD results indicate the presence of mullite, anorthite, and amorphous aluminosilicate materials formed in the thermally treated LTA samples. The formation of these slagging crystalline and glassy phases could be attributed to either crystallisation during the cooling of the molten solution, or via solid-state reactions at elevated temperatures.

Another objective was to relate the coalescence of included minerals and the fragmentation of excluded minerals, during combustion, to the slagging propensities of South African coal samples. The feed, float and sink fractions were subjected to laboratory combustion experiments in order to determine the temperatures where various mineral interactions occur. The mode of occurrence of mineral matter played a crucial role in the formation of high-temperature mineral phases under combustion conditions. Formations of high-temperature minerals, such as mullite and cristobalite, were mainly due to the transformation reactions of kaolinite and quartz at elevated temperatures, respectively. However, the formation of anorthite at elevated temperatures can be attributed to the interaction of fluxing minerals (calcite, dolomite, pyrite and siderite) that are associated with kaolinite in the coal sample. The presence of anorthite, mullite and alumina-silicate glasses at elevated temperatures can, therefore, be used as an indication of the slagging propensity of South African coal.

It was proposed that blends of the different density fractions will reduce or minimise clinker and slag formation as well as the abrasive nature of the clinkers or slags. Possible blends to minimise clinker and slag formation include the float and sink fractions of the feed coals in varying proportions based on the specific mineralogical, petrographical and chemical data. A comprehensive knowledge of the included and excluded minerals can be used to prepare a blended feedstock for combustion processes. The operational ash-related problems in the combustion and gasification processes could be minimised by implementing this comprehensive knowledge of the transformation of coal minerals at elevated temperatures.

Keywords: Mineral matter, included and excluded minerals, reflux classification, low-temperature plasma ashing, QEMSCAN, HT-XRD

TABLE OF CONTENTS

CHAPTER 6
CONCLUDING SUMMARY

LIST OF TABLES

LIST OF FIGURES

CHAPTER 1

INTRODUCTION

1.1. Introduction and motivation

Coal is the dominant primary fuel source in South Africa by providing approximately 77% of the country's energy needs and 36% of the global energy needs. Coal-fired power stations generate more than 90% of South Africa's electricity (Ratshomo & Nembahe, 2018; Wagner *et al.*, 2018). Coal deposits in South Africa are abundant, shallow and relatively easy to mine, thus making it an affordable fuel resource. Alternative renewable energy sources will not entirely replace coal due to this abundance of coal in South Africa (Buhre *et al.*, 2006). South Africa consists of 3.5% of coal reserves globally, while the annual coal production represents 3.3% of coal production worldwide (Minerals Council South Africa, 2019). Coal is South Africa's top mining commodity revenue producer and will thus be of great significance in the future, for at least five more decades.

South African coal reserves are spread over 19 coalfields in 5 different provinces and can be classified as inertinite-rich coal with high ash yield. The coal qualities vary significantly between these coalfields as well as from the one seam to the other (Falcon & Snyman, 1986; Jeffrey, 2005; Snyman & Botha, 1993; Wagner *et al.*, 2018). An overall decline in coal quality is the result of the exploitation of the higher quality coal seams. Lower-grade coals tend to be high ash yielding coals due to the increase in the mineral matter while it may also exhibit caking behaviour during thermal treatment (Jeffrey, 2005). Coal research must, therefore, focus on maximising coal utilisation by improving process efficiencies when incorporating lower grade coal (Ratshomo & Nembahe, 2018).

Comprehensive knowledge regarding the mineral matter associations as well as the mode of occurrence of these minerals in the coal sample is fundamental when investigating and modelling the ash deposition problems related to coal utilisation (Liu *et al.*, 2005; Matjie *et al.*, 2011; Matjie *et al.*, 2016).

It is hypothesised that during the combustion of coal, various changes in the mineral matter may be observed at different temperatures. Included minerals within the macerals may interact to form minerals in the molten solution through crystallisation. Excluded minerals may interact to form high-temperature products during solid-solid state reactions as well as crystallisation. Organically associated inorganic elements within the macerals may interact with each other to form artefact minerals, gases and fine ash particles at low temperatures through volatilisation and evaporation.

Submicron minerals infilling cleat fractures in the vitrinite may transform at elevated temperatures to fly ash particles that will volatilise during the combustion of coal.

A comprehensive study is therefore proposed to gain widespread knowledge relating to the mineralogical, petrographical and chemical properties of carbon-rich and mineral-rich fractions as well as the transformations and interactions of mineral matter present in these fractions at elevated temperatures. Some of the ash-related environmental and operational problems, such as slagging, fouling, abrasion, deposition, and agglomeration that occur may be minimised or even avoided using these results from the advanced analytical techniques described in this study.

1.2 Aim and objectives of this study

The aim of this study is to qualify and quantify the various mineral matter associations and mineral liberations responsible for the industrial problems related to coal combustion. The following objectives are stipulated:

- Qualify and quantify the mineral-mineral associations (referring to the included minerals) within the feed coals as well as in the float and sink fractions (high in vitrinite coal fractions) that are responsible for the melting, sintering, slagging, deposition, fouling problems during the laboratory coal combustion studies.
- Qualify and quantify mineral liberation and mineral association (referring to the excluded minerals) within the sink fractions which are responsible for the melting, sintering, slagging, deposition, fouling problems during the laboratory coal combustion studies.
- Determine the concentrations of the organically associated inorganic elements as well as the submicron minerals associated within the macerals (minerals infilling cleat fractures in the vitrinite), which are responsible for the volatilisation of inorganic constituents and formation of fine ash during coal combustion.
- Link mineralogy of the feed coals and the density separation coal fractions (low and high vitrinite coal fractions) to the mineralogy of their corresponding ash samples.

1.3 Outline of the thesis

Chapter 1 provides an introduction to this study. The aim and objectives, problem statement and the hypothesis will be explained in the introduction chapter. An outline of the experimental procedures to be used will also be included.

In **Chapter 2**, the literature chapter, the significance of South African coal samples are explained, followed by a review of the nature of organic and inorganic constituents in coal. The mode of occurrence of mineral matter present within coal, i.e. included minerals, excluded minerals and the organically associated inorganic elements are reviewed. Industrial problems, such as melting, sintering, slagging, ash deposition and fouling, related to the coal combustion process is summarised.

The first objective of this study was to produce a mineral-rich and a maceral-rich fraction in order to comprehensively investigate the associations of minerals within the included minerals (float fraction) and excluded minerals (sink fraction). Reflux classification was a novel approach in order to produce maceral-rich fraction without liberated minerals. Advanced analytical techniques were applied in order to extend the knowledge of the chemical, mineralogical and petrographical properties of mineral-rich and carbon-rich fractions of South African coal.

The results presented and discussed in **Chapter 3** can be effectively used in order to minimise or avoid ash-deposition problems that occur during coal utilisation.

Low-temperature oxygen plasma ashing was used to determine the proportions of mineral matter contained in the feed coals, and their density separated fractions. The LTA ash (mineral matter) samples were subsequently analysed using HT-XRD under air to investigate the formation of high-temperature mineral phases.

In **Chapter 4**, the actual experimental data obtained from quantitative HT-XRD experiments, as well as the mineralogical and chemical results for the low-temperature ash (LTA) samples were used to identify the minerals which are accountable for the sintering and slagging of mineral matter. The transformation of minerals in the coals and their density separated fractions at elevated temperatures is considered to be due to the mode of occurrence of mineral matter.

The primary objective of **Chapter 5** was to relate the coalescence of included minerals (<1.5 g/cm^3 float fractions) and the fragmentation of excluded minerals (>1.9 g/cm^3 sink fractions), during combustion, to the slagging propensities of South African coal samples. By incorporating the behaviour of both included and excluded minerals under combustion conditions, the

heterogeneous nature of ash properties is considered, which were disregarded in previous traditional ash deposition predictions

In **Chapter 6,** the conclusions drawn throughout this study are summarised. Recommendations for future work in the same area of research covering any shortcomings during this study are also included.

Chapter References

Minerals Council South Africa. 2019. "Facts and Figures 2018." *Minerals Council South Africa.* September 09. Accessed February 01, 2020. https://www.mineralscouncil.org.za/industry-news/publications/facts-and-figures.

Buhre, B.J.P., Hinkley, J.T., Gupta, R.P., Nelson, P.F. & Wall, T.F. 2006. Fine ash formation during combustion of pulverised coal-coal property impacts. F*uel*, 85:185-193.

Falcon, R.M.S. & Snyman, C.P. 1986. An introduction to coal petrography: Atlas of petrographic constituents in the bituminous coals of Southern Africa. Johannesburg, RSA: The Geological Society of South Africa.

Jeffrey, L.S. 2005. Characterization of the coal resources of South Africa. *Journal of Southern African Institution of Mineral and Metallurgy*, 105(2):95-102.

Liu, Y., Gupta, R., Sharma, A., Wall, T., Butcher, A., Miller, G., Gottlieb, P. & French, D. 2005. Mineral matter–organic matter association characterisation by QEMSCAN and applications in coal utilisation. *Fuel*, 84(10):1259-1267.

Matjie, R.H., French, D., Ward, C.R., Pistorius, P.C. & Li, Z. 2011. Behaviour of coal mineral matter in sintering and slagging of ash during the gasification process. *Fuel Processing Technology*, 92:1426-1433.

Matjie, R.H., Li, Z., Ward, C.R., Bunt, J.R. & Strydom, C.A. 2016. Determination if mineral matter and elemental composition of individual macerals in coals from Highveld mines. *The Journal of The Southern African Institute of Mining and Metallurgy*, 116:169-180.

Ratshomo, K. & Nembahe, R. 2018. Department of Energy. http://www.energy.gov.za/files/media/explained/South-African-Coal-Sector-Report.pdf Date of access: 05 May 2019.

Snyman, C. & Botha, W. 1993. Coal in south Africa. *Journal of African Earth Sciences (and the Middle East)*, 16(1-2):171-180.

Wagner, J., Malumbazo, N. & Falcon, R.M.S. 2018. Southern African Coals and Carbons: Definitions and Applications of Organic Petrology: Cape Town : Struik Nature.

CHAPTER 2

LITERATURE REVIEW

Literature relevant to this study on the transformation of mineral matter in South African coal is summarised in this chapter. The nature of minerals and macerals in coal, the transformations at high temperatures as well as the associations of mineral matter within coal are described. The effect of these mineral interactions on ash-related problems, such as slagging, sintering and fouling, during coal conversion processes, will also be emphasised.

The detailed literature relevant to each article is included in Chapters 3, 4 and 5.

2.1 Introduction

Mineral matter in coal is divided into three subgroups; included (inherent) minerals, excluded (extraneous) minerals and organically associated inorganic elements. Various complex mineral interactions, phase changes, and transformations occur during coal conversion processes. These mineral transformations at elevated temperatures are the cause of ash-related industrial problems such as slagging, fouling, sintering, agglomeration, erosion and corrosion. The mode of mineral matter occurrence in the coal samples is of significance when investigating ash deposition during coal conversion processes.

2.2 South African coal deposits

Coal is a heterogeneous organic sedimentary rock formed from fossilised plant material which has been altered by the effects of heat and pressure over an extended period. Classification of different coal samples is based on the chemical and physical properties, which differ significantly from one coalfield to another. The variations in coal properties and quality, i.e. grade, type and rank, are the result of different conditions during deposition (Falcon & Ham, 1988). There are 19 coalfields in South Africa which are spread over five provinces (Jeffrey, 2005). The coal quality, properties, composition and stratigraphy, vary significantly between these coalfields and are explained in detailed by numerous authors (Falcon & Ham, 1988; Jeffrey, 2005; Smith *et al.*, 1993;

Snyman & Botha, 1993; Wagner *et al.*, 2018). Low-rank coals with high ash yield are typically used in South African conversion processes.

2.3 The nature of organic and inorganic constituents in coal

Organic and inorganic materials are present within the heterogeneous structure of coal. The organic material also referred to as the complex macerals, can be categorised into three main groups; liptinite, vitrinite and inertinite maceral groups. These organic materials have different technological, physical and optical properties, which are used in order to distinguish between the maceral constituents. Comprehensive classifications of macerals are described in the classification system compiled by the International Committee for Coal and Organic Petrology (Falcon & Snyman, 1986; Green *et al.*, 1983; ICCP, 1998; ICCP, 2001; Stach *et al.*, 1982; Van Niekerk *et al.*, 2008). The maceral constituents play a fundamental role in the establishment of nature as well as the value of coal for various utilisation processes. Benfell et al., (2001) reported that when particles contain different maceral components, they will behave differently in terms of the swelling behaviour, char structure, ash composition, reactivity and the amount of devolatilisation during coal conversion (Benfell *et al.*, 2000).

The first maceral group is liptinite, previously known as exinite, which is derived from hydrogen-rich vegetation that is not humifiable and contains mainly the remains of spores, algae, cuticles, and polymerised waxes, fats, and oils. Less than 10 vol% of liptinite typically occurs in South African coal samples. Liptinite yields the highest volatile matter during coal conversion due to the aliphatic-aromatic compounds that are rich in aliphatic side chains (Falcon & Ham, 1988; Snyman & Botha, 1993).

Vitrinite, the second maceral group, is the most reactive maceral and also abundantly present in South African coal (Wagner *et al.,* 2018). Formation of vitrinite occurs when water rapidly conceal the vegetation (branches, leaf tissue, roots, trunks, and twigs) during deposition, or when the plant material lands in a peat swamp area. This rapid burial of vegetation inhibits biochemical modification through oxidation and thus destroys the original cellular structure which results in gelification, i.e. the ‘glassy’ appearance of vitrinite. Vitrinite consists of randomly orientated aromatic nuclei which are surrounded by outlying aliphatic compounds. The outlying aliphatic chains break, while the number of aromatic nuclei increases with an increase in coal rank. The increase in coal rank coincides, in a linear fashion, with the decrease in the volatile matter and the increase in aromaticity and carbon content. Petrographic analysis is used to determine the light reflecting from the surface of vitrinite, where high reflectance correlates with high carbon

content. Vitrinite reflectance can thus be successfully used to determine coal rank (Falcon & Ham, 1988; ICCP, 2001; Wagner *et al.*, 2018).

The third maceral group is the inertinite macerals, which has a low reactivity during coal utilisation processes (Falcon & Ham, 1988). However, reactive semifusinite, a sub-group of inertinite, will perform similarly to vitrinite as a result of the comparable reflectance and volatile yield values. Inertinite formation is the result of severe degradation and alteration of plant material under aerobic oxidising conditions. Only minor chemical and physical changes occur with an increase in coal rank due to the low levels of hydrogen and the firmly bonded oxygen molecules (Falcon & Ham, 1988; ICCP, 2001; Wagner *et al.*, 2018; Ward, 2002; Ward, 2016).

The significance and value of coal during various conversion processes, such as combustion, in-situ absorption of methane, metallurgical processing as well as the potential of coal as an alternative source of hydrocarbons can be mainly attributed to the organic (maceral) constituents present in coal. South African coals typically contain more than 55% inertinite, but ranges between 20% and 80%, and can, therefore, be classified as inertinite-rich coals (Falcon & Ham, 1988; Wagner *et al.*, 2018; Ward, 2002; Ward, 2016).

The inorganic constituents of coal, also known as the mineral matter, can be grouped into three types of mineral classifications; (1) mineral salts, which are dissolved in the water and precipitated in the pores, (2) inherent mineral matter, which is part of the structure of coal, and (3) inorganic compounds associated with the organic material (Ward, 2002). Included (inherent) minerals represent a significant portion of mineral matter that is closely associated with the organic matter, i.e. the macerals. Beneficiation of included minerals is challenging due to the intimate association of these minerals with the coal matrix and therefore, included minerals will have a significant influence on the behaviour of coal during utilisation. Excluded (extraneous) minerals represents the additional mineral components and rock fragments present in coal after mining due to the contamination of the roof and floor strata. These excluded minerals can be partly beneficiated by physical methods such as density separation and reflux classification. The rock fragments present during coal combustion may result in the formation of clinkers, which can cause blockages in the equipment and impact negatively on the process (Krishnamoorthy & Pisupati, 2015; Schobert, 2013)..

Over a hundred minerals have been identified in coal samples, but less than twenty are present in significant quantities to have a practical impact. These main minerals present in coal can be grouped into seven families, as listed in Table 2-1.

Table 2-1 Main minerals found in coal samples, grouped into seven families (Matjie, 2008; Schobert, 2013; Ward, 2002).

Mineral group	Mineral	Composition
Silicates (Clay minerals)	Kaolinite	$Al_2Si_2O_5(OH)_4$
	Illite	$K_{1-1.5}Al_4(Si_{7-6}Al_{1-1.5}O_{20})(OH)_4$
	Muscovite	$K_2O.3Al_2O_3.6SiO_2.2H_2O$
	Montmorillonite	$(1-x)Al_2O_3.x(MgO, Na_2O)\cdot 4SiO_2\cdot H_2O$
	Quartz	SiO
	Feldspar	$KAlSi_3O_8$
Carbonates	Calcite	$CaCO_3$
	Dolomite	$CaMg(CO_3)_2$
	Siderite	$FeCO_3$
	Ankerite	$(Ca,Fe,Mg)CO_3$
Oxides	Rutile / Anatase	TiO_2
	Hematite	Fe_2O_3
	Magnetite	Fe_3O_4
Sulphides	Pyrite	FeS_2
	Marcasite	FeS_2
	Pyrrhotite	$Fe(1-x)S$
Sulphates	Gypsum	$CaSO_4\cdot 2H_2O$
	Alunite	$KAl_3(SO_4)_2(OH)_6$
	Bassanite	$CaSO_4\cdot ½H_2O$
	Anhydrite	$CaSO_4$
Phosphate	Apatite	$Ca_5F(PO_4)_3$
	Crandallite	$CaAl_3(PO_4)_2(OH)_5\cdot H_2O$
	Goyazite	$SrAl_3(PO_4)_2(OH)_5\cdot H_2O$

The most abundant mineral group present in coal are the clay minerals that usually consist of hydrous oxides of aluminium and silicon, which may also contain iron, alkali and alkaline earth elements in the structure. Coal samples may comprise of up to 80% clay minerals, with kaolinite

as the predominant mineral. These minerals are present in coal as dispersed mineral grains, bands, and lenticels, and contribute significantly to ash formation (Kemezys & Taylor, 1964; Raask, 1985; Spears, 2000). Approximately 20% of the total minerals present in coals consist of silica, mainly in the form of quartz.

The second group of minerals present in coal includes the main carbonates such as calcite, dolomite, siderite, and ankerite. These carbonates in coal are in solid solution state, which results in a very complex chemistry (Gluskoter, 1975). The most abundant sulphide mineral in coal is pyrite which primarily precipitates after the coalification process. The total amount of sulphides in the coal samples are less than 5% of the total minerals but require much attention due to the contribution to air pollution, which leads to acid rain. The sulphates of calcium and iron are the main sulphates that are present in coal, although at very low concentrations (Schobert, 2013).

2.4 Methods to determine the mode of occurrence of mineral matter in coal

Methods used to determine the mode of occurrence include density fractionation and sequential leaching in combination with more advanced techniques such as Computer-Controlled Scanning Electron Microscopy (CCSEM) and Quantitative Evaluation of Materials by Scanning Electron Microscopy (QEMSCAN). X-ray Diffraction and X-ray Fluorescence techniques also contribute to an understanding of the mode of occurrence of mineral matter in coal. Comprehensive knowledge of the mode of occurrence of mineral matter, i.e. the way the elements are chemically bound, can be used in order to determine the associations of minerals in coal (Maledi, 2017).

Mineral matter plays a significant role during coal utilisation, and it is therefore of utmost importance to be able to determine the concentrations as well as the mode of occurrence of mineral matter in coal. Low-temperature oxygen plasma ashing (LTA) is a technique that is used to oxidise the organic material in coal at temperatures between 120°C and 150°C, without modifying or decomposing the coal minerals. The schematic diagram of a low-temperature oxygen plasma asher is represented in Figure 2-1.

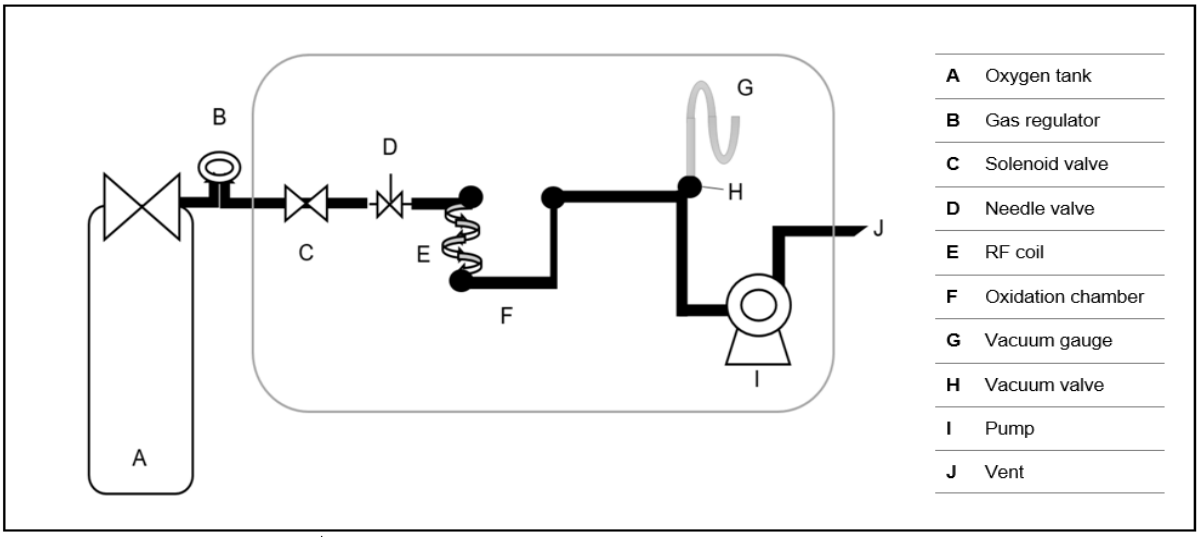

Figure 2-1 Schematic representation of a low-temperature oxygen plasma asher (Rautenbach *et al.*, 2019) adapted from (Gluskoter, 1965).

A radiofrequency oscillator is used to produce activated oxygen which is distributed over pulverised coal in order to oxidise the organic material at low temperatures. This technique was used by several authors and provided reliable and accurate results for the determination of mineral matter in coal (Frazer & Belcher, 1973; Gluskoter, 1965; Matjie *et al.*, 2016; Matjie *et al.*, 2012a; Matjie *et al.*, 2012b; Miller *et al.*, 1979; Ward, 2002; Ward, 2016; Ward *et al.*, 1999).

2.5 Transformation of minerals at elevated temperatures

Mineral matter transforms during coal utilisation through various complex reactions, and phase changes such as fusion, thermal decomposition, oxidation, reduction, dehydroxylation, volatilisation, condensation, melting, recrystallisation and solid-state reactions (Vassileva & Vassilev, 2006). The combustion conditions, mineral associations and the physical and chemical properties determine the behaviour of mineral matter during coal conversion processes.

Inorganic compounds, such as aluminosilicates, have relatively low melting points and will coalesce, soften and melt with an increase in the temperature (Schobert, 2013). During coal combustion, the included minerals, which are intimately associated with each other in the coal matrix, will react by coalescence. It is also proposed that included minerals melt at lower temperature and are therefore responsible for the volatilisation of inorganic elements, as well as the formation of slag deposits during combustion (Matjie *et al.*, 2011).

Excluded minerals will fragment and fuse before solidifying when exposed to elevated temperatures. This particle fragmentation can be the result of thermal shock due to rapid heat-up or pressure build-up, which is caused by the evolution of gaseous species during decomposition. Mechanical abrasion may also cause fragmentation when mineral particles collide with each other at high velocities (Krishnamoorthy & Pisupati, 2015; Schobert, 2013).

The transformation of excluded kaolinite at elevated temperatures starts with dehydration at temperatures from 425°C to 525°C. The formation of metakaolinite, an amorphous phase, occurs after dehydration (equation 1).

$$Al_2Si_2O_5(OH)_4 \rightarrow Al_2O_3{\cdot}2SiO_2 + 2H_2O \quad (1)$$

The transformation of kaolinite is completed at temperatures from 950°C to 1000°C (eq. 2), which results in the formation of mullite, cristobalite, and gamma-alumina.

$$Al_2O_3{\cdot}2SiO_2 \rightarrow Al_6Si_2O_{13} + SiO_2 + Al_2O_3 \quad (2)$$

Mullite and cristobalite will persist at high temperatures as solid phases and will melt at temperatures exceeding 1600°C. Van Alphen (2005) developed a fly ash formation model for South African coals, where it was predicted that included kaolinite would be released from the carbon matrix during combustion and subsequently form part of the fly ash as excluded kaolinite. Included kaolinite will cause coalescence with fluxing element-bearing minerals, such as calcite, dolomite, pyrite, and to a lesser extent with quartz to form dense ash particles (Matjie, 2008; Van Alphen, 2005).

Quartz is mainly non-reactive during coal utilisation processes. However, a sequence of transformations is observed for quartz with an increase in temperature from α-quartz, to β-quartz, to β-tridymite and finally to β-cristobalite at temperatures higher than 1400°C. Tridymite and cristobalite, the high-temperature mineral phases of quartz, may also form during solid-state interactions when the conditions are favourable (Ward, 2002; Ward, 2016). These solid-state reactions occur at significantly low rates. Therefore the hard quartz particles will mainly persist throughout the combustion process (Matjie, 2008).

Excluded carbonate minerals present in South African coals include calcite, dolomite, siderite, and ankerite. Calcium oxides will react readily with quartz and clay minerals as well as with gaseous sulphur-containing species. The decomposition temperature of calcite is in the range of 600°C to 950°C, which results in the formation of lime (eq. 3).

$$CaCO_3 \rightarrow CaO + CO_2 \quad (3)$$

When this lime reacts with sulphur oxides and water, the formation of anhydrite (eq. 4) and portlandite (eq. 5) occur respectively.

$CaO + SO_3 \rightarrow CaSO_4$ (4)

$CaO + H_2O \rightarrow Ca(OH)_2$ (5)

Bassanite is a low-temperature product of non-mineral calcium and organic sulphur (eq. 6), while anorthite and gehlenite forms at high temperatures as the result of the interaction between metakaolinite and calcium (eq. 7).

$Ca_{organic} + S_{organic}$ (low temperatures) $\rightarrow CaSO_4 \cdot ½H_2O$ (6)

$CaO + Al_2O_3 \cdot 2SiO_2 \rightarrow Ca_2Al_2SiO_7$ (gehlenite) + $CaAl_2Si_2O_8$ (anorthite) (7)

During the decomposition of dolomite and ankerite (the mixed carbonates), the calcium, magnesium, and iron are liberated and act as fluxing minerals or participate in the formation of aluminosilicates. Decomposition of dolomite occurs in two-steps to form lime and periclase during coal combustion.

$CaMg(CO_3)_2 \rightarrow CaO + MgO + 2CO_2$ (8)

Decomposition of siderite occurs between 400°C and 800°C, which leads to the formation of wustite (eq. 9).

$FeCO_3 \rightarrow FeO + CO_2$ (9)

Wustite, which also forms during the oxidation of pyrrhotite, will subsequently oxidise to hematite or magnetite (Matjie, 2008; Schobert, 2013). During Van Alphen's (2005) study on the transformation of minerals at elevated temperatures, the Drop Tube Furnace results indicated that excluded calcite would transform to calcium oxide while excluded dolomite will transform to Ca-Mg-oxide. Included calcium will enhance the slag formation by forming complexes with low melting points in the presence of silica.

Excluded pyrite will fragment at elevated temperatures and form various iron oxides, such as magnetite, hematite and maghemite. Pyrite can also decompose at temperatures from 300°C to 600°C to form pyrrhotite (eq. 10).

$FeS_2 \rightarrow FeS + S$ (10)

The atmosphere in which the sulphur decomposes is of utmost importance. In an oxidising atmosphere, the sulphur will form sulphur dioxide (eq. 11).

$$FeS_2 + O_2 \rightarrow FeS + SO_2 \quad (11)$$

In a reducing atmosphere the sulphur will form hydrogen sulphide (eq. 12).

$$FeS_2 + H_2 \rightarrow FeS + H_2S \quad (12)$$

When pyrite oxidises in the presence of air, it will form iron sulphides (Schobert, 2013).

Calcium sulphates are mainly present as gypsum, $CaSO_4 \cdot 2H_2O$, which will decompose firstly to bassanite, $CaSO_4 \cdot \frac{1}{2}H_2O$, and afterwards to anhydrite, $CaSO_4$. Anhydrite will decompose at approximately 900°C to form sulphur oxide as well as calcium oxide. Anhydrite can also be reduced in the presence of CO to calcium sulphide (eq. 13) (Schobert, 2013).

$$CaSO_4 + 4\ CO \rightarrow 4\ CO_2 \quad (13)$$

Some of the main high-temperature mineral phases that occur in South African coal samples are listed in Table 2-2.

Table 2-2 High-temperature mineral phases commonly reported in South African coal samples (Matjie, 2008; Schobert, 2013; Ward, 2002).

Mineral	Composition	Mineral	Composition
Quartz	SiO_2	Aragonite	$CaCO_3$
Cristobalite	SiO_2	Portlandite	$Ca(OH)_2$
Tridymite	SiO_2	Lime	CaO
Metakaolinite	$Al_2O_3 \cdot 2SiO_2$	Periclase	MgO
Mullite	$Al_6Si_2O_{13}$	Wustite	FeO
Sillimanite	Al_2SiO_5	Hematite	Fe_2O_3
Anorthite	$CaAl_2Si_2O_8$	Maghemite	Fe_2O_3
Albite	$NaAlSi_3O_{13}$	Magnetite	Fe_3O_4
Pyrrhotite	Fe(1-x)S	Spinel	$MgAl_2O_4$
Anhydrite	$CaSO_4$	Gehlenite	$Ca_2Al_2SiO_7$

The associations of mineral matter in coal, i.e. included minerals, excluded minerals or organically-bound inorganic materials contribute significantly to the ash formation mechanism during thermal utilisation processes. The interaction of mineral matter during coal utilisation processes will lead to the formation of fly ash and bottom ash, slag deposit formation due to crystallisation and fusion of mineral matter at elevated temperatures as well as the formation of fouling deposits due to volatilisation and condensation (Gupta *et al.*, 1998; Raask, 1985; Ward, 2002).

2.6 Industrial ash related problems

Ash deposition occurs as a result of the transformation of minerals during heat treatment of coal and is of significant concern due to operational problems such as sintering, agglomeration, fouling, slagging, erosion and corrosion.

Slagging and fouling are a result of ash deposition within the boilers. Slagging occurs when a fluid phase adheres to a surface exposed to the flames' radiation. Slag deposits are described as fused, molten or semi-molten deposits found on the water walls within the boiler (Unsworth *et al.*, 1988).

There are various factors which contribute to slagging such as molten fly ash particles sticking to the surface, fly ash particles carried by the gas flow to the boiler walls, as well as the low excess air environment resulting in a reduced atmosphere. Slag formation occurs as a result of fluxing minerals that react with metakaolinite and subsequently decrease the ash fusion temperatures (AFT) (Van Dyk *et al.*, 2009). The slag build-up may result in the formation of a molten phase due to the increase of the surface temperature. The surface of the slag deposit may also act as an efficient fly ash collector. Large slag deposits may break loose from the boiler wall and cause damages to the bottom of the furnace. It furthermore reduces the heat transfer rate resulting in dramatic fouling deposits due to the increase of the temperature within the convective pass. There are some units which are designed to handle the slag formation, but others cannot operate when running slag is present. The slag can cause significant damages and unscheduled outages for maintenance and cleaning purposes.

Fouling occurs when the ash deposits attach to convective heat exchange surfaces exposed to high temperatures such as reheaters, superheaters, and economisers. Only small amounts of molten phases are present in fouling deposits. With the decrease in the rate of heat transfer and the subsequent increase in the gaseous temperature, sulfates condense out of the gaseous

phases producing sufficient liquid amounts, which result in an expansion of the fouling deposits. Severe fouling will lead to an increase in the pressure drop throughout the tubes, which will initiate the formation of bridging across the tubes, resulting in the inevitable shutdown of the boilers (Bryers, 1996; Matjie *et al.*, 2012a).

Sintering and agglomeration are used interchangeably by some authors, but it is, in fact, two different aspects. Sintering occurs when the ash particles undergo partial melting and are bonded together in order to lower the surface tension. When the particles bond together, the system energy decreases while the strength of the predominantly solid structure improves (German, 1996; Nel, 2009; Schobert, 2013). The melt phase binds the particles to each other and results in the coalescence of the initial ash particles into larger particles. According to Kang (2004), sintering can be classified by the growth of the grains, as well as by densification (Kang, 2004).

Agglomeration is a process where large clusters of ash particles form during heat treatment. During agglomeration, the fluid phase responsible for binding the particles does not originate from the composition of the agglomerated particles. The coating on the surface of the particles may act as the glue which binds the agglomerates together. During agglomeration, the size of the cluster increases and no grain growth of individual ash particles can be observed (Arastoopour *et al.*, 1988; Nel, 2009; Schobert, 2013). Sintering of agglomerated particles may occur at elevated temperatures (Arastoopour *et al.*, 1988). The sintering and agglomeration of ash particles may lead to the formation of hard aggregates and clinkers within the operational unit, which will make the collection of ash difficult and may cause the fluidised beds to be de-fluidised (Schobert, 2013).

Corrosion and erosion are two additional ash-related operational problems which can occur during coal utilisation. Erosion is the result of hard mineral particles which impacts on the surface of gasifiers and combustors. The degree of erosion in a unit depends on the shape, size and hardness of the ash particle, as well as on the angle and velocity on which the particle impacts the surface. Quartz is an excellent example of a mineral particle that can cause erosion inside boilers. Corrosion occurs inside the gasifiers or combustors when sulphuric acid or hydrogen chloride is produced from other minerals present in the ash. These boilers are made from alloys, such as stainless steel, which contains a tightly bonded oxide layer that protects the inner layer. When the ash deposits onto this inner layer, it may react with the protective layer on the metal and compromise its ability to protect the metal from corrosion.

2.7 Slagging and fouling prediction indices

Numerous authors have investigated the empirical prediction indices, which are based on the ash chemistry of coal and used to predict the slagging tendencies of coal during combustion (Barroso *et al.*, 2007; Degereji *et al.*, 2012; Lawrence *et al.*, 2008; Raask, 1985). The main indices used to predict slagging and fouling propensities are summarised in Table 2-3.

Table 2-3: Empirical indices used to predict slagging and fouling propensities of coal

Empirical index	Formula	Propensity (fractions and percentages)	
Base/Acid Ratio: (B/A_R)	$\frac{Fe_2O_3+CaO+MgO+Na_2O+K_2O}{SiO_2+Al_2O_3+TiO_2}$	Low: <0.4 or >0.7	High: from 0.4 to 0.7
Silica percentage: (Si_R)	$\frac{SiO_2 \times 100}{SiO_2+Fe_2O_3+CaO+MgO}$	Low: 72 to 80% Medium: 65 – 72%	Severe: 50 – 65%
Iron to calcium ratio: (Fe/Ca_R)	Fe_2O_3 / CaO	Low: <0.3 or >3.0	High: 0.3 to 3.0
Slagging factor	B/A ratio x Sulphur in coal	Low: <0.6 Medium: 0.6 to 2.0	High: 2.0 to 2.6 Severe: >2.6
Fouling factor	B/A ratio x Na_2O % in ash	Low: <0.2 Medium: 0.2 to 0.5	High: 0.5 to 1.0 Severe: >1.0

The limitations of these empirical indices are that it applies to specific coal under specific conditions. The elemental composition results, as determined by X-ray Fluorescence, are used in these indices, and incorporate the total acidic and basic elements within included and excluded minerals. When subjecting South African coal properties to these empirical indices, very low or no slag formation are predicted. However, slagging and clinker formation does exist in South African boilers due to the reactions of mineral matter at elevated temperatures. South African coal samples can be characterised as high ash yielding coal with low proportions of basic elements and high proportions of acidic elements in the ash.

Consequently, the empirical methods will not accurately predict the slagging tendencies of South African coals, because the ash composition is not a true reflection of the behaviour of mineral matter during combustion. These indices may be used as a guide for the prediction of slagging and fouling propensities, however with caution as it does not incorporate the mode of occurrence of mineral matter in coal (Lawrence *et al.*, 2008; Van Dyk *et al.*, 2009; Vuthaluru & French, 2008). By investigating the transformation of included and excluded minerals during combustion, an alternative slag prediction method can be developed which is based on the mode of occurrence of mineral matter.

Chapter References

Arastoopour, H., Huang, C. & Weil, S. 1988. Fluidisation behaviour of particles under agglomeration conditions. *Journal of Chemical Engineering Science*, 43.

Barroso, J., Ballester, J. & Pina, A. 2007. Study of coal ash deposition in an entrained flow reactor: Assesment of traditional and alternative slagging indices. *Fuel Processing Technology*, 88:865-876.

Benfell, K.E., Liu, G., Roberts, D.G., Harris, D.J., Lucas, J.A., Bailey, J.G. & Wall, T. 2000. Modeling char combustion: The influence of parent coal petrography and pyrolysis pressure on the structure and intrinsic reactivity of its char. (*In*. Combustion Institute organised by. p. 2233-2241).

Bryers, R.W. 1996. Fireside slagging, fouling, and high-temperature corrosion of heat-transfer surface due to impurities in steam-raising fuels. *Progress in Energy and Combustion Science*, 22(1):29-120.

Degereji, M.U., Ingham, D.B., Ma, L., Pourkashanian, M. & Williams, A. 2012. Numerical assessment of coals/blends slagging potential in pulverized coal boilers. *Fuel*, 102:345-353.

Falcon, R.M.S. & Ham, A.J. 1988. The characteristics of Southern African coals. *Journal of Southern African Institution of Mineral and Metallurgy*, 88(5):145-161.

Falcon, R.M.S. & Snyman, C.P. 1986. An introduction to coal petrography: Atlas of petrographic constituents in the bituminous coals of Southern Africa. Johannesburg, RSA: The Geological Society of South Africa.

Frazer, F.W. & Belcher, C.B. 1973. Quantitative determination of the mineral-matter content of coal by a radiofrequency-oxidation technique. *Fuel*, 52(1):41-46.

German, R.M. 1996. Sintering theory and practice. *Solar-Terrestrial Physics*:568.

Gluskoter, H.J. 1965. Electronic low temperature ashing of bituminous coal *Fuel*, 44:285-291.

Gluskoter, H.J. 1975. Mineral matter and trace elements in coal: ACS Publications.

Green, P.D., Johnson, C.A. & Thomas, K.M. 1983. Applications of laser Raman microprobe spectroscopy to the characterization of coals and cokes. *Fuel*, 62(9):1013-1023.

Gupta, R., Wall, T., Kajigaya, I., Miyamae, S. & Tsumita, Y. 1998. Computer-controlled scanning electron microscopy of minerals in coal—implications for ash deposition. *Progress in Energy and Combustion Science*, 24(6):523-543.

ICCP. 1998. ICCP (International Committee for Coal and Organic Petrology). The new vitrinite classification (ICCP System 1994). *Fuel*, 77(5):349-358.

ICCP. 2001. ICCP (International Committee for Coal and Organic Petrology). The new inertinite classification (ICCP System 1994). *Fuel*, 80(4):459-471.

Jeffrey, L.S. 2005. Characterization of the coal resources of South Africa. *Journal of Southern African Institution of Mineral and Metallurgy*, 105(2):95-102.

Kang, S.-J.L. 2004. Sintering: densification, grain growth and microstructure: Elsevier.

Kemezys, M. & Taylor, G.H. 1964. Occurrence and distribution of minerals in Australian coals. *Journal of the Institute of Fuel*, 37:389-397.

Krishnamoorthy, V. & Pisupati, S.V. 2015. A critical review of mineral matter related issues during gasification of coal in fixed, fluidized, and entrained flow gasifiers. *Energies*, 8(9):10430-10463.

Lawrence, A., Kumar, R., Nandakumar, K. & Narayanan, K. 2008. A Novel tool for assessing slagging propensity of coals in PF boilers. *Fuel*, 87:947-950.

Maledi, N.B. 2017. Characterisation of mineral matter in South African coals using micro-raman spectroscopy and other techniques.

Matjie, R., Li, Z., Ward, C.R., Bunt, J. & Strydom, C. 2016. Determination of mineral matter and elemental composition of individual macerals in coals from Highveld mines. *Journal of the Southern African Institute of Mining and Metallurgy*, 116(2):169-180.

Matjie, R.H. 2008. Sintering and slagging of mineral matter in South African coals during the coal gasification process. University of Pretoria.

Matjie, R.H., French, D., Ward, C.R., Pistorius, P.C. & Li, Z. 2011. Behaviour of coal mineral matter in sintering and slagging of ash during the gasification process. *Fuel Processing Technology*, 92(8):1426-1433.

Matjie, R.H., Ward, C.R. & Li, Z. 2012a. Mineralogical Transformation in Coal Feedstocks during Carbon Conversion, based on Packed-Bed Combustor Tests: Part 1 Bulk Coal and Ash Studies. *Coal Combustion and Gasification products*, 4:45-54.

Matjie, R.H., Ward, C.R. & Li, Z. 2012b. Mineralogical transformations in coal feedstock during carbon conversion, Based in packed-bed combustor tests: Part 2. Behavior of individual particles. *Coal Combustion and Gasification products*, 4:55-67.

Miller, R.N., Yarzab, R.F. & Given, P.H. 1979. Determination of the mineral-matter contents of coals by low-temperature ashing. *Fuel*, 58(1):4-10.

Nel, M.V. 2009. The influence of coal–associated trace elements on sintering and agglomeration of a model coal mineral mixture. North-West University.

Raask, E. 1985. The mode of occurrence and concentration of trace elements in coal. *Progress in Energy and Combustion Science*, 11(2):97-118.

Rautenbach, R., Matjie, R.H., Strydom, C.A., Bunt, J.R., Ward, C.R., French, D. & Van Alphen, C. 2019. Evaluation of mineral matter transformations in low-temperature ashes of South African coal feedstock samples and their density separated cuts using high-temperature X-ray diffraction. *International Journal of Coal Preparation and Utilization*:1-28.

Schobert, H.H. 2013. Composition, properties and classification of coals. Chemistry of Fossil Fuels and Biofuels. Cambridge: Cambridge University Press. p. 295-322).

Smith, R., Eriksson, P. & Botha, W. 1993. A review of the stratigraphy and sedimentary environments of the Karoo-aged basins of Southern Africa. *Journal of African Earth Sciences (and the Middle East)*, 16(1-2):143-169.

Snyman, C. & Botha, W. 1993. Coal in south Africa. *Journal of African Earth Sciences (and the Middle East)*, 16(1-2):171-180.

Spears, D. 2000. Role of clay minerals in UK coal combustion. *Applied Clay Science*, 16(1-2):87-95.

Stach, E., Mackowsky, M.-T., Teichmuller, M., Taylor, G.H., Chandra, D. & Teichmuller, R. 1982. Textbook of coal petrology. 2. Vol. 2. Berlin: Gebruder Borntraeger.

Unsworth, J.F., Barratt, D.J., Park, D. & Titchener, K.J. 1988. Ash formation during pulverized coal combustion: 2. The significance of crystalline anorthite in boiler deposits. *Fuel*, 67(5):632-641.

Van Alphen, C. 2005. Factors influencing fly ash formation and slag deposit formation (slagging) on combusting a South African pulverised fuel in a 200 MWe boiler. University of the Witwatersrand Johannesburg, South Africa.

Van Dyk, J., Benson, S., Laumb, M. & Waanders, B. 2009. Coal and coal ash characteristics to understand mineral transformations and slag formation. *Fuel*, 88(6):1057-1063.

Van Niekerk, D., Pugmire, R.J., Solum, M.S., Painter, P.C. & Mathews, J.P. 2008. Structural characterization of vitrinite-rich and inertinite-rich Permian-aged South African bituminous coals. *International Journal of Coal Geology*, 76(4):290-300.

Vassileva, C.G. & Vassilev, S.V. 2006. Behaviour of inorganic matter during heating of Bulgarian coals: 2. Subbituminous and bituminous coals. *Fuel Processing Technology*, 87(12):1095-1116.

Vuthaluru, H. & French, D. 2008. Ash chemistry and mineralogy of an Indonesian coal during combustion: part 1 drop-tube observations. *Fuel Processing Technology*, 89(6):595-607.

Wagner, J., Malumbazo, N. & Falcon, R.M.S. 2018. Southern African Coals and Carbons: Definitions and Applications of Organic Petrology: Cape Town : Struik Nature.

Ward, C.R. 2002. Analysis and significance of mineral matter in coal seams. *International Journal of Coal Geology*, 50(1-4):135-168.

Ward, C.R. 2016. Analysis, origin and significance of mineral matter in coal: An updated review. *International Journal of Coal Geology*, 165:1-27.

Ward, C.R., Spears, D., Booth, C.A., Staton, I. & Gurba, L.W. 1999. Mineral matter and trace elements in coals of the Gunnedah Basin, New South Wales, Australia. *International Journal of Coal Geology*, 40(4):281-308.

CHAPTER 3

MINERALOGICAL, CHEMICAL AND PETROGRAPHIC PROPERTIES OF SELECTED SOUTH AFRICAN POWER STATIONS' FEED COALS AND THEIR CORRESPONDING DENSITY SEPARATED FRACTIONS USING FLOAT-SINK AND REFLUX CLASSIFICATION METHODS.

Rudelle Rautenbach, Christien A. Strydom, John R. Bunt, Ratale H. Matjie, Quentin P. Campbell & Chris Van Alphen

This work is published in the *International Journal of Coal Preparation and Utilization* **2019**, 39:8,421-446, **DOI:** 10.1080/19392699.2018.1533551

Abstract

Three South African feed coal samples for the combustion process were beneficiated to produce carbon-rich and mineral-rich fractions. The mineralogical, petrographical, and chemical properties of these feed coals and their density separated fractions were investigated using XRD, XRF, QEMSCAN, electron microprobe, and petrography analyses. This work was conducted with the goal of better understanding the processes and operational problems which could possibly occur during coal utilisation, with particular focus on the included and excluded mineral matter transformational behaviour at elevated temperatures. The conventional float-sink and reflux classification methods used were shown to successfully eliminate liberated minerals and produced maceral-rich float fractions (98%) macerals. The main differences between the feed coals were related to the mode of occurrence of mineral matter. Integration of these different analytical techniques allowed for better determination of the concentrations of mineral matter responsible for industrial ash related problems. In this paper, we propose that blends of the different density fractions will reduce or minimise clinker and slag formation as well as the abrasive nature of the clinkers or slags. Possible blends to minimise clinker and slag formation include the float and sink fractions of the feed coals in varying proportions based on the specific mineralogical, petrographical and chemical data.

Keywords: Mineral matter, included and excluded minerals, reflux classification, QEMSCAN, electron microprobe

3.1 Introduction

The occurrence of the different types of mineral matter and organic matter (macerals) in coal are reported extensively in the literature (Falcon & Snyman, 1986; Harvey & Ruch, 1986; Stach *et al.*, 1982; Van Niekerk *et al.*, 2008; Ward, 2002). It is known that included minerals are mainly <20 µm and typically associated with the coal matrix (macerals), while the excluded and extraneous minerals are contained in rock fragments or ultra-fine components attached to the coal surface. The presence of these rock fragments may be due to contamination of floor and roof strata during the coalification and mining processes and can be separated from the coal by physical methods such as density separation and gravity concentration techniques. Heterogeneous clinkers which result in severe blockages of carbon conversion and combustion equipment may be formed as a result of these rock fragments attaching to the aluminium silicate molten solution of the interaction of the included mineral with the fluxing minerals during coal utilisation (Matjie *et al.*, 2011; Matjie *et al.*, 2008; Matjie *et al.*, 2012a; Matjie *et al.*, 2012b). In addition, the transformation and volatilisation of mineral matter during the combustion of coal may lead to industrial ash-related problems such as slagging, deposition and fouling. These inevitable industrial problems influence the efficiency of the boilers as well as the maintenance and operating costs (Van Alphen, 2005). Slagging behaviour of coal can be determined by using empirical indices in order to predict the slagging propensity. These empirical indices, based on the ash chemistry, have been studied by several authors explaining the practical implication as well as the definitions of the indices (Barroso *et al.*, 2007; Degereji *et al.*, 2012; Lawrence *et al.*, 2008; Raask, 1985). The major problem with these indices is the discrepancies reported when these indices are extrapolated in order to accommodate coals from another source with different characteristics. It can thus be concluded from these previous studies that the application of the existing empirical indices is mainly limited to the particular coal as well as the specific combustion system. Included minerals (fluxing and clays minerals) are the main source in the slag phase which cause the bonding, therefore must be included in the slagging propensity predictions (Van Dyk *et al.*, 2009).

A further mineral matter group includes the organically associated inorganic elements which only occur in minor proportions within the coal macerals. However, they play a major role in the formation and volatilisation of particulate matter (PM), fine and ultrafine ash particles, fly ash particles and polluting gases (sulphur oxides, nitrogen oxides, hydrogen sulfide, and carbonyl sulfide) during the coal combustion and carbon conversion processes (Buhre *et al.*, 2006; Matjie, 2008; Van Alphen, 2005; Zhang *et al.*, 2006). These elements are therefore considered to influence the fine/ultrafine ash particles and fly ash formation mechanisms during the coal combustion processes (Van Alphen, 2005). It has been reported that the non-mineral inorganic

elements (e.g. Ca, Mg) present in lignitic coals react with aluminum silicate (metakaolinite) released from the transformation of the kaolinite mineral to form fused agglomerates during the combustion process (Quann & Sarofim, 1986).

Macerals (vitrinite, liptinite, and inertinite) are major components of coal and fundamental in the determination of coal type. According to Benfell *et al*. (2000) coals with varying maceral composition will behave differently in terms of reactivity, caking behaviour, char structure, volatile matter emissions as well as the ash composition. Detailed information on the mode of occurrence of mineral matter and organic matter is thus of utmost importance for the utilisation of coal (Benfell *et al.*, 2000; Liu *et al.*, 2005).

It has been found that the classification of particles based on size and density can be accomplished by using a reflux classifier that combines the advantages of an inclined vessel with the flow conditions of a fluidised bed (Campbell *et al.*, 2015; Nguyentranlam & Galvin, 2004). The reflux classification technology is based on the Boycott phenomenon which explains that the rate of particle segregation from a liquid increases rapidly within a vessel with an incline compared to segregation within a vertical vessel (Boycott, 1920). Campbell *et al*. (2015) performed studies on South African coal samples using a laboratory-scale reflux classifier and found that fractionation of coal is possible using this water-only reflux classification. The reflux classifier data produced, based upon ash distribution and washability, is similar to the results from the traditional physical float-sink methods.

Soundarrajan *et al*. (2012) studied the variation in the organic and inorganic materials within density and size separated coal fractions and concluded that the density fractions >1.6 g/cm^3 relate primarily to industrial ash-related problems as it contributed more than 28% to the overall ash content. The differences between inorganic and organic materials are, therefore, more evident in the density fractions than in the bulk size distribution (Soundarrajan *et al.*, 2012).

The primary objective of this study, the first study of its kind on these specific South African power station feed coals, was to test the effectiveness of the reflux classification process on the beneficiation of South African feed coals for the combustion process, in order to produce carbon-rich and mineral-rich fractions. The secondary objective of this study was to obtain a better understanding of the mineralogical, petrographical and chemical properties of carbon-rich and mineral-rich fractions from the feed coals using advanced and traditional analytical techniques.

Quantitative Evaluation of Materials by Scanning Electron Microscopy (QEM*SEM, now termed QEMSCAN) is an advanced analytical technique that provides reliable data on the mineralogy of coal and coal ash samples. QEMSCAN was developed in Australia by CSIRO for the

determination of mineral proportions as well as the characterisation of precious minerals and base metals (Creelman *et al.*, 1993; Galbreath *et al.*, 1996; Gottlieb *et al.*, 1990). In this study, South African feed coals to the combustion process as well as their density separated coal fractions were investigated using various analytical techniques, including ultimate, proximate, petrographic, mineralogical, QEMSCAN, and electron microprobe (EMP) analyses. Analytical results obtained from this study, may be of benefit in understanding the processes that take place during coal utilisation. Some of the inevitable operational (slagging, deposition, abrasion, fouling, and agglomeration) and environmental problems that could take place in different private and parastatal sectors of the coal utilisation industry may be avoided or minimised using these results.

3.2 Experimental procedure

Approximately 100 kg of coarse combustion-feed coal (−75 + 1.7 mm) was collected from three different South African power plants. The coarse feed coal was submitted to the South African Bureau of Standards (SABS) laboratories in Secunda for density separation using the float-sink method. The method involved using the specific densities of the mixtures of benzene, Perchloroethylene, and TBE (Tetrabromoethane) in order to produce three fractions; a float fraction <1.5 g/cm^3, a middling fraction, i.e. between 1.5 g/cm^3 and 1.9 g/cm^3, and a sink fraction that are >1.9 g/cm^3. For the purpose of this paper, only the feed coals, the float and the sink fractions of the three coals were investigated. The density separation experiments were performed based on the procedure described by SANS/ISO 7936 by SABS laboratories, Secunda. The feed coals, as well as the density-separated fractions, were crushed to −1 mm particles using a Samuel Osborne (SA) LTD jaw crusher in combination with a ball mill containing stainless steel balls. Representative samples of the prepared coal samples were then submitted to Bureau Veritas Laboratories for proximate analysis using standard methods to measure the ash content (ISO 1171:2010), inherent moisture (ISO 11722:1999) and volatile matter (ISO 562:2010). The ultimate analysis of the coal samples was carried out according to the ISO 29541:2010 method, while the total sulphur content was determined using the ISO 19579:2006 standard procedure; these analyses were also conducted by Bureau Veritas.

The pulverised feed and float samples (−1 mm) were further screened to produce a finer coal particle size range (−500 µm +350 µm) and subjected to reflux classification in order to produce clean density fractions without liberated or excluded minerals, thus producing a float fraction containing increased proportions of macerals and less mineral matter. Reflux classification experiments were conducted on the coal samples using the laboratory scale reflux classifier at

the School of Chemical and Minerals Engineering at the North-West University and the design is fully described in (Campbell *et al.*, 2015). The RC setup can be observed in Fig. 3-1. The cross-sectional diameter of the reflux classifier is 0.105 m with 23 steel plates arranged at a 70° angle and 3.5 mm apart. Approximately 500 g feed coal particles (−500 µm +350 µm) were loaded in the fluidisation zone and the batch separation method was followed. A certain fluidisation flow rate was selected in order to produce a corresponding density fraction. In order to produce the float fractions, a flow rate of 35 L/min were used while a flow rate of 60 L/min were used to produce the sink fractions. These flow rates used were as determined by (Campbell *et al.*, 2015).

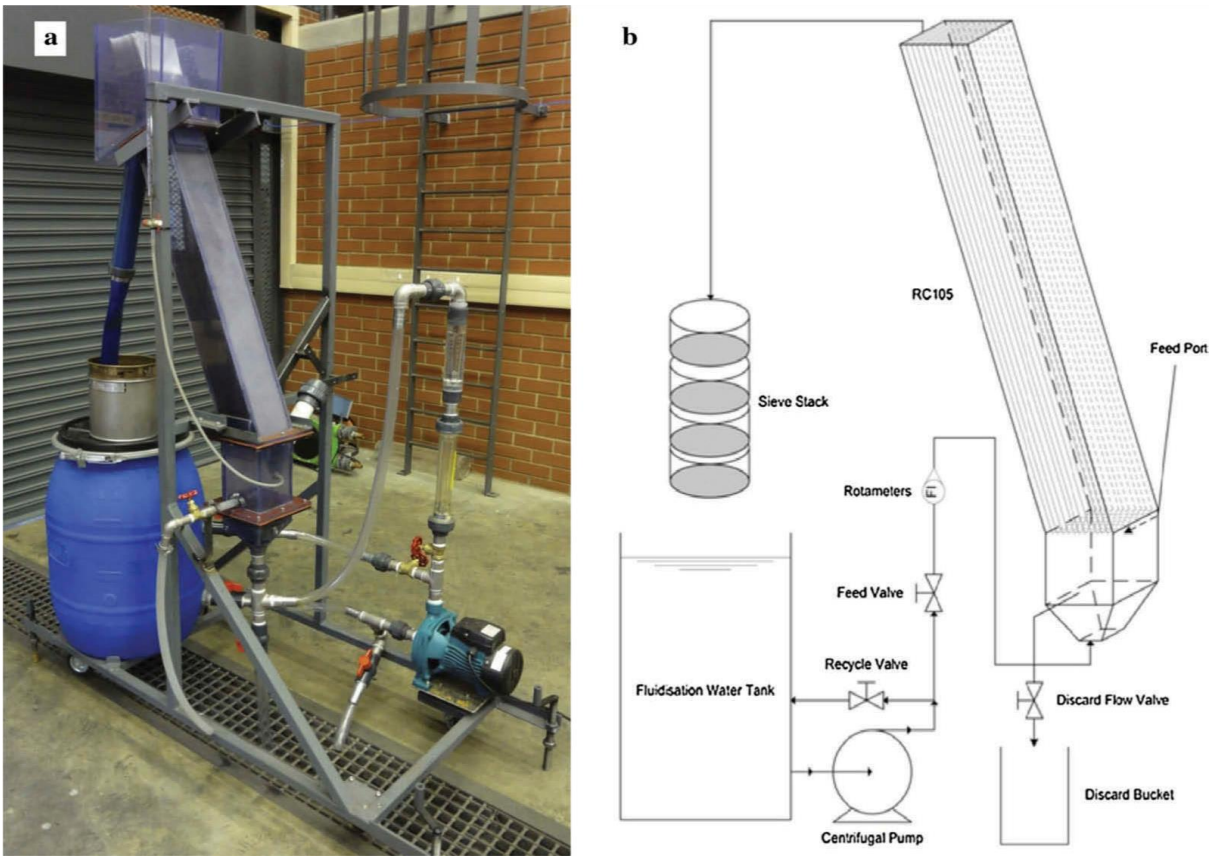

Figure 3-1 Reflux classifier setup at the North West University adapted from (Campbell *et al.*, 2015).

3.2.1 Analytical methods

X-ray diffraction (XRD) analyses were conducted on the feed coal samples and density separated fractions in order to identify the crystalline phases and amorphous material present within the samples. A PANalytical X'Pert Pro instrument equipped with a Co X-ray tube as well as an X'Celerator detector was used to identify the different phases. Each coal sample was spiked with

20% Si (Aldrich, 99.9% purity) and was subsequently micronised in a McCrone micronising mill. Identification, as well as the determination of the concentrations of crystalline phases and amorphous material in the spiked coal sample, were achieved by using X'Pert Highscore plus and an ICDD (International Centre for Diffraction Data) program while quantification of the phases were based on the Rietveld method (Rietveld, 1969).

X-ray fluorescence (XRF) was used to determine the concentrations of the elements present in the coal samples and density separated coal fractions using a PANalytical Axios MAX XRF instrument. The pressed samples were irradiated using an Rh X-ray tube while a Super Q database, calibrated with a range of approved standards (OMNIAN), was used to determine the concentrations of selected elements (Norrish & Hutton, 1969).

Feed coal and density separated coal fraction samples were submitted to the University of Johannesburg in Johannesburg, South Africa, for petrographic and electron microprobe (EMP) analyses. The crushed samples (−1 mm particle size) were set in epoxy resin, while a Struers Tegraforce polisher was used to prepare polished sections based on the ISO 7404–2 method. Analyses of the polished sections were achieved by using a Zeiss Axioimager petrographic microscope at an x500 magnification. Vitrinite reflectance was determined by using the Fossil Hilgers systems attached to the microscope, based on the ISO 7404–3 method, while maceral analysis was conducted according to the ISO 7404–4 method, by using a semi-automated point counting stage fitted to the microscope. A Cameca SX 100 electron microprobe was used to determine the elemental content of the macerals through wavelength-dispersive X-ray spectrometry (ISO7404-2, 1985; ISO7404-4, 1985).

The coal samples under investigation were also submitted to Eskom, Sustainability Division Research, Testing and Development department for QEMSCAN analysis. A scanning electron microscope (SEM) was used to create digital images of the feed coal as well as density separated fractions through Energy Dispersive X-ray (EDX) and Backscattered Electron (BSE) signals. Each pixel in these images corresponds to a specific mineral or phase type (Liu *et al.*, 2005; Matjie *et al.*, 2008). Characteristics of the different particles, density distribution of the particles as well as the modal proportions of the minerals were determined by using a FEG (Field Emission Gun) based QEMSCAN 650 from FEI. The pulverised samples were mixed with standard molten carnauba wax and allowed to cure in a 30 mm mould. Polished sections of the solid wax were then prepared in order to expose the mineral particles within the samples. An electron beam in the SEM was positioned at specified points and 1000 count X-ray spectrum were then produced which measured the elemental proportions. The mineral or amorphous phases as well as the

morphology of the particles in the sample at each point were then evaluated using the elemental proportions measured.

3.3 Results and discussion

3.3.1 Proximate and Ultimate analyses

The proximate analysis results for the feed coals as well as the density separated coal fractions (float and sink) are summarised in Table 3-1. The main differences between the feed coals observed from proximate analysis (reported on an air-dried basis) are the ash yield as well as the fixed carbon percentages. Coal A consists of the highest ash yield (36%) and the lowest fixed carbon content (40.3%). Coal B has an ash yield of 33% and fixed carbon content of 43.3%. The lowest ash yield and highest fixed carbon content were observed for Coal C, 25% and 48.6%, respectively. These results are in accordance with previous studies conducted on South African coal samples (Matjie *et al.*, 2016; Matjie *et al.*, 2015; Pinetown *et al.*, 2007). As expected, the ash yield for the sink fractions is high, ranging from 60% to 68%, in comparison to the float fractions with low ash yields of 7.8% to 12.4%.

The float fractions also contain higher volatile matter contents (27.5% to 33%), while a decrease is observed for the sink fractions (16% to 17%). As expected, the fixed carbon content is more concentrated in the float fractions (55.5% to 57.9%), and consequently relatively low in the sink fractions (13.6% to 20.4%). The density separation step has thus successfully concentrated the carbon content and the volatile matter in the float fractions (<1.5 g/cm^3) while lowering the ash content. When comparing the volatile matter and fixed carbon content for all the samples (based on a dry ash free basis), similar proportions can be observed which indicates that the main differences between the coals are related to the mode of occurrence of the mineral matter within the carbon-matrix or macerals.

Ideal combustion conditions will utilize feed coals that have high fixed carbon contents and low ash yields in order to minimize slagging and fouling inside the boiler. The yields of the float and sink fractions after density separation techniques are reported in Table 3-1. The yields of float and sink fractions after reflux classification treatment were not significantly high (40–60%) with the exception of Coal B float with a relatively high yield of 75%. According to the analyses of the reflux classification-treated fractions, reported in Section 3.6, the reflux classification successfully eliminated liberated minerals or excluded minerals and concentrated the vitrinite in the float fractions. The mass yields after the float-sink separation method was relatively low, although sufficient amount of material was collected in order to conduct the study.

Table 3-2 indicates the ultimate analysis results for the feed coals, as well as for the float and sink fractions. High concentrations of carbon can be observed for the feed coals (76% to 80%, air-dried basis), with lower hydrogen (4% to 5%) and nitrogen (1.7% to 1.9%) concentrations.

Table 3-1 Proximate analysis results for the feed coals, float, and sink fractions.

Sample identification		Feed A	Float A	Sink A	Feed B	Float B	Sink B	Feed C	Float C	Sink C
Moisture (%)	*a.d.b.*	2.0	2.7	1.8	3.2	3.9	2.2	4.5	4.1	2.3
Ash (%)	*a.d.b.*	35.9	7.8	62.9	32.9	12.4	68.1	25	10.5	60.3
Volatile Matter (%)	*a.d.b.*	21.8	33	16.4	20.6	28.2	16.1	21.9	27.5	17
Fixed carbon (%)	*a.d.b.*	40.3	56.5	18.9	43.3	55.5	13.6	48.6	57.9	20.4
Volatile Matter (%)	*d.a.f.*	35.1	36.9	46.5	32.2	33.7	54.2	31.1	32.2	45.5
Fixed carbon (%)	*d.a.f.*	64.9	63.1	53.5	67.8	66.3	45.8	68.9	67.8	54.5
% yield of fractions after float-sink separation			13	24		12	16		22	5
% yield of fractions after reflux classification			46	75		41	53		59	58

Note: a.d.b.: air dried basis; d.a.f.: dry ash basis

Table 3-2 Ultimate analysis results for the coals, float, and sink fractions.

Sample Identification	Feed A	Float A	Sink A	Feed B	Float B	Sink B	Feed C	Float C	Sink C
Carbon (%)	79.6	82.2	67.1	76.6	78.3	51.9	79.5	78.2	62.9
Hydrogen (%)	4.7	5.3	4.8	4.0	4.5	4.7	3.9	4.3	3.5
Nitrogen (%)	1.7	1.9	1.6	1.9	2.0	1.5	1.9	2.1	1.7
Total Sulphur (%)	2.1	0.9	4.8	0.5	0.6	0.6	0.7	0.6	1.9
Oxygen (% by difference)	13.9	10.7	26.5	17.4	15.2	41.8	14.6	15.4	32.0

These values are comparable with those obtained from previous studies done on South African coals (Matjie *et al.*, 2015; Van Dyk *et al.*, 2009). The sulphur content in the feed coals is relatively low, although when comparing the three feed coals, significantly higher amounts of sulphur is present in coal A. The float fractions contain higher concentrations of carbon, in accordance with the results in Table 3-1, as well as slightly higher nitrogen concentrations than the sink fractions. The oxygen proportions, calculated by difference, are more concentrated in the sink fractions.

Higher concentrations of oxygen in the sink fractions could be due to high concentrations of oxide minerals (kaolinite and quartz) concentrated in these fractions (Table 3-3). The higher volatile matter present in the float fractions (Table 3-1) correlates to the higher hydrogen and nitrogen contents (Table 3-2), when compared to the sink fractions. These values are representative of typical South African coal samples that are used in the combustion process (Van Dyk *et al.*, 2009).

3.3.2 Mineralogy of Feed Coals and Density Separated Fractions

The XRD results obtained for the powdered feed coals from the different South African power stations, as well as their density-separated fractions (floats and sinks) are presented in Table 3. The feed coal crystalline species consist mainly of quartz and kaolinite, and minor proportions of calcite, while dolomite is present in significantly higher proportions in coal A than in coals B and C. This is in accordance with previous studies on the mineralogy of South African coal resources (Matjie *et al.*, 2016; Van Dyk *et al.*, 2009). Minor proportions of pyrite, muscovite, illite, and anatase are also present in the feed coals.

A significant decrease in the quartz, kaolinite, and calcite concentrations are observed in the float fractions for all three coals, while the dolomite and calcite cleats associated within carbon matrix were more concentrated. The XRD detected low or no proportions of iron-containing minerals in the float fractions of coals A, B, and C, and feed coals (Table 3-3), due to the submicron iron-containing minerals (pyrite and siderite) particles (<1 nm crystallites) that could be dispersed in the carbon matrix which is amorphous material. These submicron mineral grains (crystallites) particles present in the float samples and feed coals could be below the detection limit of XRD, and they cannot be detected by XRD (Chinchón *et al.*, 1993).

As expected a high concentration of amorphous content, which is organic carbon, is also observed for the float fractions. Traces of microcline, goyazite, and fluorapatite are observed in the float fractions. According to (Matjie, 2008; Matjie *et al.*, 2011), the high temperature transformation products (calcium oxide, ferrous oxide, magnesium oxide) of the included fluxing minerals (calcite, dolomite, FeS_2) which are strongly associated with kaolinite in the carbon-matrix particles, react with the high temperature transformation (metakaolinite and reactive silica) of the included kaolinite to form CaO-MgO-FeO bearing aluminosilicate melt. Hard minerals such as anorthite and mullite crystallize from the melt and contribute significantly to abrasion or erosion of plant equipment during coal combustion and gasification processes (Hlatshwayo *et al.*, 2009). Some heated rock fragment particles from the surroundings attach to the melt to form large heterogeneous clinkers that are associated with slagging and boiler/gasifier blockage problems.

Therefore, the use of the float fractions alone without blending with the feed coals in the combustion process is postulated to result in severe slagging and fouling which will lead to lower carbon efficiency due to the high amorphous content. According to Van Dyk et al. (2009) in order to reduce ash-related problems during coal utilisation, the mineral reactions and bonding behaviour of the amorphous phase should be investigated.

Table 3-3 XRD results for the feed coals and density separated fractions (w/w %).

	Feed A	Float A	Sink A	Feed B	Float B	Sink B	Feed C	Float C	Sink C
Quartz	7.5	6.3	10.0	1.0	0.5	4.5	7.1	3.0	16.8
Kaolinite	18.0	11.7	27.7	20.2	8.8	59.6	18.7	9.0	26.3
Calcite	2.1	0.4	1.1	3.2	3.4	3.9	1.5	0.3	5.4
Pyrite	0.3		3.0	0.9		0.5	1.6		1.3
Muscovite	0.1	1.3		4.0	0.8	0.2	4.1		
Illite	1.2	0.6		3.5			1.6		
Microcline		0.8			0.8				
Portlandite			0.1			0.2			0.1
Goyazite		0.3			0.1			0.1	0.1
Dolomite	9.5	0.5	5.1	0.5	0.2	0.2	0.7	1.0	2
Anatase	0.2	0.6	0.2	0.2	0.3		0.2	0.1	0.5
Rutile				0.1		0.1			
Gypsum	0.8								
Fluorapatite	0.2	0.4			0.4			0.3	
Graphite	0.4						2.8		
Mineral matter	39.9	22.9	47.2	33.6	15.3	69.2	35.5	13.8	52.5
Amorphous/organic carbon content	59.6	77	52.9	66.3	84.6	30.8	61.6	86	47.5

From Table 3-3 it is evident that the quartz, kaolinite, and calcite, which are extraneous minerals, tend to be concentrated in the sink fractions (rock fragments such as sandstone, siltstone, mudstone, and carbonaceous shale). Traces of portlandite are also present in the sink fractions. These rock fragments are reported to be mainly non-reactive during heat treatment and will consequently result in unreactive sink fractions during carbon conversion and are therefore not a preferred feedstock (Matjie *et al.*, 2011).

The percentage mineral distribution of kaolinite, quartz, and the fluxing element-bearing minerals, such as dolomite, pyrite, and calcite, within the density fractions can be observed in Fig. 3-2. Kaolinite and quartz in the rock fragments are concentrated in the sinks A, B, and C, i.e. the higher density fraction, thus associated with excluded minerals and correlates to previous studies on density-separated fractions of South African coal samples (Matjie, 2008). The percentage mineral distribution for the kaolinite and quartz are less than 10% in the float fractions, while the percentage distribution of fluxing element-bearing minerals are extremely low in the float fraction of coal A and significantly higher in coal C float and coal B float fractions (Fig. 3-2).

It is evident that coal C contains significant amounts of fluxing element bearing minerals associated with excluded minerals as well as included minerals in the float fraction, with corresponding low proportions of clay minerals. Coal B on the other hand contains more clay minerals associated with excluded minerals in the sink fraction than fluxing element-bearing minerals. These percentage mineral distribution values across the density-separated fractions of the three feed coals imply that the modes of occurrences of mineral matter are indeed very different. The mineral matter in these three coals is expected to transform and interact with each other differently during the combustion or carbon conversion process (Matjie, 2008; Van Alphen, 2005). During coal utilisation, these fluxing element-bearing minerals in the coal B float and coal C float fractions, may lead to the formation of a melt, i.e. slagging, by interacting with the aluminum silicate.

Subsequently, the ash fusion temperature of these clay minerals present in the coal will be lowered (Matjie *et al.*, 2006). In addition, the abundance of extraneous minerals in the sinks fraction from coals A, B and C (Fig. 2) may contribute significantly to wear on mechanical equipment during coal- or ash-handling operations (Hlatshwayo *et al.*, 2009; Kalmanovitch *et al.*, 1986).

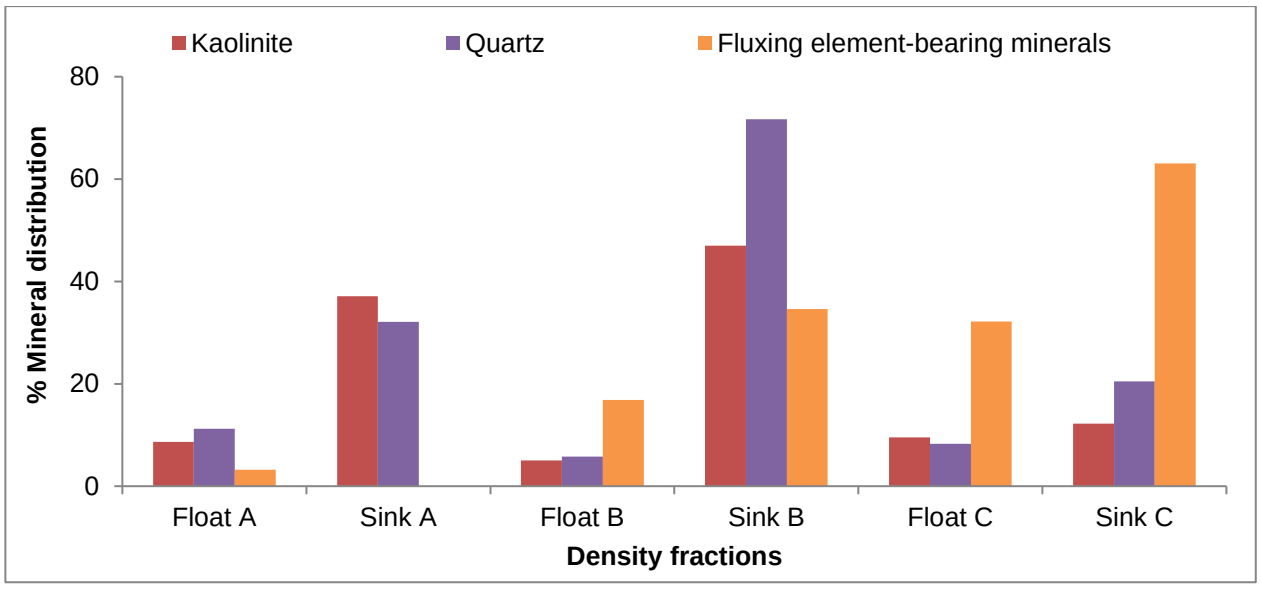

Figure 3-2 **The percentage mineral distribution within the density separated fractions derived from XRD analysis.**

3.3.3 XRF analysis

Inorganic elements present in the coal ashes for the three coals and corresponding density separated fractions are reported as oxides in Table 3-4. Silica (SiO_2) and Alumina (Al_2O_3) are the dominant components in the coal ashes, ranging between 40% and 60% for the silica and 20% to 40% for the alumina. Fe_2O_3, TiO_2, CaO, and MgO are present in relatively low but still notable proportions, while P_2O_5, K_2O and SO_3 are present in significantly low proportions. TiO_2, P_2O_5, CaO, and MgO are more concentrated in the float fractions than in the sink fractions. It has been reported in literature that the higher proportions of TiO_2 in the float fractions correlates with the Ti concentrations present in the vitrinite (Matjie *et al.*, 2016; Van Alphen, 2005).

Higher proportions of silica and alumina are present in the sink fractions, except for coal C sink, which contains lower amounts of alumina than for the float fraction. The XRF results that are reported in Table 3-4 are in good agreement with the XRD results reported in Table 3-3 and Fig. 3-2. This increase in the Si and Al proportions in the sink fractions were also observed in previous studies on South African coal samples (Matjie *et al.*, 2011; Van Dyk *et al.*, 2009).

The percentage element distributions of SiO_2, Al_2O_3 and fluxing elements (Na, Ca, Mg, K, and Fe) can be observed in Fig. 3-3. Considerably high percentage distribution of fluxing elements in comparison to the SiO_2 and Al_2O_3 is evident for all three samples, which is in agreement with the percentage of mineral distributions in Fig. 3-2. Coal A exhibits a higher concentration of fluxing elements in the sink fraction, i.e. associated with excluded minerals, while coal B and coal C show

a higher percentage distribution of fluxing elements in the float fractions, i.e. associated with included minerals. It is proposed that during the carbon conversion process that the fluxing elements (Na, K, Ca, Mg, and Fe) from included fluxing minerals associated with included kaolinite may react with the reactive aluminum silicate (metakaolinite) and consequently contribute to slagging (Matjie, 2008). From the results in Fig. 3-3 it is evident that float A and sink A from feed coal A, float B from feed coal B and float C from feed coal C could exhibit more slagging of mineral matter during coal conversion, due to the higher percentage distribution of fluxing elements from the fluxing minerals that are associated with kaolinite.

Table 3-4 XRF results for the feed coals and the density separated fractions.

	Feed A	Float A	Sink A	Feed B	Float B	Sink B	Feed C	Float C	Sink C
SiO_2	50.7	53.4	54.2	46.5	41.3	51.6	54.3	47.3	58.8
Al_2O_3	28.8	28.1	29.4	36.1	31.9	39.4	27.4	29.9	23.6
Fe_2O_3	3.4	3.7	8.4	4.0	2.8	2.8	4.0	3.2	3.6
TiO_2	2.0	5.0	1.5	2.1	4.0	2.3	1.8	4.3	1.6
P_2O_5	1.5	1.7	0.2	0.2	0.5	0.1	0.7	1.2	0.2
CaO	9.0	6.3	4.1	8.1	17.8	2.7	8.2	10.7	10.5
MgO	3.4	0.6	0.8	1.1	1.0	0.4	2.1	1.5	0.9
Na_2O	0.5	0.0	0.0	0.6	0.0	0.0	0.3	0.1	0.0
K_2O	0.7	1.2	1.0	0.9	0.2	0.5	0.8	0.8	0.6
SO_3	0.0	0.0	0.5	0.3	0.4	0.2	0.5	0.8	0.2

3.3.4 Petrographic analysis

When comparing the petrographic results of the three feed coal samples, summarised in Table 3-5, it is evident that coal A and coal C consist of different macerals content, whereas coal B is more comparable with coal C. Relatively high vitrinite content was observed for coal A feed in comparison with coal B and coal C, however this trend is reversed for the inertinite content, where coal A contained the lowest percentage (40.6%) and coal C the highest percentage inertinite (66.7%). Significant mineral matter content is observed for the feed coal samples ranging from 17.3%, for coal C, to 32.7%, present in coal A. Liptinite contributes less than 5% to the macerals content, which is observed in all three feed coals, as well as in the float and sink fractions. The three feed coal samples can be classified as inertinite-rich, medium rank C bituminous coal and is typical of South African coal samples (Snyman, 1989; Snyman, 1998).

As expected, the vitrinite content is enriched in the float fractions, when compared to the feed coals, and decreased substantially in the sink fractions. These results are in accordance with previous studies on the densities of macerals (Borrego *et al.*, 1997) where it was determined that the densities of the macerals vary from lightest to heaviest in the order: liptinite >vitrinite >inertinite. The inertinite is concentrated in the sink fractions, i.e. the heaviest fraction, while the lighter macerals are concentrated in the less dense float fractions. The mineral matter percentage increased significantly in the sink fractions, thus linking the vitrinite enriched float fractions and the mineral-rich sink fractions.

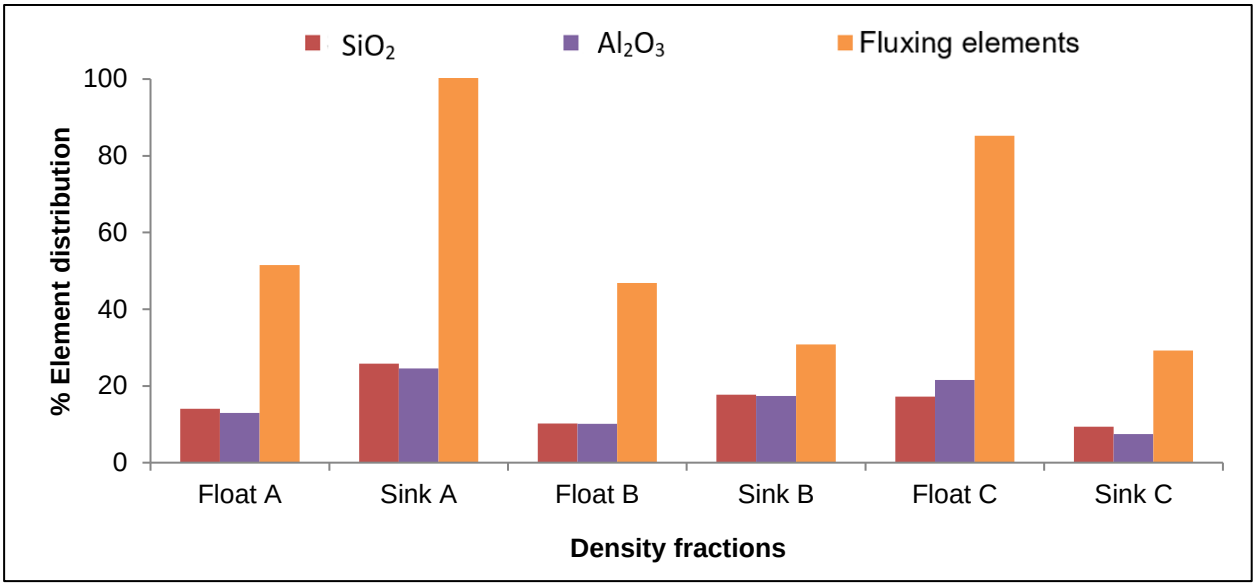

Figure 3-3 The elemental distribution within the density separated fractions derived from XRF analysis

The petrographic properties can be observed in Fig. 3-4, where (i) represents a feed coal (Coal A) with calcite cleats visible within a vitrinite band. The second image (ii) represents a float fraction (Coal A) which containing inertodetrinite, while the third image (iii) shows a sink fraction (Coal A) containing pyrite and carbonate cleats visible. These images were taken with an oil immersion lens under reflected, white light and x500 magnification. From these images, it is evident that the coal samples contained mineral cleats within the coal matrix and this can be liberated during pulverisation.

Comparison between mineral matter values calculated from XRD data, QEMSCAN and petrographic results (Tables 3-3, 3-5 and 3-6) showed similar trends and are in broad agreement in terms of the qualitative results. However, the XRD and QEMSCAN reported similar proportions of mineral matter in the same feed coal samples. The same trends of the proportions of mineral

matter in South African coals were obtained when using a low-temperature asher as previously reported by (Matjie *et al.*, 2016).

Table 3-5 Petrographic results (vol. %).

	Feed A	Float A	Sink A	Feed B	Float B	Sink B	Feed C	Float C	Sink C
Maceral group (mineral matter included)									
Vitrinite (%)	22.3	74.3	4.8	10.5	41.8	4.3	14.3	38.6	4.0
Inertinite (%)	40.6	19.1	23.7	59.5	48.5	14.7	66.7	53.3	30.8
Liptinite (%)	4.4	4.1	1.0	1.2	4.4	0.2	1.8	3.7	0.0
Mineral matter (%)	32.7	2.5	70.5	28.8	5.3	80.8	17.3	4.3	65.2
Maceral group (mineral matter free)									
Vitrinite (%)	33.1	76.2	16.3	14.8	44.1	22.4	17.3	40.3	11.5
Inertinite (%)	60.4	19.6	80.3	83.6	51.3	76.5	80.6	55.8	88.5
Liptinite (%)	6.5	4.2	3.4	1.6	4.6	1.0	2.2	3.9	0.0

Variations in the results can be attributed to the differences between analytical techniques and sampling location as well as the fact that XRD data reflect mass fractions as percentages, while petrographic data are reported as volume percentages. QEMSCAN data of minerals and mineral matter in the selected particles in the coals and coal ash are based on the calculations and conversions of the elemental proportions. QEMSCAN determined high proportions of mineral matter in the feed coals and sink fractions of these coals. Whilst low proportions of mineral matter are reported in the float fractions of the feed coals (Table 3-6). This could be attributed to the high content of the organic carbon present in the float fractions. If this equipment can be used effectively as complementary techniques, useful data of the sampled analysed can be generated.

Table 3-6 Relative proportion of mineral matter determined by different analytical techniques.

Mineral matter	Coal A feed	Coal A float	Coal A sink	Coal B feed	Coal B float	Coal B sink	Coal C feed	Coal C float	Coal C sink
XRD	39.9	22.9	47.2	33.6	15.3	69.2	35.5	13.8	52.5
Petrography	32.7	2.5	70.5	28.8	5.3	80.8	17.3	4.3	65.2
QEMSCAN	40.2	1.9	76.5	40.4	4.2	82.0	30.3	3.8	80.0

3.3.5 Electron microprobe analysis

The electron microprobe (EMP) analysis allows for the determination of concentrations of organically associated inorganic elements within individual macerals. The EMP results are presented in Table 3-7. They may assist in the investigation of mineral matter interactions which are responsible for the slagging and fouling problems during coal combustion and carbon conversion processes.

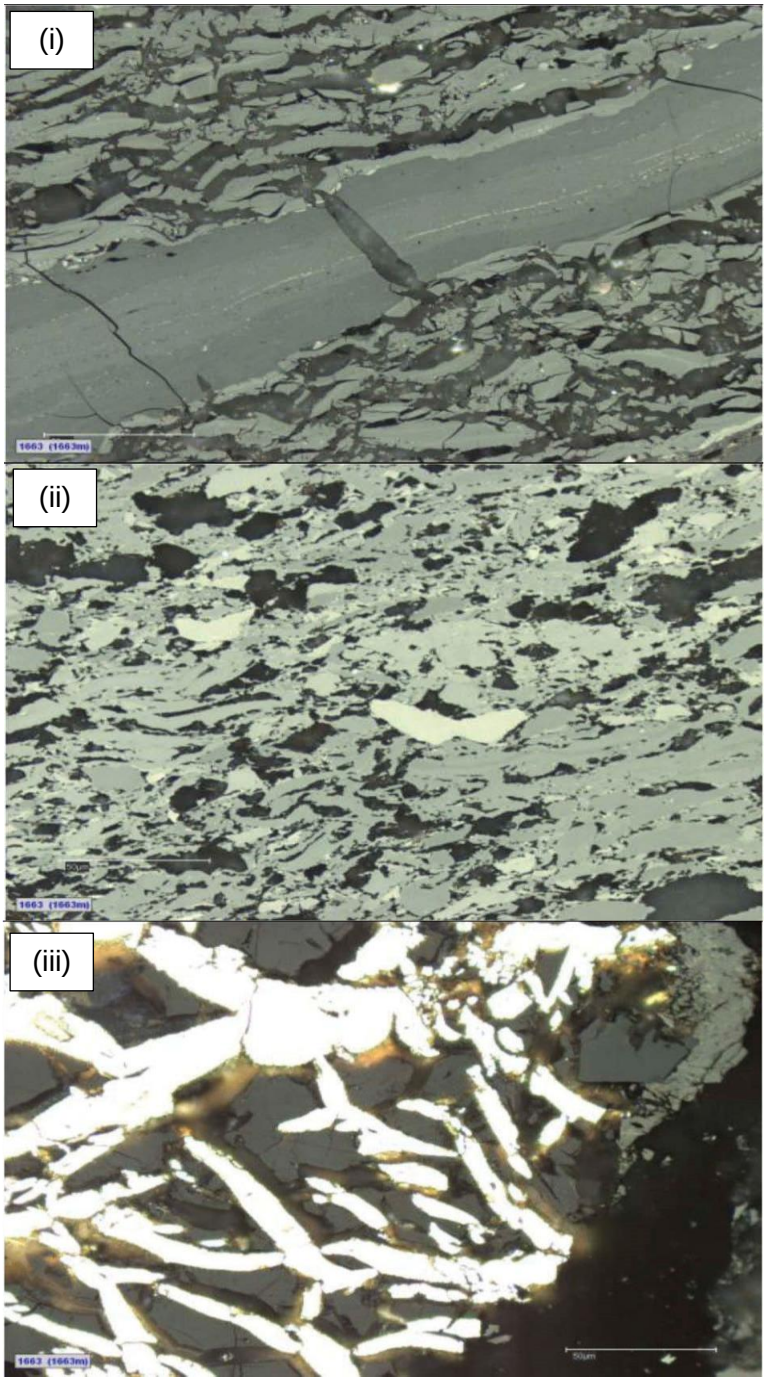

Figure 3-4 **Photographs showing the petrographic properties of (i) Feed coal, (ii) Float fraction, and (iii) Sink fraction, produced from Coal A. The scale bar represents 50 microns.**

Table 3-7 Electron microprobe results for the feed coals as well as the density separated fractions.

Percentage %		C	N	O	Al	Ca	Fe	K	Mg	Na	S	Si	Ti	Total
Coal A feed	V	76.5	3.5	18.0	0.2	0.0	0.2	0.0	0.0	0.0	0.8	0.1	0.1	99.30
	I	81.4	2.4	14.2	0.1	0.0	0.3	0.0	0.0	0.0	0.5	0.1	0.0	99.12
Coal A float	V	78.4	2.4	14.4	0.1	0.0	0.1	0.0	0.0	0.0	0.8	0.1	0.2	96.36
	I	83.4	2.9	9.6	0.1	0.0	0.1	0.0	0.0	0.0	0.5	0.3	0.0	96.94
	L	77.8	2.3	17.9	0.3	0.1	0.5	0.1	0.0	0.0	1.1	0.6	0.1	100.66
Coal A sink	V	75.2	3.1	18.2	0.1	0.0	0.2	0.0	0.0	0.0	0.7	0.1	0.5	98.03
	I	80.4	2.8	13.7	0.3	0.0	0.2	0.0	0.0	0.0	0.5	0.2	0.0	98.17
Coal B feed	V	73.0	2.7	20.8	0.3	0.0	0.1	0.0	0.0	0.1	0.7	0.2	0.7	98.38
	I	80.5	2.8	12.6	0.2	0.1	0.1	0.0	0.0	0.1	0.2	0.2	0.1	96.98
	L	77.6	2.6	17.2	0.0	0.0	0.2	0.0	0.0	0.0	1.0	0.0	0.0	98.75
Coal B float	V	71.9	2.8	21.3	0.3	0.1	0.1	0.0	0.0	0.1	0.4	0.2	0.6	97.61
	I	81.6	2.9	10.9	0.1	0.0	0.1	0.0	0.0	0.0	0.3	0.1	0.0	96.05
	L	70.2	0.8	19.6	1.7	0.0	0.0	0.0	0.0	0.2	0.7	1.0	0.3	94.56
Coal B sink	V	73.4	2.4	18.7	0.1	0.1	0.1	0.0	0.0	0.1	0.5	0.0	0.4	95.84
	I	78.9	3.4	12.4	0.6	0.0	0.1	0.0	0.0	0.1	0.2	0.6	0.3	96.59
Coal C feed	V	71.3	3.8	21.8	0.3	0.1	0.2	0.0	0.0	0.1	0.5	0.1	0.3	98.57
	I	82.4	3.3	11.2	0.2	0.2	0.2	0.0	0.0	0.1	0.3	0.2	0.0	98.09
Coal C float	V	70.5	4.0	22.5	0.2	0.1	0.2	0.0	0.0	0.1	0.5	0.1	0.5	98.65
	I	81.4	3.8	11.9	0.0	0.1	0.3	0.0	0.0	0.0	0.3	0.0	0.0	97.89
Coal C sink	I	78.5	2.3	13.5	0.2	0.1	0.2	0.0	0.0	0.1	0.3	0.2	0.0	95.44

V: Vitrinite, I: Inertinite, L: Liptinite

Photomicrographs prepared for EMP analysis can be observed in Fig. 3-5. These were taken under x100 magnification with no oil and under a white reflected light. A large quartz particle was inserted in the middle as a reference point.

(i)

(ii)

(iii)

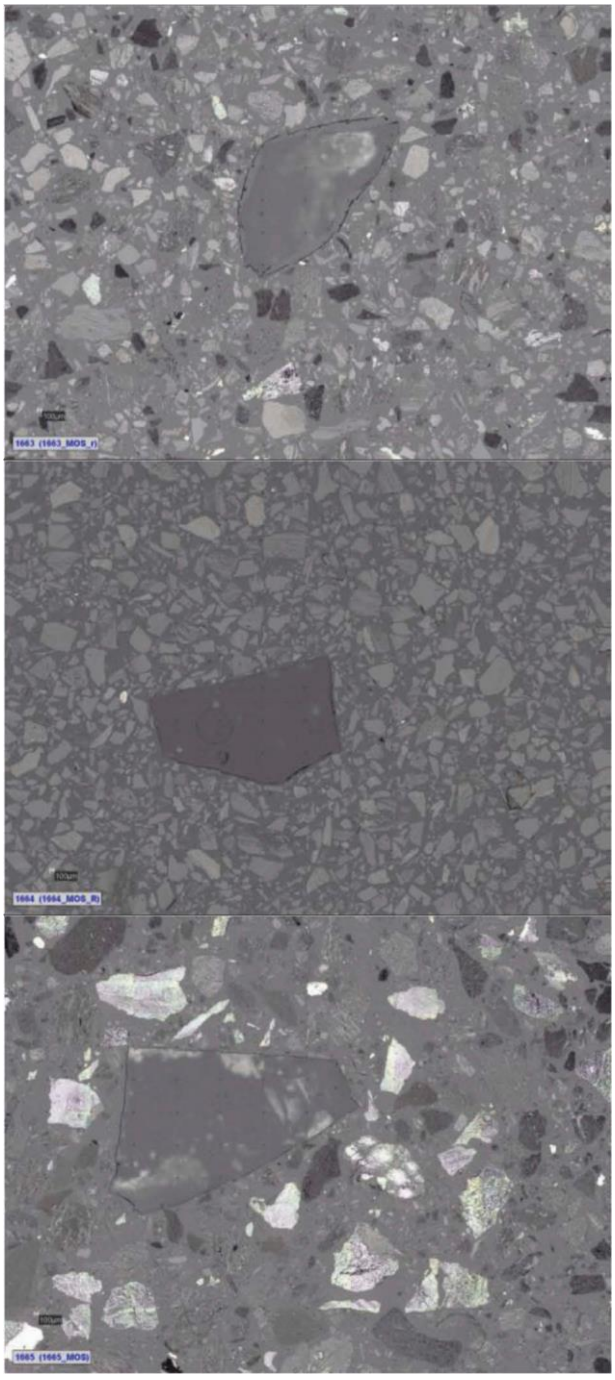

Figure 3-5 Photographs prepared for EMP analysis, (i) Feed coal, (ii) float fraction, (iii) sink fraction, produced from Coal A. Scale bar represents 50 micron.

The carbon proportions in the vitrinite macerals vary from 70% to 78% in the coal samples probed, while inertinite macerals have higher carbon percentages, ranging from 78% to 83%. Vitrinite macerals contained higher proportions of oxygen, which ranged from 14% to 22.5%, while a decrease in the oxygen percentages was observed in the inertinite macerals (9% −14%). These EMP results for the coal samples analysed in this study are consistent with observations made in other studies (Mastalerz & Gurba, 2001; Matjie *et al.*, 2016; Ward & Gurba, 1998; Ward *et al.*, 2008). In almost all cases the concentrations of these elements in the vitrinite macerals are approximately double those in the inertinite components within the same sample.

The organic nitrogen proportions showed similar percentages for the inertinite and vitrinite macerals with a less distinct relationship, although a significantly low proportion of organic nitrogen was observed for the liptinite maceral within the Coal B float sample. A low proportion of organic nitrogen in the liptinite group could be attributed to the high aliphatic hydrocarbons and low aromatic hydrocarbons which are associated with the organic nitrogen (Hackley & Cardott, 2016).

Organic sulphur percentages within the vitrinite macerals ranged from 0.4% to 0.8% and showed a decrease in the inertinite macerals, which contained organic sulphur percentages of 0.2–0.5%. The absence of a high concentration of iron in these coal macerals confirms that the sulphur is organic species in nature and, that the higher organic sulphur concentrations do not include the content of sulphur from pyrite in the coal macerals concerned.

Low percentages of Al, Si, Ca, Fe, and Ti are observed (i.e. <0.05%), for the vitrinite as well as the inertinite macerals, although not for all the samples investigated. The Al and Si proportions are similar within the same coal sample and are an indication of submicron included kaolinite present in the coal samples. However, an increase in the Si percentage was observed for inertinite within the coal A float fraction and can be assigned to include submicron quartz or organic Si. A higher percentage of Ti was observed in the vitrinite macerals, compared to the inertinite macerals. The Fe percentage in the liptinite maceral (coal A float) was significantly higher, and is in agreement with above-mentioned results where coal A float showed high concentrations of Fe present.

The evaluated coal samples did not contain significant proportions of organic potassium, which suggest that the potassium, mainly associated with clay minerals, and does not occur as organic potassium within the coal samples. Similar trends were observed for EMP analysis of coal samples by various authors (Li *et al.*, 2010; Matjie *et al.*, 2016; Ward *et al.*, 2008). Qualification and quantification of such elements in the macerals in the feed coals, through either electron microprobe analysis or more conventional studies, may assist to minimize the potential for

corrosion, slagging, and fouling in operating combustion and gasification plants (Creelman *et al.*, 2013). The emission of gases and/or fine particulates with the potential for adverse environmental impacts may also be avoided and minimalised.

3.3.7 QEMSCAN and Reflux Classification Results

Figure 3-6 contains the false-colour images produced from QEMSCAN results for the feed, float and sink fractions produced from Coal A. These are representative for all three coal samples. The feed coal (i) is a mixture of the float and the sink fractions with included minerals as well as excluded minerals present. In this case, the float fractions (ii) were reflux classified prior to QEMSCAN analysis. As a result, the vitrinite and included minerals are successfully concentrated in the float fraction because the density separation using float-sink method was followed by reflux classification cleaner step after size-reduction. Excluded minerals, i.e. the rock fragments are present in the sink fractions as observed in Fig. 3-6 (iii).

The modal proportion of minerals in the samples can be observed in Fig. 3-7 for; i) Feed coals, ii) Coal A, iii) Coal B and iv) Coal C. Similar trends are observed in the modal proportions for the feed coals B and C, while coal A feed exhibited a different modal proportion of minerals. Coal A was more enriched in vitrinite with less fusinite and reactive semi fusinite compared to coals B and C, while significantly less clay minerals were also observed in coal A. The modal proportion of minerals in the density fractions (ii to iv) are in accordance with the feed coal analysis. High proportions of clay minerals were observed in the sink fractions while the vitrinite reported to the float fraction as expected (Koekemoer, 2010; Matjie *et al.*, 2011; Matjie *et al.*, 2008).

Microlithotype classification was done based on the mineral concentrations and proportions within one particle and can be observed in Fig. 3-8; i) Feed coals, ii) Coal A, iii) Coal B and iv) Coal C. Microlithotypes are the microscopic bands of mineral matter and macerals within the coal sample (Falcon & Falcon, 1987; Falcon & Snyman, 1986).

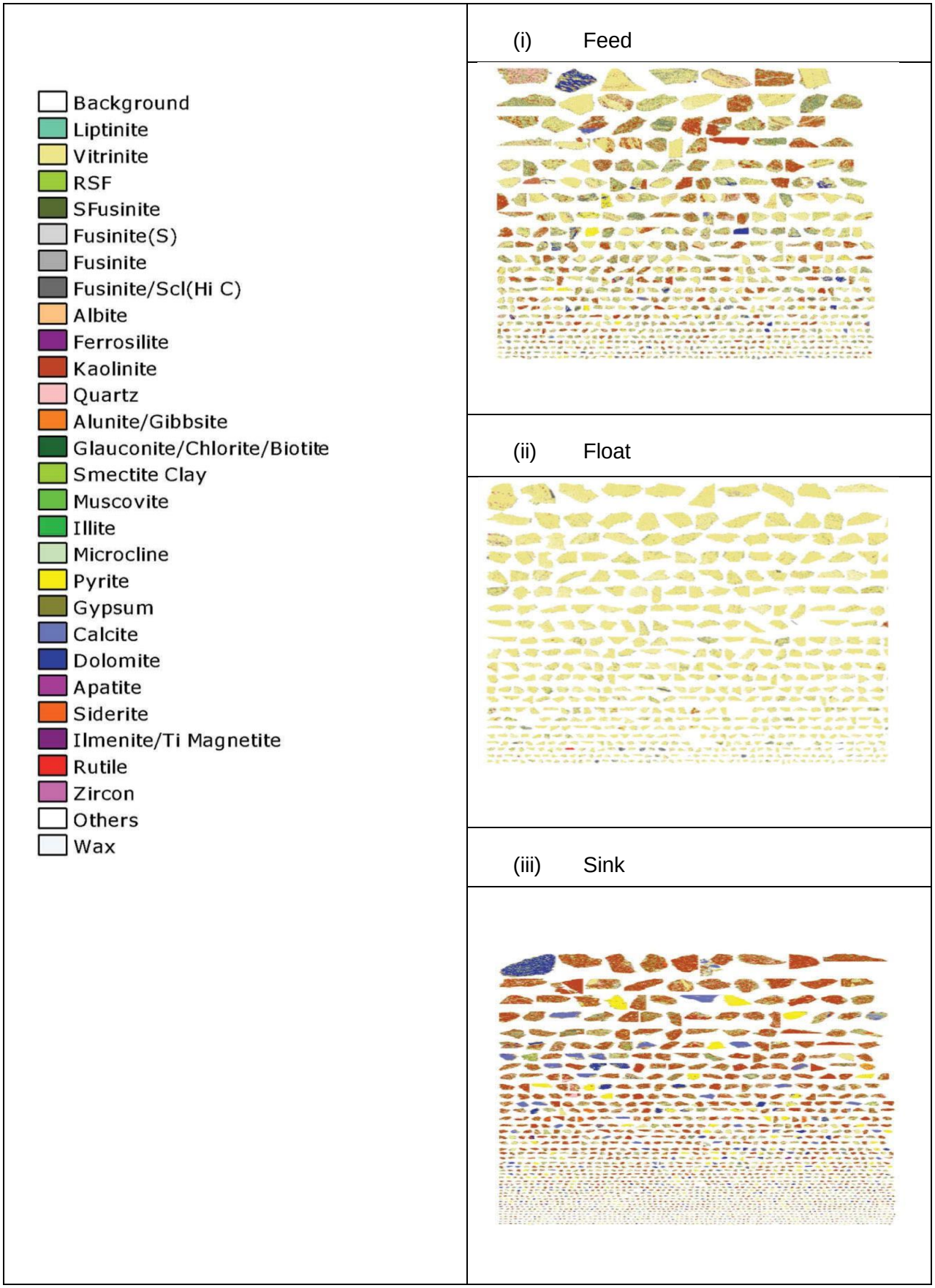

Figure 3-6 False colour QEMSCAN images for (i) Feed coal, (ii) Float fraction and (iii) Sink fractions, produced from Coal A.

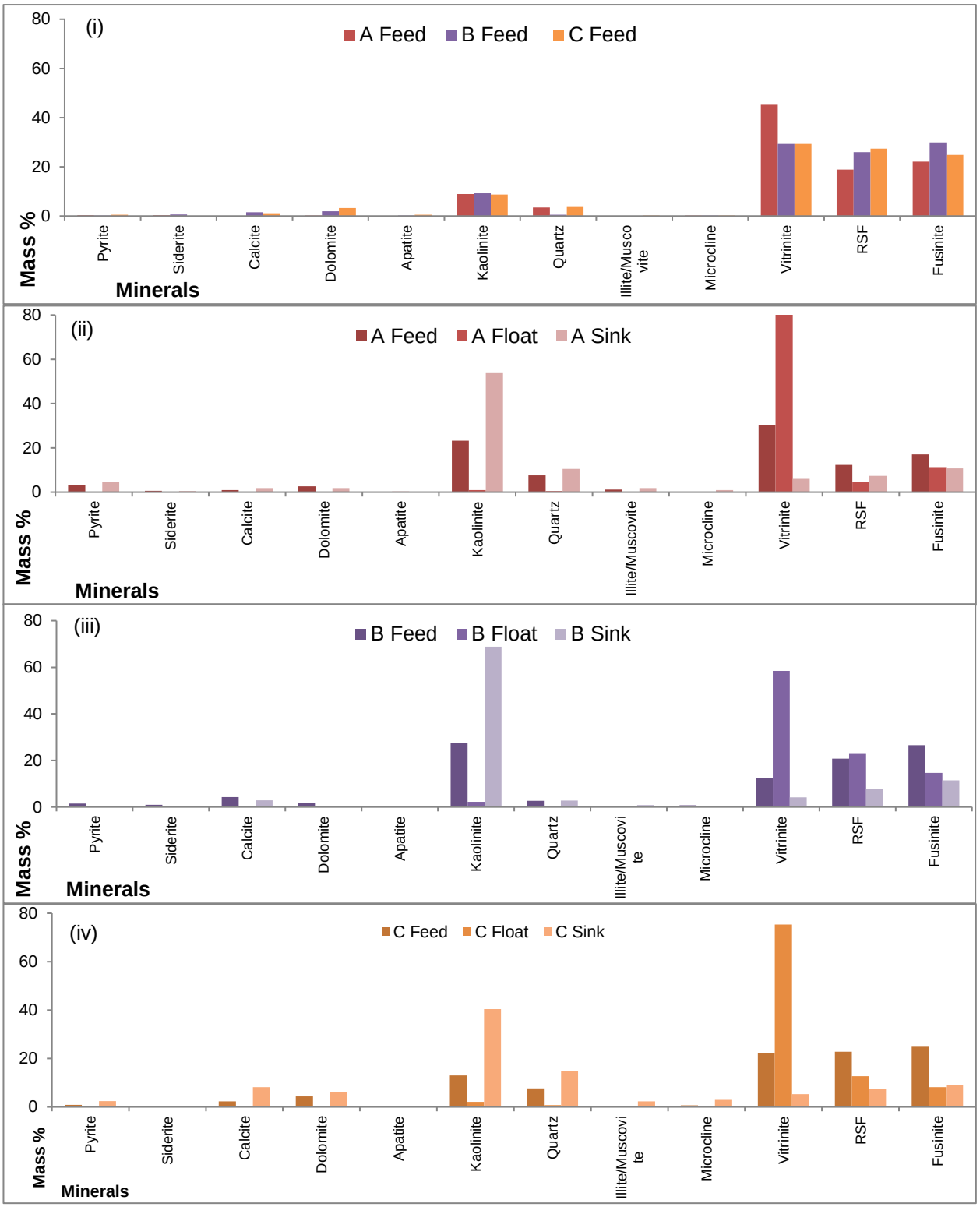

(i) Three different feed coals; (ii) Coal A feed, float and sink; (iii) Coal B feed, float and sink; (iv) Coal C feed, float and sink

Figure 3-7 Modal proportions of minerals and macerals in the feeds, floats and sinks

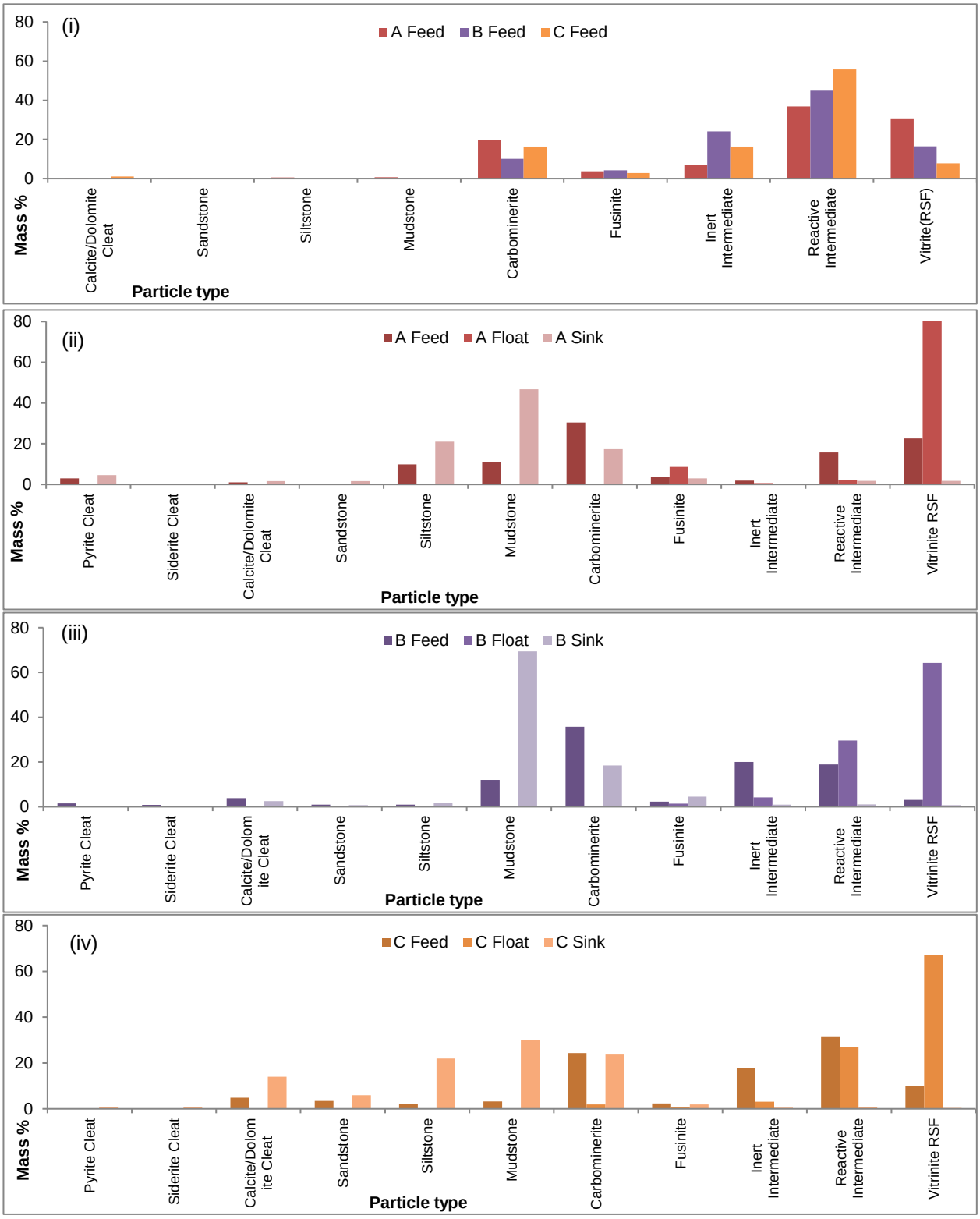

Figure 3-8 **Microlithotype characterisation of i) Three different feed coals, ii) Coal A feed, float and sink iii) Coal B feed, float and sink and iv) Coal C feed, float, and sink.**

As expected, and in accordance with previous results, the coal A float fraction consisted of a significantly high proportion of vitrinite (88%). Fusinite and reactive intermediate are also present in lower concentrations (<10%).

The sink fractions are high in mudstone, siltstone, and pyrite concentrations, as expected since it is related to the kaolinite and quartz contents. Lower concentrations of carbominerite, fusinite, inert intermediate, reactive intermediate, as well as vitrinite are observed for the sink fractions in comparison to the feed coal. The carbominerite group refers to mineral-maceral associations and are concentrated in the denser sink fractions. Reactive intermediate (referring to maceral-maceral associations) are predominantly present in the feed coal and float fractions of coals B and C, and not present in the sink fractions. An increase in mineral groups can be observed for the dense sink fractions, while macerals and intermediate groups are concentrated in the lighter float fractions, thus confirming the effectiveness of the separation of organic matter and minerals through float-sink techniques (Koekemoer, 2010).

In Fig. 3-9, the effect of the reflux classifier can be observed where float fractions, produced via the float-sink method, were subjected to reflux classification. It is evident that the float sample after reflux classification contained approximately 10% more vitrinite with no or less included clay minerals, while small proportions of included clay minerals were still present in the float sample before reflux classification. Reflux classification concentrated the floats from the float-sink experiments successfully by eliminating the included rock fragments and included clay cleats which were present in the float fraction due to liberation of minerals during pulverisation.

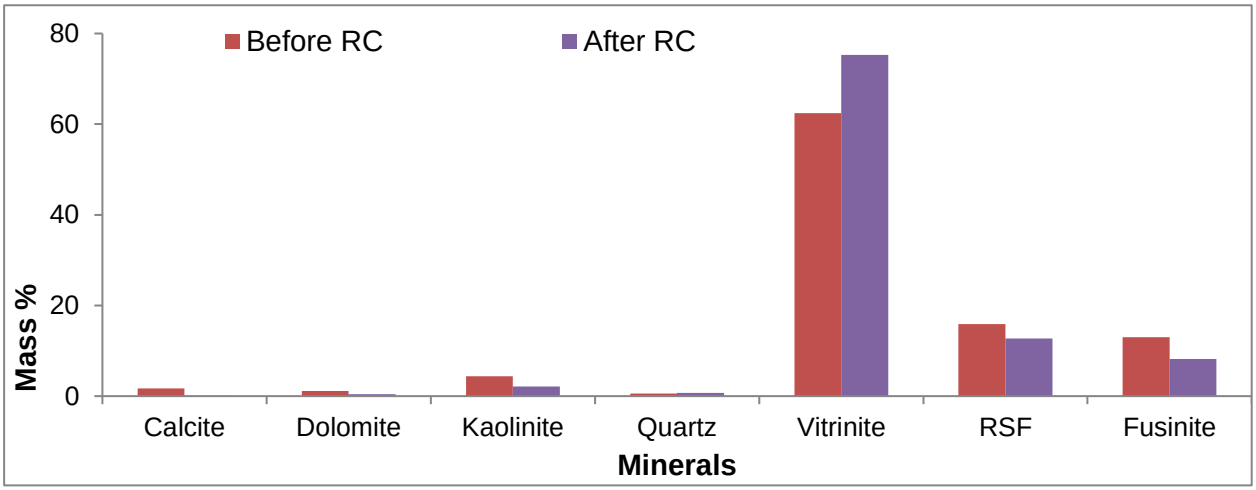

Figure 3-9 The effect of reflux classification based on modal proportions.

The difference between QEMSCAN data from the two-density separation methods used in this study is illustrated in Fig. 3-10. For this comparison a feed coal sample was subjected to the traditional float-sink method using dense medium, while another feed coal sample was subjected to reflux classification in order to produce a float sample <1.5 g/cm^3. In order to produce a clean float fraction with mainly included minerals, i.e. high vitrinite content and no or less clay minerals present, the feed coal must be subjected to the float-sink method, followed by reflux classification.

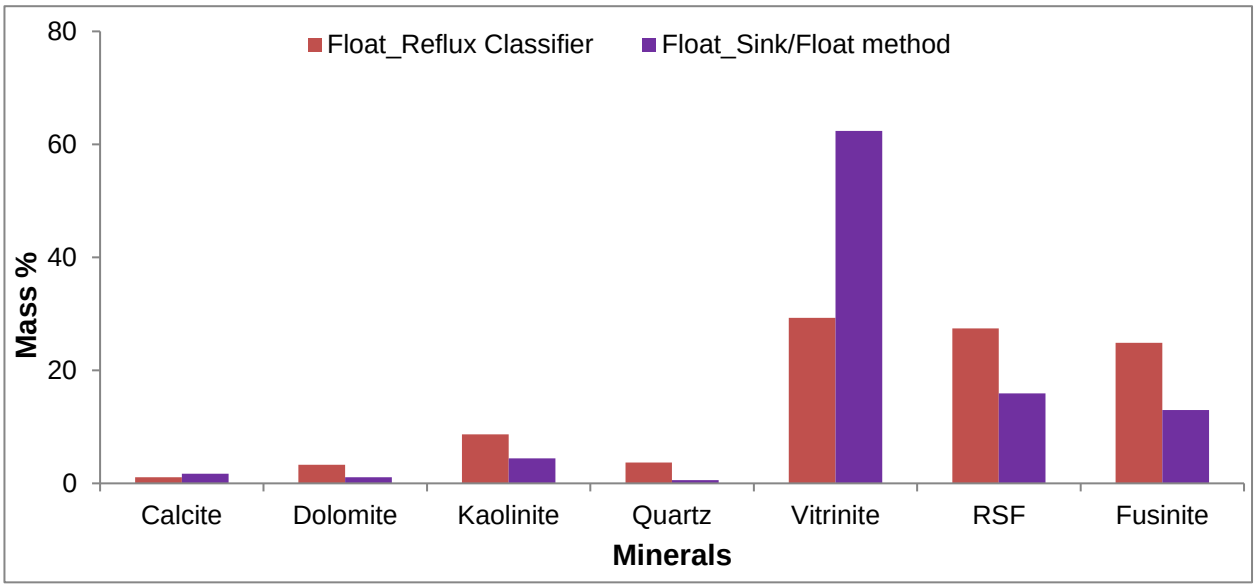

Figure 3-10 Comparison of QEMSCAN data obtained from two beneficiation techniques, i.e. density separated separation through sink-float method and reflux classification.

Comparison of QEMSCAN and XRD results indicated similar trends, especially qualitative rather than quantitative, although it will be difficult to achieve full agreement between the data due to differences in analytical techniques. The XRD analysis is used to qualitatively and quantitatively detect coarse crystalline minerals in a sample, while the concentration of the total proportion of the elements present in the submicron and coarse minerals (i.e. within included, excluded as well as organically associated inorganic elements) are determined by using QEMSCAN (Ayling *et al.*, 2012). Similar trends of the kaolinite associations within the different density fractions can be observed when comparing the QEMSCAN analysis results with the XRD results, where the proportion of kaolinite decreased in the float fractions and increased significantly in the sink fractions. QEMSCAN, on the one hand, showed higher concentrations of kaolinite measured for the feed as well as the sink samples compared to the XRD results, although significantly lower proportions of kaolinite were measured in the float fractions using QEMSCAN. XRD measurements for calcite were significantly higher than depicted in the QEMSCAN results, and a similar trend was observed for the XRD results of dolomite in Coal A. However, the QEMSCAN results for dolomite concentrations in coal B and C were significantly higher than the XRD results.

It has been explained by (Matjie *et al.*, 2011) that the irregularities in the detection of dolomite and calcite between QEMSCAN and XRD may be due to the difficulty in distinguishing the dolomite from calcite within cleat infillings. With regards to the proportion of quartz measured, QEMSCAN did not detect any quartz in the float fraction; this is due to the reflux classification of the float fractions prior to QEMSCAN analysis. XRD detected significantly higher concentrations of quartz from the float-sink experiments in the sink fractions compared to the QEMSCAN analysis.

In conclusion, XRD is a bulk technique and QEMSCAN is a microscopic technique. Useful data that was generated from these two complementary techniques can be used effectively during a method of comparative study by the implementation of these data in the coal combustion and carbon conversion processes, in order to minimize or avoid slagging, fouling, abrasion, and pollution problems. Based on the mineralogical and chemical results obtained in this study, slightly higher slagging and abrasion tendencies were observed for Coal A in comparison with the other coal and density separated fraction samples that have very low slagging tendencies as well as very low abrasion tendencies. Analytical results obtained from this study could be used in the blending strategies of the float and sink fractions in order to prepare feed coal which will be suitable for the utilisation in the coal combustion and carbon conversion processes.

3.3.8 Predictive Slagging Behaviour

The empirical indices used to predict slagging propensities and behaviour are summarised in Table 3-8. These empirical indices are based on the total elements in the ash of the coal samples that were determined by XRF. As expected, these indices do not predict any slagging (low slagging) behaviour for South African coals. Although the slag and clinker formation in South African boilers are formed as a result of the included mineral matter, i.e. mineral-mineral and mineral-maceral interactions at elevated temperatures. These empirical indices, however, are based on the total basic and acidic oxides in both included and excluded minerals and thus will not indicate the initial temperature for slagging. Severe slagging coals must have a slagging factor of >2.6, silica percentage of between 50 and 65, and a base to acid ratio of <0.4 or >0.7. Due to the high proportions of total acidic elements in South African coal ash samples and low proportions of total basic elements, these slagging indices will not predict the slagging behaviour for South African coals accurately.

Table 3-8 Empirical indices predicting slagging behaviour based on ash analysis.

	Feed A	Float A	Sink A	Feed B	Float B	Sink B	Feed C	Float C	Sink C
Slagging factor (F_s) (B/A_R x %S)	0.42	0.13	0.82	0.09	0.17	0.04	0.13	0.12	0.36
Slagging tendencies	L.S	L.S	L.S	L.S	L.S	L.S	L.S	L.S	L.S
Base – Acid Ratio (B/A_R) (Fe_2O_3 + CaO + MgO + Na_2O + K_2O)/(SiO_2 + Al_2O_3 + TiO_2)	0.20	0.14	0.17	0.17	0.28	0.07	0.18	0.20	0.19
Slagging tendencies	L.S	L.S	L.S	L.S	L.S	L.S	L.S	L.S	L.S
Silica percentage (Si_R) (SiO_2 x 100)/(SiO_2+Fe_2O_3+CaO+MgO)	76.2	83.5	80.3	77.9	65.7	89.7	79.2	75.4	79.7
Slagging tendencies	L.S	L.S	L.S	L.S	L.S	L.S	L.S	L.S	L.S
Silica to alumina ratio (Si/A_R) (SiO_2/Al_2O_3)	1.76	1.90	1.85	1.29	1.29	1.31	1.98	1.58	2.49
Slagging tendencies	M.S	M.S	M.S	M.S	M.S	M.S	M.S	M.S	M.S
Iron to calcium ratio (Fe/Ca_R) (Fe_2O_3/CaO)	0.37	0.58	2.03	0.5	0.16	1.04	0.49	0.30	0.34
Slagging tendencies	H.S	H.S	H.S	H.S	L.S	H.S	H.S	H.S	H.S

Note: L.S; Low Slagging. H.S; High Slagging

3.4 Conclusions

Physical methods including float-sink washability and reflux classifier were used in this study to effectively separate maceral-rich and mineral-rich fractions from the three South African feed coals. Advanced analytical techniques such as QEMSCAN, light-element electron microprobe analysis and X-ray diffraction have been combined with conventional methods (proximate and ultimate analysis, ash analysis, and petrographic studies) to evaluate the mineral and organic matter in feed coals from South African coal mines and their density separated coal fractions used as feedstocks for combustion and carbon conversion processes.

From the mineralogical and chemical results obtained, the main differences between the three feed coals are related to the mode of occurrence of mineral matter. From these characteristic results, it is evident that mineralogical and chemical results differ significantly between the high and low-density coal fractions, thus emphasizing the importance to incorporate the mineralogical

and chemical results for the density fractions when applying a model on ash-related problems such as slagging and fouling.

From the QEMSCAN results, it was evident that the reflux classification successfully eliminated liberated materials, which formed during pulverisation, in order to produce a high maceral-rich float fraction (98% macerals). This implies that density separation via the float-sink method followed by reflux classification successfully reduced the mineral matter content of the float fractions, while concentrating the macerals, volatile matter, fixed carbon, and nitrogen contents in the lower density separated fractions. In accordance with these results, it is evident from QEMSCAN, petrographic and XRD results, that the float fractions was maceral-rich due to the high amorphous/organic carbon content in the float fractions. The fluxing elements are also concentrated in the float fractions of coal B and coal C, except for coal A, which exhibited a higher fluxing (Fe) element association with pyrite in the mineral-rich sink fraction.

Higher percentages of kaolinite, pyrite, dolomite/calcite, and quartz distributions, as well as high proportions of silicon (reported as elemental oxide; SiO_2) and aluminum as (Al_2O_3) are reported in the sink fractions (rock fragments) of the feed coals. The sink fractions of feed coal A and feed coal C contained higher proportions of hard minerals such as quartz, pyrite, and microcline in comparison to the sink fraction C, and may be responsible for abrasion of plant equipment during utilisation.

Included kaolinite and included submicron quartz particles that are associated with the fluxing included dolomite, calcite and pyrite minerals within the coal macerals in the float fractions of coals B and coal C, will cause severe slagging when utilised alone during coal combustion and carbon conversion processes and is not recommended. However, a blend between the float and sink fractions from these feed coals, based upon the mineralogical, chemical, and petrographic results reported in this study, may be an optimal feedstock to the combustion process.

Light-element electron microprobe techniques results (carbon, oxygen, nitrogen, and organic sulphur contents) for the macerals contained in the feed coals are in good agreement with those obtained when using the conventional analysis (ultimate analysis). The vitrinite in the feed coals and density separated fractions contained less carbon and more oxygen, and have significantly higher concentrations of organic nitrogen and organic sulphur, than the inertinite macerals in the same coal samples. The electron microprobe detected minor proportions of organically associated inorganic elements, including Ca, Al, Si, Mg, and Ti in the coal macerals. The presence of minor non-mineral Ca and Mg in the coal samples may interact with metakaolinite from the transformation of submicron included kaolinite to form clinkers and slags in the plant equipment at elevated temperatures, which are associated with coal combustion and carbon

conversion processes. The interaction of pyrite, kaolinite, and organic sulphur in the coal macerals at elevated temperatures may also be responsible for the evolution of corrosive gases (hydrogen sulfide and sulphur oxides), the formation of ultrafine ash particles during the coal combustion and carbon conversion processes.

An integration of these different analytical techniques during the characterisations of the coal samples produced from this investigation permits better determination of the concentrations of included fluxing minerals (pyrite, dolomite, and calcite), included submicron kaolinite, microlithotypes, and organically associated inorganic elements. These fluxing cleat minerals, as well as organically associated inorganic elements found in the coal samples appear to be responsible for clinkers and slags formation, as well as volatilisation of inorganic elements and sulphur emissions associated with these and other activities.

Based on the slagging indices reported in Table 3-8, the overall predictions for South African coals do not exhibit slagging behaviour, or very low slagging behaviour. However, there are ash deposition and slag formation problems in South African boilers which can be explained by investigating the included and excluded mineral matter interactions during coal utilisation. An alternative method for the prediction of slagging behaviour must be investigated, which includes the mineral matter as well as the mode of occurrence of minerals, in order to predict the slagging behaviour of South African coals.

Any opinion, finding or conclusion or recommendation expressed in this material is that of the authors and the NRF does not accept any liability in this regard. Belinda Venter at the North West University, Department of Geology, Prof Nikki Wagner and Dr. Christian Reinke at the University of Johannesburg, Department of Geology, Shinelka Singh at Eskom and Vincent Dube at SABS Secunda, are thanked for assistance with different aspects of the analytical program. The work presented in this paper is based on the research financially supported by the South African Research Chairs Initiative of the Department of Science and Technology (DST) and National Research Foundation (NRF) of South Africa (Coal Research Chair Grant Nos. 86880, UID85643, UID85632). The authors would also like to thank Sasol for their financial contributions in order to complete this study.

Chapter References

Ayling, B., Rose, P., Petty, S., Zemach, E. & Drakos, P. 2012. QEMSCAN (Quantitative evaluation of minerals by scanning electron microscopy): capability and application to fracture characterization in geothermal systems. (*In*. Thirthy-Seventh Workshop on Geotherm Reservoir Engineering organised by Stanford University, Stanford, California.

Barroso, J., Ballester, J. & Pina, A. 2007. Study of coal ash deposition in an entrained flow reactor: Assesment of traditional and alternative slagging indices. *Fuel Processing Technology*, 88:865-876.

Benfell, K.E., Liu, G., Roberts, D.G., Harris, D.J., Lucas, J.A., Bailey, J.G. & Wall, T. 2000. Modeling char combustion: The influence of parent coal petrography and pyrolysis pressure on the structure and intrinsic reactivity of its char. (*In*. Combustion Institute organised by. p. 2233-2241).

Borrego, A.G., Alvarez, D. & Menendez, R. 1997. Effects of inertinite content in coal on char structure and combustion. *Energy Fuels*, 43:702-761.

Boycott, A. 1920. Sedimentation of blood corpuscles. *Nature*, 104(2621):532-532.

Buhre, B.J.P., Hinkley, J.T., Gupta, R.P., Nelson, P.F. & Wall, T.F. 2006. Fine ash formation during combustion of pulverised coal-coal property impacts. F*uel*, 85:185-193.

Campbell, Q.P., Le Roux, M. & Smith, I.G.T. 2015. Water-only laboratory coal fractionation using the reflux classifier. *Minerals Engineering*, 83:59-63.

Chinchón, J.S., Vázquez, E., Alastuey, A. & López-Soler, A. 1993. X-ray diffraction analysis of oxidizable sulphides in aggregates used in concrete. *Materials and Structures*, 26(1):24-29.

Creelman, R.A., Agron-Olshina, N. & Gottlieb, P. 1993. The characterisation of coal and the products of coal combustion using QEM*SEM, Final Report, . CSIRO Division of Mineral and Process Engineering, Clayton, Victoria, Australia.

Creelman, R.A., Ward, C.R., Schumacher, G. & Juniper, L. 2013. Relation between coal mineral matter and deposit mineralogy in pulverized fuel furnaces. *Energy Fuels*, 27:5714-5724.

Degereji, M.U., Ingham, D.B., Ma, L., Pourkashanian, M. & Williams, A. 2012. Numerical assessment of coals/blends slagging potential in pulverized coal boilers. *Fuel*, 102:345-353.

Falcon, L.M. & Falcon, R.M.S. 1987. The petrographic composition of Southern African coals in relation to friability, hardness, and abrasive indices. *Journal of Southern African Institution of Mineral and Metallurgy*, 87(10):323-336.

Falcon, R.M.S. & Snyman, C.P. 1986. An introduction to coal petrography: Atlas of petrographic constituents in the bituminous coals of Southern Africa. Johannesburg, RSA: The Geological Society of South Africa.

Galbreath, K., Zygarlicke, C., Casuccio, G., Moore, T., Gottlieb, P., Agron-Olshina, N., Huffman, G., Shah, A., Yang, N., Vleeskens, J. & Hamburg, G. 1996. Collaborative study of quantitative coal mineral analysis using computer-controlled scanning electron microscopy. *Fuel*, 75(4):424-430.

Gottlieb, P., Agron-Olshina, N., Sutherland, D.N., Ho-Tun, E. & Creelman, R.A. 1990. Characterisation of mineral matter in coal and the products of coal combustion, Final Report. CSIRO Division of Mineral and Process Engineering.

Hackley, P.C. & Cardott, B.J. 2016. Application of organic petrography in North American shale petroleum systems: A review. *International Journal of Coal Geology*, 163:8-51.

Harvey, R.D. & Ruch, R.R. 1986. Mineral matter in Illinois and other US coals. *(In* Vorres, K.S., *ed.* Mineral matter in Coal Ash and Coal. Washington, D.C.: American Chemical Society Symposium Series. p. 10-40).

Hlatshwayo, T.B., Matjie, R.H., Li, Z. & Ward, C.R. 2009. Mineralogical Characterization of Sasol Feed Coals and Corresponding Gasification Ash Constituents. *Energy & Fuels*, 23(6):2867-2873.

ISO7404-2. 1985. ISO 7404-2 International Standards Organisation: Standards South Africa.

ISO7404-4. 1985. ISO 7404-4 International Standards Organisation: Standards South Africa.

Kalmanovitch, D.P., Sanyal, A. & Williamson, J. 1986. Slagging in boiler furnaces: A prediction technique based on high temperature phase equilibria. *Inst. Energy*, 58:120-123.

Koekemoer, A.F. 2010. The influence of minerals content and petrographic composition on the gasification of inertinite rich high ash coal. Potchefstroom, South Africa: North-West University.

Lawrence, A., Kumar, R., Nandakumar, K. & Narayanan, K. 2008. A Novel tool for assessing slagging propensity of coals in PF boilers. *Fuel*, 87:947-950.

Li, Z., Ward, C.R. & Gurba, L.W. 2010. Occurrence of non-mineral inorganic elements in macerals of low-rank coals. *International Journal of Coal Geology*, 81:242-250.

Liu, Y., Gupta, R., Sharma, A., Wall, T., Butcher, A., Miller, G., Gottlieb, P. & French, D. 2005. Mineral matter–organic matter association characterisation by QEMSCAN and applications in coal utilisation. *Fuel*, 84(10):1259-1267.

Mastalerz, M. & Gurba, L.W. 2001. Determination of nitrogen in coal macerals using electron microprobe technique-experimental procedure. *International Journal of Coal Geology*, 47:23-30.

Matjie, R., Li, Z., Ward, C.R., Bunt, J. & Strydom, C. 2016. Determination of mineral matter and elemental composition of individual macerals in coals from Highveld mines. *Journal of the Southern African Institute of Mining and Metallurgy*, 116(2):169-180.

Matjie, R.H. 2008. Sintering and slagging of mineral matter in South African coals during the coal gasification process. University of Pretoria.

Matjie, R.H., French, D., Ward, C.R., Pistorius, P.C. & Li, Z. 2011. Behaviour of coal mineral matter in sintering and slagging of ash during the gasification process. *Fuel Processing Technology*, 92(8):1426-1433.

Matjie, R.H., Li, Z., Ward, C.R. & French, D. 2008. Chemical composition of glass and crystalline phases in coarse coal gasification ash. *Fuel*, 87(6):857-869.

Matjie, R.H., Li, Z., Ward, C.R., Kosasi, J., Bunt, J.R. & Strydom, C.A. 2015. Mineralogy of Furnace Deposits Produced by South African coals during Pulverized-Fuel Combustion tests. *Energy Fuels*, 29(12):8226-8238.

Matjie, R.H., Van Alphen, C. & Pistorius, P.C. 2006. Mineralogical characterisation of Secunda gasifier feedstock and coarse ash. *Minerals Engineering*, 19(3):256-261.

Matjie, R.H., Ward, C.R. & Li, Z. 2012a. Mineralogical Transformation in Coal Feedstocks during Carbon Conversion, based on Packed-Bed Combustor Tests: Part 1 Bulk Coal and Ash Studies. *Coal Combustion and Gasification products*, 4:45-54.

Matjie, R.H., Ward, C.R. & Li, Z. 2012b. Mineralogical transformations in coal feedstock during carbon conversion, Based in packed-bed combustor tests: Part 2. Behavior of individual particles. *Coal Combustion and Gasification products*, 4:55-67.

Nguyentranlam, G. & Galvin, K.P. 2004. Applications of the Reflux Classifier in solid-liquid operations. *International Journal of Mineral Processing*, 73:83-89.

Norrish, K. & Hutton, J. 1969. An accurate X-ray spectrographic method for the analysis of a wide range of geological samples. *Geochimica et cosmochimica acta*, 33(4):431-453.

Pinetown, K.L., Ward, C.R. & Van der Westhuizen, W.A. 2007. Quantitative evaluation of minerals in coal deposits in the Witbank and Highveld Coalfields, and the potential impact on acid mine drainage. *International Journal of Coal Geology*, 70:166-183.

Quann, R.J. & Sarofim, A.F. 1986. A scanning electron microscopy study of the transformations of organically bound metals during lignite combustion. *Fuel*, 65:40-46.

Raask, E. 1985. The mode of occurrence and concentration of trace elements in coal. *Progress in Energy and Combustion Science*, 11(2):97-118.

Rietveld, H.M. 1969. A Profile refinement method for Nuclear and Magnetic structures. *Journal of Applied Crystallography* 2:65-71.

Snyman, C.P. 1989. The role of coal petrography in understanding the properties of South African coal. *International Journal of Coal Geology*, 14:83-101.

Snyman, C.P. 1998. Coal. *(In* Wilson, M.G.C. & Anhaeusser, C.R., *eds*. The Mineral Resources of South Africa. South Africa: Council of Geoscience. p. 136-205).

Soundarrajan, N., Krishnamurthy, N. & Pisupati, S.V. 2012. Physical and Chemical Characterization of coal particles used as entrained flow gasifier feedstock: Heterogeneity in mineral matter distribution. *Energy Procedia*, 14:1735-1740.

Stach, E., Mackowsky, M.-T., Teichmuller, M., Taylor, G.H., Chandra, D. & Teichmuller, R. 1982. Textbook of coal petrology. 2. Vol. 2. Berlin: Gebruder Borntraeger.

Van Alphen, C. 2005. Factors influencing fly ash formation and slag deposit formation (slagging) on combusting a South African pulverised fuel in a 200 MWe boiler. University of the Witwatersrand Johannesburg, South Africa.

Van Dyk, J., Benson, S., Laumb, M. & Waanders, B. 2009. Coal and coal ash characteristics to understand mineral transformations and slag formation. *Fuel*, 88(6):1057-1063.

Van Niekerk, D., Pugmire, R.J., Solum, M.S., Painter, P.C. & Mathews, J.P. 2008. Structural characterization of vitrinite-rich and inertinite-rich Permian-aged South African bituminous coals. *International Journal of Coal Geology*, 76(4):290-300.

Ward, C.R. 2002. Analysis and significance of mineral matter in coal seams. *International Journal of Coal Geology*, 50(1-4):135-168.

Ward, C.R. & Gurba, L.W. 1998. Occurrence and distribution of organic sulphur in macerals of Australian coals using electron microprobe techniques. *Organic Geochemistry*, 28:635-647.

Ward, C.R., Li, Z. & Gurba, L.W. 2008. Comparison of elemental composition of macerals determined by electron microprobe to whole-coal ultimate analysis data. *International Journal of Coal Geology*, 75:157-165.

Zhang, L., Ninomiya, Y. & Yamashita, T. 2006. Occurrence of inorganic elements in condensed volatile matter emitted from coal pyrolysis and their contributions to the formation of ultra-fine particulates during coal combustion. *Energy Fuels*, 20:1482-1489.

CHAPTER 4

EVALUATION OF MINERAL MATTER TRANSFORMATIONS IN LOW-TEMPERATURE ASHES OF SOUTH AFRICAN COAL FEEDSTOCK SAMPLES AND THEIR DENSITY SEPARATED CUTS USING HIGH-TEMPERATURE X-RAY DIFFRACTION

Rudelle Rautenbach, Ratale H. Matjie, Christien A. Strydom, John R. Bunt, Colin R. Ward, David French, and Chris van Alphen

This work is published in the *International Journal of Coal Preparation and Utilsation,* **2019,** Published Online 22 October 2019. DOI: 10.1080/19392699.2019.1677629

Abstract

Coal mineral matter is the leading cause of inevitable ash problems (fouling and slagging) during the combustion of coal. Low-temperature ash (LTA) samples of feed coals and the density separated fractions were subjected to high-temperature X-ray diffraction (HT-XRD) to identify the mineral reactions occurred at elevated temperatures under oxidizing conditions. Excluded minerals were mainly contained in the sink fractions, while included minerals were mainly present in the float fractions. QEMSCAN results indicate that the mineral associations in carbominerites and included minerals in Feeds A, B and C and sinks B and C are responsible for the melt formation during HT-XRD experiments. HT-XRD results indicate the presence of mullite, anorthite, and amorphous aluminosilicate materials formed in the thermally treated LTA samples. The formation of these slagging crystalline and glassy phases could be attributed to either crystallisation during the cooling of the molten solution, or via solid state reactions at elevated temperatures. A comprehensive knowledge of the included and excluded minerals can be used to prepare a blended feedstock for combustion processes. The operational ash-related problems in the combustion and gasification processes could be minimised by implementing this comprehensive knowledge of the transformation of coal minerals at elevated temperatures.

Keywords: Mineral matter, density separated fractions, low-temperature plasma ashing, HT-XRD

4.1 Introduction

Coal is an essential sedimentary fossil fuel with a significant role as a primary fuel source worldwide (Falcon & Ham, 1988; Falcon & Snyman, 1986; Jeffrey, 2005). More than 90% of the electricity generated in South Africa is produced from coal power stations, while the coal-to-liquids and metallurgical industries also rely heavily on coal as a feedstock (Falcon & Ham, 1988; Falcon & Snyman, 1986; Jeffrey, 2005; Snyman, 1998). This dependence on coal as the primary fuel source and feedstock are not likely to change in the near future due to the vast coal resource quantities as well as the costs of coal mining, which are relatively cheap when compared to alternative energy sources (Jeffrey, 2005). Although coal resources are in abundance, the quantity of higher grade coals is decreasing, while lower grade coals are being increasingly utilised. These lower grade coals contain significantly more mineral matter than higher grade coals. Mineral matter in coal undergoes various reactions during thermochemical processes (pyrolysis, gasification and combustion). These reactions include transformation, decomposition, agglomeration, dehydration, volatilisation, solid-phase interactions, melting, and recrystallisation (Bryers, 1996; Creelman *et al.*, 2013; Matjie, 2008; Matjie *et al.*, 2015; Raask, 1985; Reifenstein *et al.*, 1999; Van Dyk *et al.*, 2006). Minerals in coal can occur as included minerals (inherent minerals) associates with other minerals and the organic matter, i.e., the macerals. Minerals can be liberated from the organic matter and occur as distinct/discrete particles, i.e., excluded or extraneous minerals in the rock fragments (Creelman *et al.*, 2013).

Mineral matter can be successfully investigated by isolating it from the organic matter through low-temperature oxygen plasma ashing, which has been proven to be a successful and effective technique by previous authors (Frazer & Belcher, 1973; Gluskoter, 1965; Matjie *et al.*, 2016; Matjie *et al.*, 2012a; Matjie *et al.*, 2012b; Pinetown *et al.*, 2007; Ward, 2002; Ward, 2016). Low-temperature oxygen plasma ashing oxidizes coal macerals without changing the minerals by operating at low temperatures between 100°C and 150°C. During this LTA analysis, activated oxygen is produced by an electromagnetic field through a radio-frequency oscillator. This activated oxygen is passed over pulverised coal samples, which results in the decomposition of the macerals while the minerals remain unaffected. The inorganic element carboxylates in the macerals transform to new minerals (artifacts that are not present in the original coals) which are the pitfall of the LTA technique (Frazer & Belcher, 1973; Matjie, 2008). When the oxidation is completed, the ash residues will be gray, which confirms the absence of any organic matter. LTA is possibly the most reliable technique to calculate the total percentage of mineral matter in coal (Frazer & Belcher, 1973; Miller *et al.*, 1979; Ward, 2002; Ward, 2016). Other inorganic elements that are associated with water-soluble inorganic salts can be dissolved in the pore water or be

present as dissolved inorganic element carboxylates contained in the macerals (Frazer & Belcher, 1973; Miller *et al.*, 1979). The composition and mode of occurrence of mineral matter in coals need to be investigated and characterised as it plays a vital role in the ash slagging and fouling, ash deposition and agglomeration problems during coal combustion and gasification (Bryers, 1996; Creelman *et al.*, 2013; Jeffrey, 2005; Matjie *et al.*, 2016; Matjie, 2008; Matjie *et al.*, 2011; Matjie *et al.*, 2012a; Matjie *et al.*, 2012b).

Slagging occurs when molten ash formed at high temperature (ranging from 1100°C to 1600°C) adheres to boiler surfaces. Fluxing cations (Ca2+, Fe2+, Mg2+, and K+) -bearing minerals, and fluxing non-mineral inorganics in the coal water pores react with aluminosilicates at high temperatures, thus lowering the ash fusion temperature and subsequently initiate slag formation (Van Dyk *et al.*, 2009). The slag deposits that form inside the boiler result in a decrease of efficiency and adversely affect the thermal behaviour of the equipment which can ultimately lead to the shutdown of equipment to remove these deposits (Matjie, 2008; Van Dyk *et al.*, 2006).

In-depth knowledge of the associations and mode of occurrence of mineral matter in different coals is of utmost importance for various coal combustion and gasification processes. Despite this significance, only limited studies on the characterisation of mineral matter in South African coal can be found in the literature (Mahlaba *et al.*, 2011; Matjie *et al.*, 2016; Matjie *et al.*, 2011; Matjie *et al.*, 2012a; Matjie *et al.*, 2012b; Pinetown *et al.*, 2007; Van Dyk *et al.*, 2009; Van Dyk *et al.*, 2006).

Van Dyk *et al.* (2006) studied the transformation of minerals during coal gasification. They compared the ash fusion temperature (AFT) to slag formation determined by qualitative high-temperature X-ray diffraction (HT-XRD) and FactSage modeling. Low quantities of slag (melt) were present at 1000°C according to HT-XRD and FactSage results, which did not correlate with the AFT analysis results as expected. They concluded that by utilizing various techniques, such as HT-XRD and FactSage, insightful information regarding mineral transformations at high temperatures, could be obtained. The interpretation of the reacted minerals, as well as the flow properties, can be improved by using alternative techniques to AFT analysis (Van Dyk *et al.*, 2006).

The quantitative HT-XRD analysis can be followed to evaluate the transformations of minerals contained in coal at high temperatures during the coal combustion experiments. The HT-XRD results could then be used to identify the problems related to coal combustion and the formation of fouling and slagging deposits in boilers. The chemistry of the combustion products or modeling

of the phase equilibrium was formerly used to make assumptions regarding the mineral transformations that occur during combustion. Dynamic studies of the mineral interactions at high temperatures can be achieved, while the effects of various parameters can also be evaluated by HT-XRD analysis (French *et al.*, 2001).

The previous test-work conducted on South African coals mainly focused on the chemistry and mineralogy of the feed samples, while very little information is available on the mineral matter of South African feed coals as well as on their density separated fractions (float and sink fractions). Earlier investigations of mineral matter from South African coals focused on the transformation of minerals during gasification and the impact of mineral matter on acid mine drainage (Matjie *et al.*, 2016; Matjie, 2008; Matjie *et al.*, 2008; Pinetown *et al.*, 2007).

The objectives of this study, the first of its kind on these specific South African power station feed coals and their density separated fractions, are to improve the existing knowledge of the mineral matter in South African coals. Advanced quantitative analytical techniques such as quantitative HT-XRD as well as Quantitative Evaluation of Materials by Scanning Electron Microscopy (QEMSCAN) analysis were used to investigate the behaviour of included minerals, excluded minerals, and non-mineral inorganic elements.

The feed coal, as well as the float and sink cuts, were investigated to evaluate the mineral occurrences and interactions separately within the float and sink fractions before comparing it to the feed coal. Low-temperature oxygen plasma ashing was used to determine the proportions of mineral matter contained in the feed coals, and their density separated fractions. The LTA ash (mineral matter) samples were subsequently analysed using HT-XRD under air to investigate the formation of high-temperature mineral phases. The low temperature ashes of South African feed coals and their density separated fractions that were heated in the HT-XRD tests were characterised by XRD and X-ray fluorescence (XRF) analysis techniques. The actual experimental data obtained from the quantitative HT-XRD tests as well as the mineralogical and chemical results for the LTA samples were used to identify the minerals which are accountable for the sintering and slagging of mineral matter. The transformation of minerals in the coals and their density separated cuts at elevated temperatures is considered to be due to the mode of occurrence of mineral matter during HT-XRD tests under oxidizing conditions.

4.2 Experimental procedures

4.2.1 Sample Preparation

Three feedstock coal samples were selected from different power stations representing three coalfields which are situated in different South African provinces (Limpopo, Free State, and Mpumalanga). Three run of mine (ROM) materials from three South African coal stockpiles were sampled and utilised in this study. The ISO1988:1975 and ISO13909-4:2016 methods were followed to obtain 100 kg representative sample with the particle size distribution (PSD) of <75mm+0.54mm taken from each South African power station coal stockpile.

The coarse ROM material (approximately 100 kg of Feed A, Feed B, and Feed C) was subsequently submitted for density separation using the conventional float-sink method by the South African Bureau of Standards (SABS) laboratories in Mpumalanga, Secunda. The float-sink experiments were based on the standard method defined by SANS/ISO 7936 by SABS laboratories. Three fractions were produced by using the specific densities of the mixtures of TBE (Tetrabromoethane), benzene and perchloroethylene; float fractions <1.5 g/cm^3, middlings (<1.5 g/cm^3 + <1.9 g/cm^3) and sink fractions that are >1.9 g/cm^3. The middlings fraction were not included in this study, because the main objective of this study was to better understand the behaviour of inherent mineral matter in the float fractions, extraneous minerals in the sink fractions and mixture of inherent mineral matter and extraneous minerals in the ROM feed coals at elevated temperatures during the laboratory combustion experiments under oxidizing condition. The proximate analysis results for the feed coals (Feeds A, B, and C), as well as their density separated cuts are reported by Rautenbach *et al.,* (2019) and can be observed in Table 4-1 (Rautenbach *et al.*, 2019).

The feed samples, as well as the two density separated fractions (float and sink samples) were crushed using a jaw crusher (Samuel Osborne LTD) and a ball mill with stainless steel balls to achieve a particle size of <500 µm. Representative samples were sent to Australia (University of New South Wales (UNSW)) for low-temperature plasma ashing as well as XRD and XRF analyses. The experimental procedure can be observed in Figure 4-1.

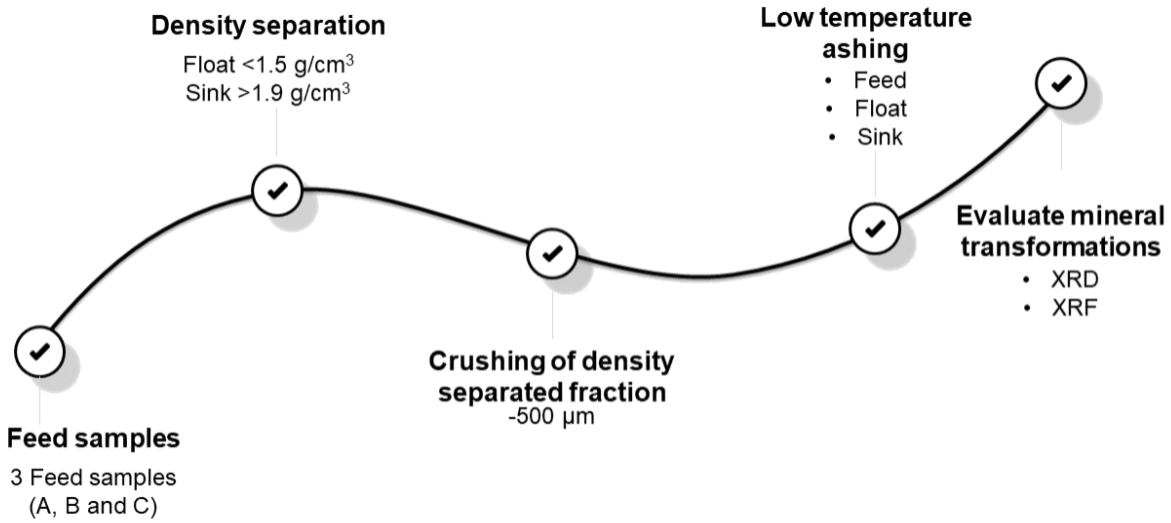

Figure 4-1 Schematic representation of the experimental procedure for feed coals.

4.2.2 QEMSCAN Analysis

The QEMSCAN analysis was followed to characterize the coal samples, and their respective density separated fractions by the Sustainability Division Research, Testing, and Development at Eskom, South Africa. Rautenbach *et al.,* (2019) reported the QEMSCAN analysis details as well as the results. Tables 4-2 to 4–4 contain the mineral-maceral association results based on the QEMSCAN results reported by (Rautenbach *et al.*, 2019).

Table 4-1 Proximate analysis results for feed coals with their density separated fractions (air-dried-basis), and % yield of density separated fractions (Rautenbach *et al.*, 2019).

	Feed A	Float A	Sink A	Feed B	Float B	Sink B	Feed C	Float C	Sink C
Moisture %	2.0	2.7	1.8	3.2	3.9	2.2	4.5	4.1	2.3
Ash %	35.9	7.8	62.9	32.9	12.4	68.1	25.0	10.5	60.3
Volatile matter %	21.8	33.0	16.4	20.6	28.2	16.1	21.9	27.5	17.0
Fixed carbon %	40.3	56.5	18.9	43.3	55.5	13.6	48.6	57.9	20.4
% yield of fractions after density separation		13	24		12	16		22	5

Table 4-2 Mineral and maceral associations in Feed A, Float A and Sink A fractions based on QEMSCAN results (vol.%).

CL: Cleats ST: Stone CM: Carbominerites INC: Included minerals

	Feed A				Float A				Sink A			
	CL	ST	CM	INC	CL	ST	CM	INC	CL	ST	CM	INC
Pyrite	71.0	3.2	25.8						83.6	9.3	7.1	
Siderite			100.0						43.8	43.8	12.5	
Calcite	16.7	50.0	33.3						85.1	5.4	9.5	
Dolomite	24.0	4.0	68.0	4.0					24.0	10.0	66.0	
Albite										100.0		
Ferrosillite										66.7	33.3	
Kaolinite		49.6	39.1	11.3		25.0	75.0		0.8	79.5	19.1	0.6
Quartz		54.8	35.6	9.6			100.0		0.8	82.7	16.5	
Mica										100.0		
Illite		80.0	20.0							89.3	10.7	
Microcline		75.0	25.0							85.7	14.3	
Rutile						100.0						
Vitrinite	0.7	3.0	20.0	76.3			100.0		8.0	26.4	42.5	23.0
Reactive semifusinite		16.4	44.3	39.3			100.0		3.5	46.5	40.7	9.3
Semifusinite		3.6	21.8	74.5			100.0			26.1	39.1	34.8
Fusinite (S)		6.5	29.0	64.5			100.0		2.5	35.0	45.0	17.5
Fusinite		13.5	42.3	44.2			100.0		1.5	41.8	41.8	14.9
Fusinite/Sclerotinite		2.1	4.2	93.8			100.0			11.1	5.6	83.3

Table 4-3 Mineral and maceral associations in Feed B, Float B and Sink B fractions based on QEMSCAN results (vol. %).

CL: Cleats ST: Stone CM: Carbominerites INC: Included minerals

	Feed B				Float B				Sink B			
	CL	ST	CM	INC	CL	ST	CM	INC	CL	ST	CM	INC
Pyrite	71.4		28.6					100.0	100.0			
Siderite	50.0	12.5	25.0	12.5				100.0	50.0	50.0		
Calcite	67.5	5.0	20.0	7.5				100.0	65.2	21.7	13.0	
Dolomite	17.6	11.8	41.2	29.4				100.0	33.3	33.3	33.3	
Apatite		100.0								100.0		
Albite			100.0							100.0		
Ferrosilite			100.0							66.7	33.3	
Kaolinite	0.4	39.3	45.7	14.6		7.1	14.3	78.6	0.1	89.9	9.6	0.4
Quartz		42.9	42.9	14.3						76.0	24.0	
Illite		33.3	66.7							100.0		
Microcline		100.0										
Rutile[Ti]										100.0		
Alunite/Gibbsite										100.0		
Vitrinite			26.9	72.1				100.0		25.0	35.0	40.0
Reactive semifusinite	1.0	6.2	44.3	48.5				98.0		51.4	37.1	11.4
Semifusinite		1.0	22.7	76.3				100.0		30.0	50.0	20.0
Fusinite(S)			28.8	71.2				100.0		27.3	36.4	36.4
Fusinite	0.6	4.3	35.6	59.5				100.0	1.4	39.1	39.1	20.3
Fusinite/Sclerotinite			12.0	88.0				100.0		10.0		90.0

Table 4-4 Mineral and maceral associations in sample Feed C, Float C and Sink C fractions based on QEMSCAN results (vol. %).

CL: Cleats ST: Stone CM: Carbominerites INC: Included minerals

	Feed C				Float C				Sink C			
	CL	ST	CM	INC	CL	ST	CM	INC	CL	ST	CM	INC
Pyrite	14.3		42.9	42.9				100.0	61.5	20.0	18.5	
Siderite									66.7	33.3		
Calcite	61.9		14.3	23.8	85.7		7.1	7.1	81.8	13.8	4.4	
Dolomite	66.7		20.5	12.8	62.5			37.5	80.0	10.8	9.2	
Apatite			66.7	33.3						100.0		
Albite									33.3	50.0	16.7	
Ferrosilite			50.0	50.0						80.0	20.0	
Kaolinite		24.2	50.0	25.8		25.0	34.4	40.6	3.2	83.8	11.7	1.3
Quartz		45.7	32.9	21.4			33.3	66.7	0.7	87.6	11.4	0.3
Mica		100								90.9	9.1	
Illite										91.7	8.3	
Microcline		100								95.8	4.2	
Rutile[Ti]										100.0		
Alunite							100			66.7	33.3	
Vitrinite		0.7	14.0	85.3		0.3	3.8	95.9	12.5	28.6	33.9	25.0
Reactive semifusinite	1.3	3.8	30.8	64.1			7.3	92.7	10.3	41.2	32.4	16.2
Semifusinite			13.0	87.0			3.6	96.4	13.3	26.7	33.3	26.7
Fusinite(S)			13.8	86.2			7.1	92.9		35.7	28.6	35.7
Fusinite		2.3	23.8	73.8			6.9	93.1	8.0	29.9	32.2	29.9
Fusinite/Sclerotinite			5.0	95.0				100.0				100.0

4.2.3 Low-temperature Oxygen Plasma Ashing, Mineralogical and Chemical Analyses

Nine prepared feed coal and density separated samples (three feeds, three floats, and three sinks) were ashed at UNSW using an International Plasma Corporation (IPC) low-temperature asher. The established LTA procedure is described by Gluskoter (1965) and is useful in isolating the mineral matter from the organic matter (Gluskoter, 1965). The schematic representation of an oxygen plasma asher can be observed in Figure. 4-2.

The XRD analysis (Matjie, 2008; Matjie *et al.*, 2008; Matjie *et al.*, 2015; Rietveld, 1969; Taylor, 1991) was followed to determine proportions of minerals present in the LTA samples of coal feedstock and their density separated fractions. The XRF analysis (Matjie, 2008; Matjie *et al.*, 2015; Norrish & Hutton, 1969; Rietveld, 1969) was employed to determine proportions of inorganic elements present ion the Low-temperature ashes of South African feed coals and their density separated fractions produced at the UNSW laboratories.

4.2.4 HT-XRD Analysis

The prepared LTA samples were subjected to HT-XRD at Coal and Environmental Research Technology, Sasol, South Africa. A Panalytical X'Pert PRO recorded the HT-XRD patterns, equipped with a multipurpose diffractometer. The scans were executed in air inside an Anton Paar HTK 2000 HT-XRD chamber.

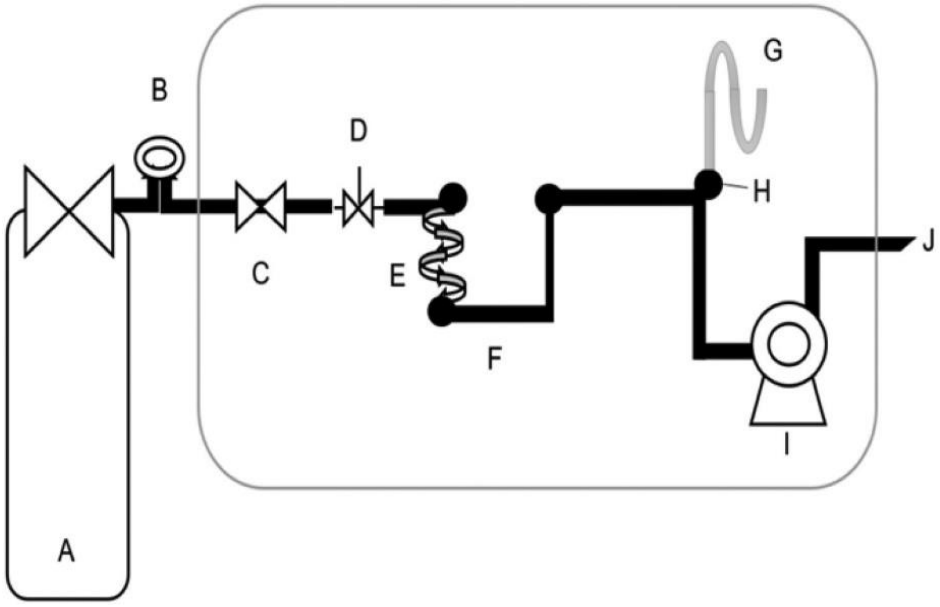

A	Oxygen tank
B	Gas regulator
C	Solenoid valve
D	Needle valve
E	RF coil
F	Oxidation chamber
G	Vacuum gauge
H	Vacuum valve
I	Pump
J	Vent

Figure 4-2 Schematic representation of the low-temperature oxygen plasma asher (Gluskoter, 1965).

The powdered samples were placed on a Platinum heating strip (with a Pt and a Pt/Rh thermocouple attached) and the HT-XRD scans were recorded every 100°C from room temperature (RT) (± 30°C) up to 1400°C after which the sample was cooled down to room temperature again (± 35°C). The experimental conditions are summarised in Table 4-5.

Siroquant™ is a software package developed and refined by Taylor and Rietveld which was used to interpret the HT-XRD results (Matjie *et al.*, 2008; Taylor, 1991). Mineral data of metakaolinite ($Al_2O_3.2SiO_2$) in the Siroquant database was used to represent the amorphous content in the LTA samples during HT-XRD tests, based on the method described by Ward *et al.,* (2005). Each HT-XRD diffractogram was processed with the data of metakaolinite included, which allowed for quantitative XRD analysis. This procedure of analysing an unspiked sample rather than spiking the sample with CaF_2, crystalline zinc, or synthetic corundum to achieve quantitative XRD results is fully described in the literature (Ward & French, 2005).

Table 4-5 Experimental conditions of HT-XRD analysis.

Instrument settings	HT-XRD	Instrument settings	HT-XRD
Temperature range	RT – 1400°C – RT, every 100°C	Scan from (deg 2θ)	5
Heating/Cooling rate	20°C/min	Scan to (deg 2θ)	65
Sample stage	Anton Paar HTK 2000 chamber	Step size (deg 2θ)	0.0334225
High voltage (kV)	40	Time per step (s)	41
Tube current (mA)	40	Scanning	Continuous
Divergence slit (deg)	1/4	Total time (min)	10
Anti-scatter slit	1/2	X-ray tube	Co radiation LFF
Soller slits (rad)	0.04	Wavelength (Å)	1.78897
Mask (mm)	10 (fixed)	Gas atmosphere	Air
Filter	Fe	Scan program	General HT Scan-2
Detector	X'Celerator		

Note: RT is room temperature

4.3 Results and Discussion

4.3.1 Mineral Associations Based on QEMSCAN Results

The mineral association results for Feed A, Feed B, and Feed C presented in Tables 4-2 to 4–4, respectively, are based on the QEMSCAN results which are reported in Rautenbach *et al.,* (2019). Pyrite/siderite/calcite/dolomite cleats represent particles with more than 60 vol. % of the respective mineral, i.e., either pyrite/siderite/calcite/ dolomite or less than 40 vol. % macerals. Stone fragments include particles with less than 40 vol. % macerals and more than 60 vol. % of any combination of quartz/kaolinite/ microcline/mica. Carbominerites represent the particles with 20 vol. % to 40 vol. % included minerals and between 60 vol. % and 80 vol. % macerals. The included minerals are associated with the carbon matrix. Matjie *et al.,* (2011) conducted research work on South African coal samples and the behaviour of mineral matter during gasification (Matjie *et al.*, 2011). Scanning electron micrographs from this investigation can be observed in Figure. 4-3, where the difference in cleats, carbominerites, and stone fragments are demonstrated.

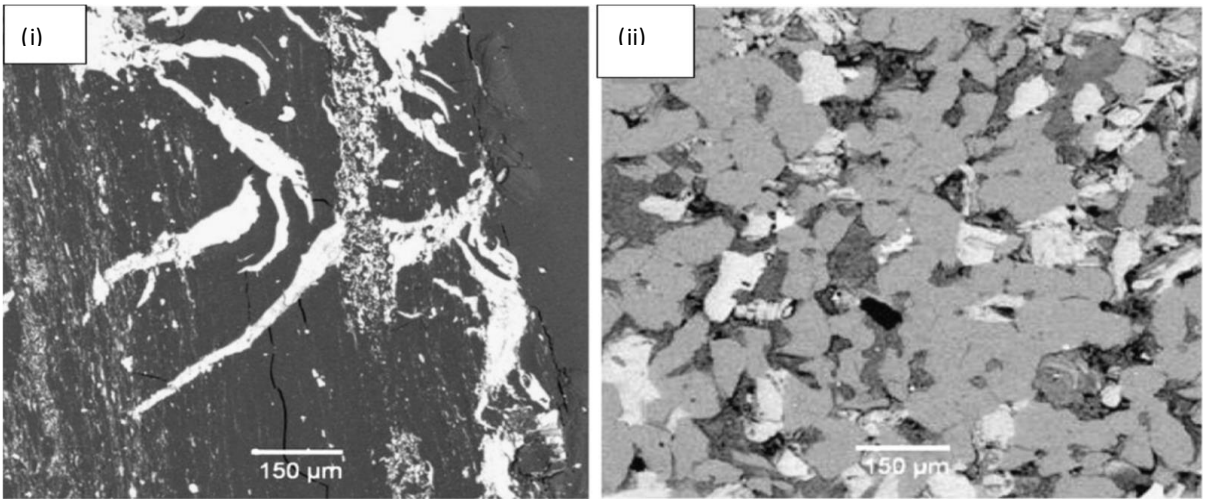

Figure 4-3 Micrographs of a South African feed coal created by back-scattered electrons. (i) represents cleat formations filled with carbominerites, and (ii) is a general view of pyrite grains (white), potassium feldspar (light grey), quartz (mid-grey), and kaolinite grains (dark-grey) present in a sandstone particle (Matjie *et al.*, 2011).

The mineral associations within Feed A, float, and sink fractions are reported in Table 4-2. With regards to Feed A, an association of fluxing minerals, i.e., pyrite (FeS_2) (± 70%) with calcite ($CaCO_3$) and dolomite ($CaMg(CO_3)_2$) in the cleat was observed. A significant amount of calcite is associated with pyrite and dolomite in the stone fragments, while the association of these fluxing

minerals with kaolinite ($Al_2Si_2O_5(OH)_4$) in the stone is also evident. In the carbominerite particles present in Feed A, the fluxing minerals are closely associated (pyrite-siderite-calcite-dolomite) with kaolinite as well as with vitrinite (i.e., association with carbon matrix can be observed).

The included minerals, in Feed A, contain no fluxing minerals, except a small amount of dolomite, while the association with kaolinite-quartz-vitrinite is observed. The stone fragments and carbominerites contaminated coal during coalification and mining through roofs and floors. These fragments, as well as the included minerals present in Feed A carbon-rich particles, will form a melt (slag) due to the association of fluxing minerals with kaolinite.

The modes occurrence of minerals and macerals in Float A were completely different from other coal feeds, and their density separated fractions mined in South Africa, as reported in Table 4-2. No fluxing mineral (either pyrite, calcite, siderite or dolomite) and kaolinite associations are observed in the included minerals of Float A. However, an association of maceral and mineral is observed between kaolinite-quartz-vitrinite. The mineral-maceral association in Float A (kaolinite-quartz-vitrinite) is not expected to cause a melt during the heating of the LTA sample of Float Ain the HT-XRD under air and thus should not lead to slag formation.

Associations among pyrite-calcite-siderite-dolomite and less than 1% kaolinite are observed in the cleats of Sink A. Smaller amounts of fluxing minerals are associated with each other in the stone fragments, although high proportions of kaolinite and quartz are associated with these fluxing minerals in the stone fragments of Sink A. The stone fragments, present in Sink A, are expected therefore to cause slag formation at elevated temperatures during the HT-XRD analysis under an air atmosphere. Significant amounts of dolomite are associated with high amounts of vitrinite (organic matter) and lesser amounts of pyrite, calcite, siderite, kaolinite and quartz in the carbominerites of Sink A. Less than 1% kaolinite is associated with vitrinite containing the inherent minerals in the carbon-rich particles in the Sink A. Carbominerite particles present in Sink A are also expected to lead to slag formation due to the mineral associations (Table 4-2).

In Table 4-3, the mineral and maceral associations within Feed B, float B, and sink B fractions can be observed. The mineral-maceral associations of pyrite-calcite-dolomitesiderite-kaolinite and macerals are mainly observed in the cleats of Feed B. Siderite-calcite -dolomite associations with kaolinite and quartz are observed in the stone fragments of Feed B, while pyrite-calcite-dolomite-siderite are associated with kaolinite-quartz-vitrinite in the carbominerites present in Feed B. The associations within the included minerals in Feed B, are similar to the associations in the stone fragments, where no pyrite was present, while calcite-dolomite-siderite are associated with included kaolinite and quartz, as well as with the organic matrix (i.e., the macerals). Slagging

behaviour will thus be mainly observed in the stone fragments and carbominerites present in Feed B, while less slagging is expected to be observed in the included minerals of Feed B.

All the fluxing minerals present in Float B (pyrite, calcite, dolomite, and siderite) are associated with the included kaolinite, while 100% of vitrinite present in Float B are associated with included minerals (fluxing minerals and kaolinite). High slagging is therefore expected to be observed at elevated temperatures for Float B under an oxidizing atmosphere during HT-XRD analysis.

All the pyrite present in the sink B fraction (Table 4-3) is associated with siderite, calcite, and dolomite in the cleats of Sink B. Low to no slagging behaviour will thus be expected from the cleats in Feed B due to the significantly low proportion of kaolinite association. The stone fragments present in Sink B will melt during the HT-XRD measurements due to the association of siderite, calcite, dolomite, and quartz with approximately 90% kaolinite. Association of calcite with dolomite, quartz, vitrinite and a small amount of kaolinite are observed in the carbominerites of Sink B. The low included mineral content in the carbon rich particles (macerals) are contained in Sink B and are not likely to form slag at elevated temperatures under oxidizing conditions.

The mineral-maceral associations determined for Feed C, float C and sink C fractions are reported in Table 4. Similar mineral-maceral associations are observed in Feed C as in Feed A, however, kaolinite is only associated with quartz in the stone fragments, while no association between fluxing minerals and kaolinite were reported in these stone fragments for Feed C. Pyrite-calcite-dolomite associated with kaolinite, quartz and vitrinite were observed in the carbominerite particles as well as the included mineral particles in Feed C. Slag formation is expected to occur when Feed C is combusted during HT-XRD due to the mineral associations in the carbominerite particles and included mineral particles.

The mineral associations differ significantly in Float C (Table 4) when compared to Float A (Table 2) and Float B (Table 3). Calcite association with dolomite is observed in the cleats of Float C, while calcite association with kaolinite, quartz and small amounts of vitrinite is observed in the carbominerites of Float C. With regards to the included minerals in Float C, the associations of 100% pyrite with calcite, dolomite, kaolinite, and quartz were observed. A high proportion of vitrinite is also reported in the included minerals, thus also associated with fluxing minerals-kaolinite-quartz. During the combustion of Float C, slagging is expected to occur not only due to the included mineral associations but also due to the mineral associations within the carbominerites.

The associations of high amounts of the fluxing minerals, pyrite-calcite-dolomite-siderite, with a small proportion of kaolinite, are recorded for the cleats in Sink C. Significantly high amounts of

kaolinite and quartz are associated with pyrite-calcite-dolomite-siderite in the stone fragments of Sink C, with lesser amounts of kaolinite and quartz associated with the fluxing minerals as well as with vitrinite in the carbominerites. As expected, the low included mineral particles present in Sink C are mainly associated with organic material (macerals).

Previous research work conducted on South African coal samples, and the mineral associations within gasifier feedstock samples found that pyrite is mainly present as liberated particles, i.e., excluded mineral matter which correlates with the results presented in Table 2–4, where pyrite was found to be mainly present in the cleats of the samples (Matjie, 2008). Dolomite is associated with calcite, while calcite has a strong association with coal and to a lesser extent with dolomite, quartz, and kaolinite (Matjie, 2008). Quartz and kaolinite are strongly associated with coal, which correlates with the results for Feed C, in Table 4, where associations of quartz and kaolinite with the included mineral matter are the highest. Furthermore, it is reported that quartz is also associated with kaolinite which suggests that quartz grains are included in the kaolinite particles (Matjie, 2008; Matjie *et al.*, 2012b).

4.3.2 Low-temperature Oxygen Plasma Ashing

The results presented in Table 6 indicate the mineral matter contents in the coals, and their density separated fractions. The differences in the LTA percentages between the float and the sink fractions are due to the mode of occurrence of mineral matter in the coal sample. The float fractions contain significantly less mineral matter when compared to the sink fractions. Similar trends in the LTA percentages were observed by Matjie *et al.,* (2011). Thus low mineral matter contents are included in the carbon matrix, i.e., associated with the organic matter, while significantly larger proportions of the mineral matter are present as excluded minerals in the rock fragments (Matjie *et al.*, 2011).

Table 4-6 LTA (mineral matter) in coal samples (wt. %).

	Feed A	Float A	Sink A	Feed B	Float B	Sink B	Feed C	Float C	Sink C
LTA %	44.3	17.5	66.0	41.5	18.5	82.5	31.6	15.2	51.5

4.3.3 Mineralogy of LTA Samples

The XRD diffractograms of the prepared LTA samples of the feed coals and their density separated fractions can be observed in Figures 4–6. The mineral distributions across the density separated fractions are compared in Figure 4-7. The significant proportions of minerals present

in all LTA samples are kaolinite ($Al_2Si_2O_5(OH)_4$) and quartz (SiO_2) with minor proportions of pyrite (FeS_2), dolomite ($CaMg(CO_3)_2$) and calcite ($CaCO_3$). Kaolinite is present in approximately equal amounts in both the float and the sink fractions of Feed A, indicating that it is uniformly distributed between the included and excluded minerals. A significantly higher concentration of kaolinite is present in the sink fraction for Feed B, and a higher concentration of kaolinite is associated with the float fraction in Feed C.

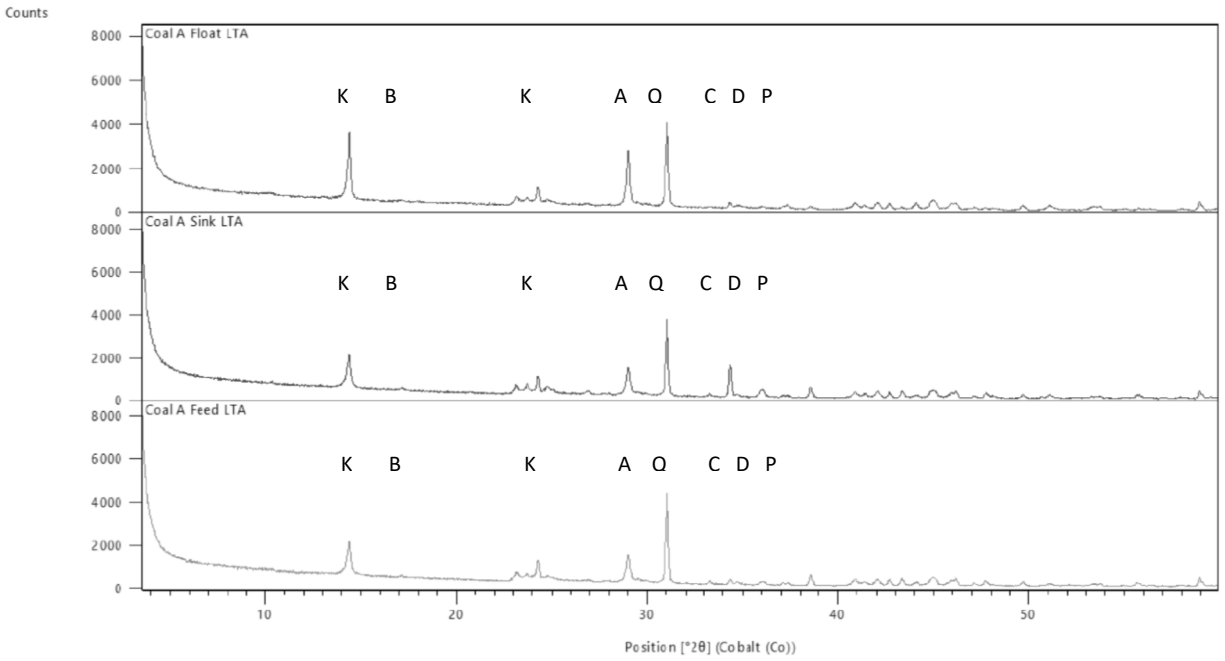

K: Kaolinite B: Bassanite A: Anatase Q: Quartz C: Calcite D: Dolomite P: Pyrite

Figure 4-4 XRD diffractograms of LTA from a) Float A, b) Sink A, and c) Feed A.

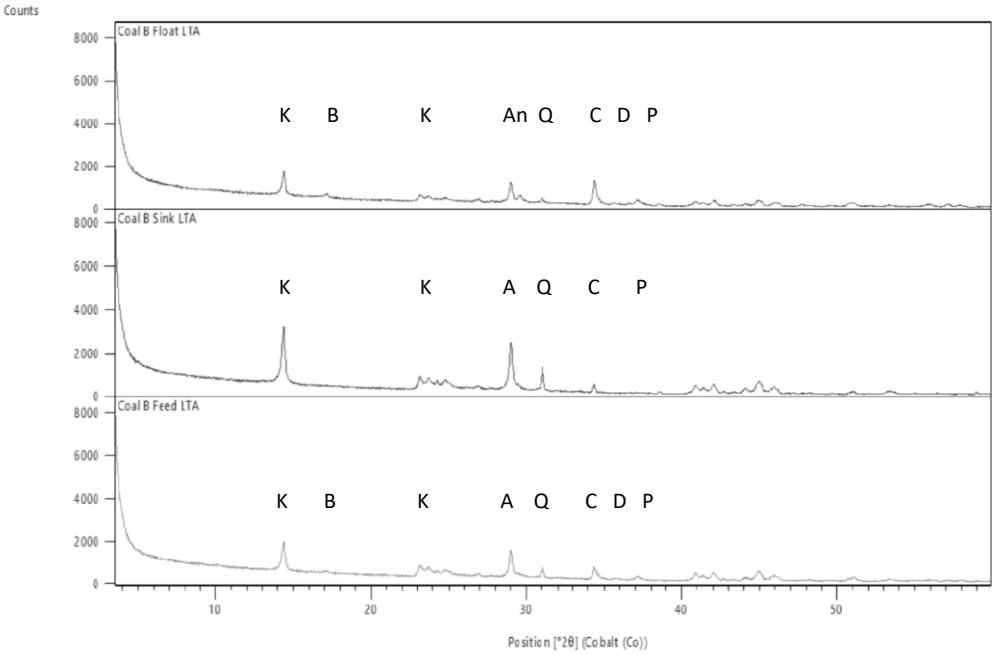

K: Kaolinite B: Bassanite An: Anhydrite A: Anatase Q: Quartz C: Calcite D: Dolomite

Figure 4-5 XRD diffractograms of LTA from a) Float B, b) Sink B, and a) Feed B.

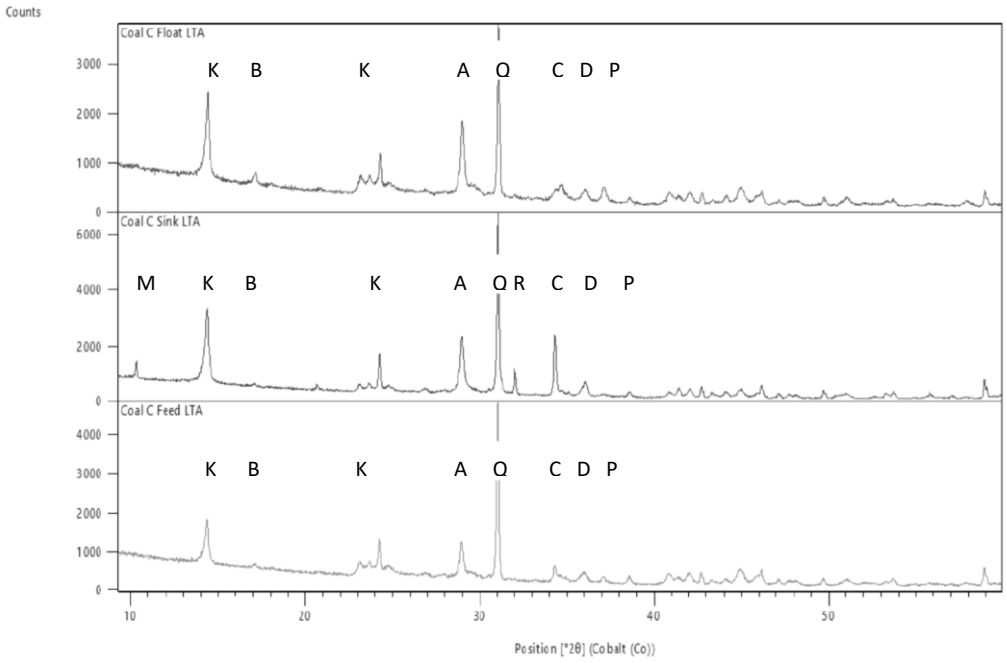

M: Muscovite K: Kaolinite B: Bassanite A: Anatase Q: Quartz
R: Rutile C: Calcite D: Dolomite P: Pyrite

Figure 4-6 XRD diffractograms of LTA from a) Float C, b) Sink C, and c) Feed C.

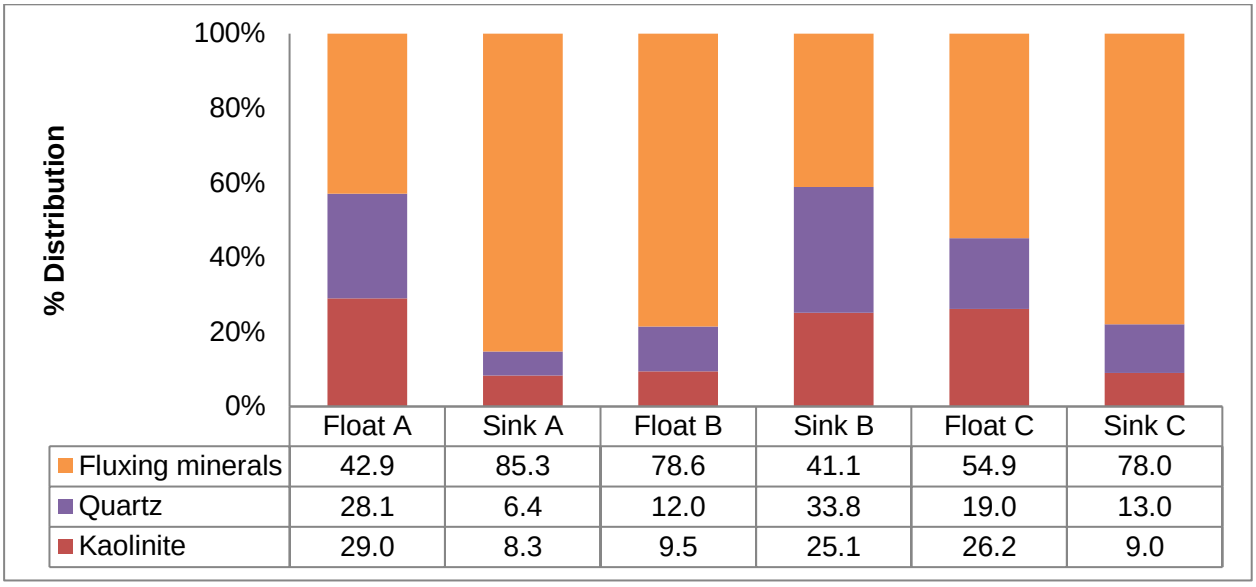

	Float A	Sink A	Float B	Sink B	Float C	Sink C
Fluxing minerals	42.9	85.3	78.6	41.1	54.9	78.0
Quartz	28.1	6.4	12.0	33.8	19.0	13.0
Kaolinite	29.0	8.3	9.5	25.1	26.2	9.0

Figure 4-7 % mineral distributions across density fractions derived from XRD analysis of LTA samples.

Quartz mainly reported to the LTA of Float A, whereas higher proportions of quartz are observed for the mineral matter of the sink fractions of Feeds B and C. It is interesting to note the significantly low proportions of quartz in the LTA samples of the feed, float and sink fractions of Feed B, which ranges between 3% and 5%. Calcite, dolomite, and pyrite mainly reported to the LTA residues of the sink fractions for Feed A and Feed C, thus present as excluded minerals. High proportions of these minerals are recorded in the LTA of Float B; however, no dolomite was detected for the LTA of Sink B. Bassanite ($CaSO_4 \cdot ½H_2O$) is an artifact mineral formed through the interaction of organic sulphur and non-mineral calcium in the coal macerals during low-temperature plasma ashing. Higher proportions of bassanite are observed in the LTA of the float fractions for Feed B and Feed C, thus associated with included minerals which correlate with findings by previous authors (Matjie *et al.*, 2011; Pinetown *et al.*, 2007; Ward, 2002; Ward, 2016).

However, a low proportion of bassanite is reported in the LTA of Sink A, indicating an association of mineral matter (organic calcium and organic sulphur) with a small proportion of macerals that were still contained in the Sink A. Anatase (TiO_2), brookite (TiO_2) and rutile (TiO_2) are polymorphs of TiO_2 with anatase being the most stable phase. LTA of Feed A, Float A and Sink A contained similar amounts of anatase, whereas the anatase present in the LTA of sample B is associated with excluded minerals. No anatase is detected for the LTA of the Feed C, Float C or Sink C fractions although brookite is present in the LTA of Feed C and Float C, while rutile is detected in the LTA of Sink C. No anatase were reported in the LTA samples of Feed C, float C and sink C

fractions which could be attributed to low quantities of anatase present in the samples below the XRD detection limit.

Anhydrite ($CaSO_4$) formation is the results of interactions between SO_2 derived from the reactions of the organic sulphur and sulphur-containing minerals present in the combustion gases and Ca, which is in the form of either organic Ca from the organic matrix or CaO transformed from the carbonate minerals. The dehydration of bassanite also forms anhydrite at elevated temperatures, which is present at 200°C in the LTA of Float B and Feed B (Matjie *et al.*, 2015; Ward, 2002; Ward, 2016). Matjie *et al.,* 2015, determined that anhydrite is abundantly present in coal samples with lower ash-yield due to the availability of higher proportions CaO formed from the transformation pf mineral matter at elevated temperatures. Gypsum, the source of anhydrite is sometimes found in South African Highveld lower-rank coals that have not been subjected to low-temperature oxygen-plasma ashing (Matjie *et al.*, 2012a). Gypsum is also present in low-rank coals stored for extended periods in stockpiles where acids (released from pyrite oxidation) have reacted with calcite or dolomite, resulting in gypsum formation (Van Alphen, 2005).

Siderite ($FeCO_3$) was only detected in the LTA of Feed A and reported to Float A, while muscovite/illite ($KAl_2(AlSi_3)O_{10}(OH)_2$)/($KAl_3Si_3O_{10}(OH)_2$) is present in the LTA of Float A. Therefore, siderite and muscovite/illite are both present in the LTA of Float A mainly as included minerals. Muscovite/illite and magnetite (Fe_3O_4) are only reported in the LTA of Sink B, thus associated with excluded minerals. Similar minerals to those listed in Table 4-2 are reported in the LTA of other South African coals (Matjie *et al.*, 2016; Matjie *et al.*, 2012a; Pinetown *et al.*, 2007).

The ‘slagging minerals’ ‘non-slagging minerals’ as well as the ratio of ‘slagging/nonslagging’ minerals are summarised in Table 4-7. The ‘slagging’ minerals represent minerals containing base types fluxing cations such as Fe^{2+}, Mg^{2+}, and Ca^{2+}. The ‘non-slagging’ minerals are the total of minerals containing Si, Al, and Ti, thus the acid type elements. The ratio of ‘slagging/non-slagging’ minerals are similar to the Base/Acid Ratio determined from elemental compositions and can thus be used to compare the different analytical techniques such as XRD, XRF, and QEMSCAN. Feeds A and C followed similar trends where more ‘slagging’ minerals reported to the sink fractions, thus associated with excluded minerals. This trend is also evident from Tables 4-1 to 4–3, where the mineral associations show that extraneous minerals reported to the sink fractions, while the included mineral matter contains in the float fractions. However, the opposite can be observed for Feed B, where more ‘slagging’ minerals are associated with included minerals in the float fraction and less in the sink fraction. These results emphasize the differences between the modes of occurrence of minerals in coal samples.

The distribution of minerals between the different float and sink fractions are compared in Figure 4-7. The significant differences between the various Feeds are the mode of occurrence of mineral matter. Quartz and kaolinite are associated with the mineral matter of the float fractions of Feeds A and C, while it is more concentrated in the mineral matter of sink fraction of Feed B.

Table 4-7 Mineralogy of LTA from coal samples based on XRD analysis (wt. %).

Minerals	Feed A	Float A	Sink A	Feed B	Float B	Sink B	Feed C	Float C	Sink C
"Slagging minerals"	14.6	7.1	28.3	9.7	27.7	5.1	10.2	7.6	21.4
"Non-slagging minerals"	82.3	75.8	69	85.6	63.4	94.9	85.9	85.1	69
Slagging/Non-slagging Ratio	0.18	0.09	0.41	0.11	0.44	0.05	0.12	0.09	0.31

The fluxing element-bearing minerals, i.e., calcite, dolomite, and pyrite, mainly occur in the sink fractions of Feeds A and C and the float fraction of Feed B. Mineral matter in these three samples will transform and behave differently when subjected to combustion and gasification conditions (Matjie, 2008; Van Alphen, 2005). The fluxing element-bearing minerals associated with kaolinite in the float fractions may interact with each other and result in a severe slag formation (Matjie *et al.*, 2006). High proportions of fluxing minerals that are associated with low proportions of kaolinite in the sink fractions could contribute to a slight slag formation.

4.3.4 Mineral Matter Chemistry

The major elemental oxide chemistry of the ashes from the coals and their density cuts are presented in Table 4-8. The principal elemental oxides present in the LTA samples are SiO_2, ranging from 36% to 55%, and Al_2O_3 ranging from 21% to 39% with minor proportions of CaO, Fe_2O_3, MgO, TiO_2, SO_3, and traces of K_2O, Na_2O, and P_2O_5. Both SiO_2 and Al_2O_3 detected in the LTA of Feed A, and Feed C are mainly present as included minerals (kaolinite and quartz). Higher proportions of these elements are contained in the LTA of Sink B, thus SiO_2 and Al_2O_3 are mainly associated with the excluded minerals (kaolinite and quartz) for Feed B. The proportions of CaO and Fe_2O_3 are higher in the LTA samples of Sink A and Sink C, thus mainly present as excluded fluxing Fe-bearing and Ca-bearing minerals in Feed A and Feed C. CaO and Fe_2O_3 mainly reported to the LTA of Float B; however it is interesting to note that a significantly high percentage of CaO (15.7%) is detected for the LTA of Float B, while only 2.1% CaO is detected in the LTA of

Sink B. This correlates with the XRD results, where dolomite was not detected due to very low/no quantities of dolomite, as well as the presence of submicron dolomite within the LTA of Sink B.

The mineral matter of Feed A contains a high percentage Fe_2O_3 which reported mostly to the sink fraction after density separation. The Fe_2O_3 percentages are lower in the LTA residues of Feeds B and C when compared to Feed A. Fe_2O_3 and MgO reported to the LTA of Float B, probably reflecting the included minerals (dolomite, calcite, and pyrite), although both elements are associated with excluded minerals in Feed C due to higher proportions observed in the LTA of Sink C (Table 4-8 and Fig. 4-6). Relatively low proportions of K_2O, Na_2O, P_2O_5, and TiO_2 that are associated with mineral matter are detected in the LTA samples. These elements are linked with mineral matter are mainly associated with included minerals (Table 4-6).

Table 4-8 XRF results for LTA samples of feed coals and their density separated fractions (wt. %) on a loss on ignition (LOI) basis.

Sample	Feed A	Float A	Sink A	Feed B	Float B	Sink B	Feed C	Float C	Sink C
SiO_2	54.4	56.3	47.4	45.0	35.6	51.1	50.4	49.3	53.2
Al_2O_3	27.8	30.7	25.2	35.5	29.0	39.3	25.5	29.0	21.0
TiO_2	1.4	1.9	1.2	1.9	3.0	2.0	1.5	2.5	1.3
Fe_2O_3	7.2	3.0	8.4	3.1	6.2	2.2	2.9	2.2	6.4
CaO	3.1	3.0	6.9	7.0	15.4	2.1	7.7	7.4	10.4
MgO	1.1	0.7	1.8	1.0	1.7	0.5	2.0	2.3	2.4
Na_2O	0.2	0.2	0.2	1.1	1.4	0.6	0.7	1.4	0.6
K_2O	0.8	0.8	0.6	0.6	0.8	0.5	0.6	0.8	1.0
P_2O_5	0.4	1.4	0.3	0.2	0.5	0.1	0.7	1.2	0.5
SO_3	2.3	0.9	6.2	2.4	4.5	0.3	4.4	2.7	2.3
Mn_3O_4	0.1	0.1	0.1	0.0	0.1	0.0	0.0	0.1	0.1
LOI	1.3	1.1	1.8	2.2	1.7	1.4	3.5	1.2	0.9

The XRF results in Table 4-8 match the XRD results and correlates with previous investigations conducted on LTA residues of South African coal (Matjie *et al.*, 2016; Matjie *et al.*, 2012a; Matjie *et al.*, 2012b; Pinetown *et al.*, 2007). The slagging propensities could be predicted by various empirical indices assuming that the coals have the same modes of occurrence of mineral matter, which is summarised in Table 4-9. The formulas used to calculate the indices included:

Base/Acid Ratio: (B/A_R) = $(Fe_2O_3+CaO+MgO+Na_2O+K_2O) / (SiO_2+Al_2O_3+TiO_2)$ (1)

Silica percentage: (Si_R) = $(SiO_2 \times 100) / (SiO_2+Fe_2O_3+CaO+MgO)$ (2)

Silica to alumina ratio: (Si/A_R) = (SiO_2 / Al_2O_3) (3)

Iron to calcium ratio: (Fe/Ca_R) = (Fe_2O_3 / CaO) (4)

The results obtained for the Base/Acid ratios, using the elemental composition, match the slagging/non-slagging minerals which are contained in the South African coal feeds evaluated in this study (Table 4-7). The Base/Acid ratio as well as the slagging/non-slagging minerals are determined from the elemental compositions and can, therefore, be used to match XRF, XRD and QEMSCAN techniques results. The similarities between these results reported in Tables 4-7 and 4-9 are an indication of the accuracy of the analytical techniques.

The empirical indices are based on the total acidic and basic elements (total element concentrations) present in the coal samples. When using these indices to predict slagging behaviours, the assumption is made that all these inorganic elements could have a similar effect on the melting behaviour of ash. Other researchers have found that the basic and acidic elements contained in the mineral matter (minerals and non-mineral inorganic elements) behave differently with varying fluxing strengths leading to difficulties when predicting the slagging behaviour of South African coals (Babcock & Company, 1923).

Slagging in South African power stations could occur as a result of included mineral matter (fluxing minerals that are associated with kaolinite/quartz in the coal). However, with regards to these empirical indices, the total basic and acidic oxides present in the minerals (both excluded and included minerals) are incorporated in the calculations. Another factor influencing these empirical predictions is the fact that the ash samples from South Africa contain very high proportions of acidic elements and low proportions of basic elements, preventing accurate prediction based on the total elemental compositions.

Table 4-9 Empirical indices predicting slagging behaviour based on ash analysis.

	Feed A	Float A	Sink A	Feed B	Float B	Sink B	Feed C	Float C	Sink C
Base/Acid Ratio (1)	0.15	0.09	0.24	0.15	0.38	0.06	0.18	0.17	0.28
Silica % (Si_R) (2)	82.76	89.47	73.52	80.28	60.23	91.53	80.09	80.48	73.46
Silica to Alumina Ratio (3)	1.96	1.84	1.88	1.27	1.23	1.3	1.97	1.7	2.53
Iron to Calcium Ratio (4)	2.35	1.00	1.23	0.43	0.41	1.05	0.38	0.31	0.62

The percentages elemental distribution of Al_2O_3 and SiO_2 which are bonded clays, and cations (Fe^{2+}, Ca^{2+}, and Mg^{2+}) which bond with the fluxing minerals across the density fractions of the LTA samples compared in Figure 4-8. Significant percentages of fluxing elements are associated with the LTA residue of Sink A, Float B and Sink C, in other words, some fluxing elements bonded with excluded minerals in Feed A and Feed C. While they are also associated with included minerals in Feed B.

From the mineralogical and elemental results reported above, it is evident that the three coal samples under investigation consist of similar qualitative mineral assemblages. Nevertheless, significant differences are observed regarding the mode of occurrence of minerals, the various origins of these minerals as well as the various quantitative mineral proportions. It was proposed, by previous authors (Matjie, 2008), that the transformed products of fluxing minerals associated with kaolinite in the LTA of the float and sink fractions may react with metakaolinite to form a molten solution, also referred to as slag. This emphasizes the importance of the improvement of knowledge relating to mineral matter transformations during combustion of coals and their density separated fractions during HT-XRD analysis.

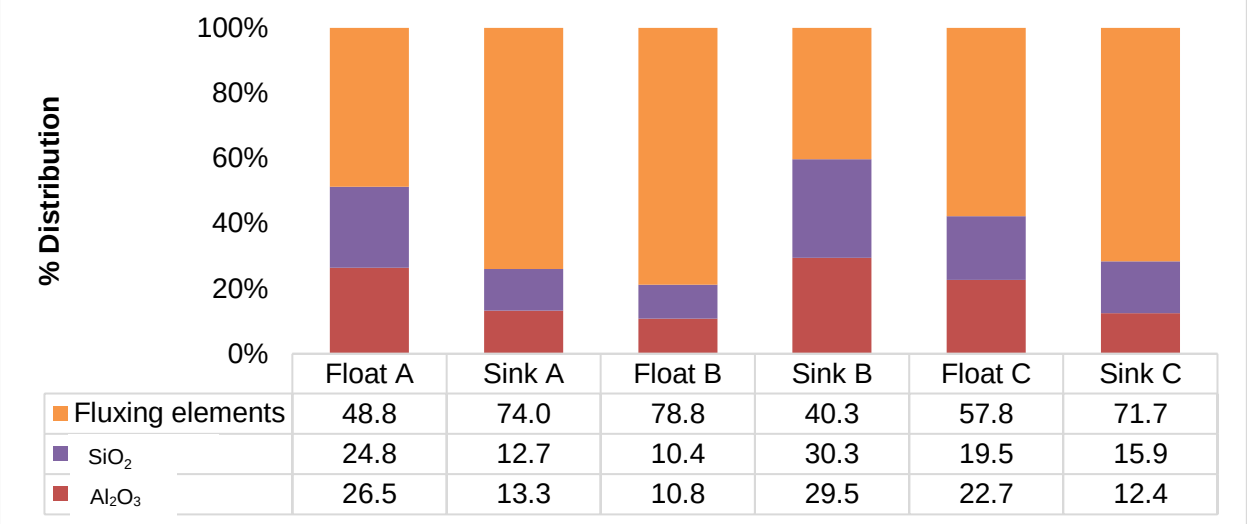

	Float A	Sink A	Float B	Sink B	Float C	Sink C
Fluxing elements	48.8	74.0	78.8	40.3	57.8	71.7
SiO_2	24.8	12.7	10.4	30.3	19.5	15.9
Al_2O_3	26.5	13.3	10.8	29.5	22.7	12.4

Figure 4-8 % elemental distribution across density fractions derived from the XRF analysis of LTA samples.

4.3.5 HT-XRD Results

The HT-XRD scans for the LTA residues of a typical feed, float, and sink samples are represented in Figure 4-9d represents a coal sample that was not subjected to low temperature plasma ashing to compare the XRD results of the low-temperature ash with the XRD results on a raw coal sample. These diffractograms are representative of LTA residues of a typical feed/float/sink fraction and raw coal under HT-XRD conditions.

The diffractograms are displayed in a sequence of increasing temperature, from 400°C up to 1400°C. With an increase in temperature, a decrease in the mineral quantities is observed as well as the formation of new minerals (e.g., mullite) at elevated temperatures. 100%

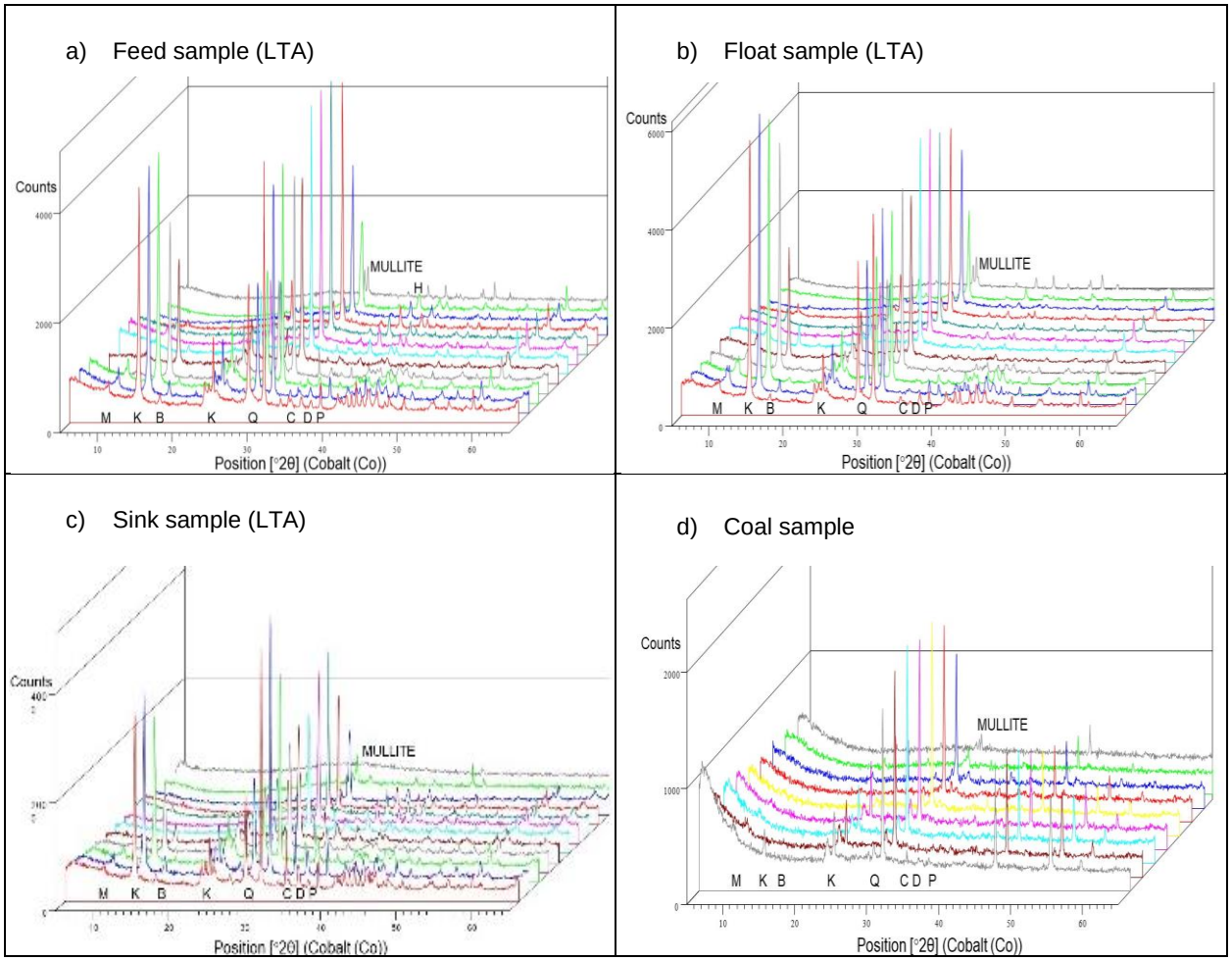

Figure 4-9 **HT-XRD scans for the LTA residues of a) Feed sample, b) Float sample, c) Sink sample; and d) Raw coal during heating up to 1400°C, recorded every 100°C.**

The influence of low-temperature ashing can be observed when comparing the LTA results (Fig. 4-9a–c)) with the HT-XRD results on the coal sample (Fig. 4-9d)). The peaks related to the dominant minerals (e.g., quartz and kaolinite) are visible in the diffractogram of the raw coal. However, the background is obscuring the minor minerals as a result of the organic matter, which is amorphous carbon present. XRD peaks obtained after low-temperature ashing (Figs 4-9a–c) are better distinguishable and will, therefore, lead to a more accurate analysis of the mineral transformations at elevated temperatures.

The quantitative HT-XRD results for the LTA samples of Feeds A, B, and C with their float and sink fractions can be observed in Figures 4-10 to 4–12, respectively. The graphs were split to view the main minerals (> 15 weight%) and the minor minerals (< 15 weight%) present in the

respective feed, float and sink fractions. The mineral transformations at high temperatures for the LTA samples of Feed A, Float A and Sink A are displayed in Figure 4-10. Quartz is usually present as large mono-mineralic elements and is therefore considered as mainly non-reactive during coal combustion and gasification processes (Bryers, 1996; Matjie *et al.*, 2015; Raask, 1985; Reifenstein *et al.*, 1999). Pure extraneous quartz is usually stable at high temperatures and non-reactive, though it depends on the mineral associations within the coal sample (Creelman *et al.*, 2013; Matjie, 2008). Impure quartz which is associated with fluxing minerals, non-fluxing mineral inorganics and kaolinite could react with reactive products of kaolinite and fluxing minerals to form

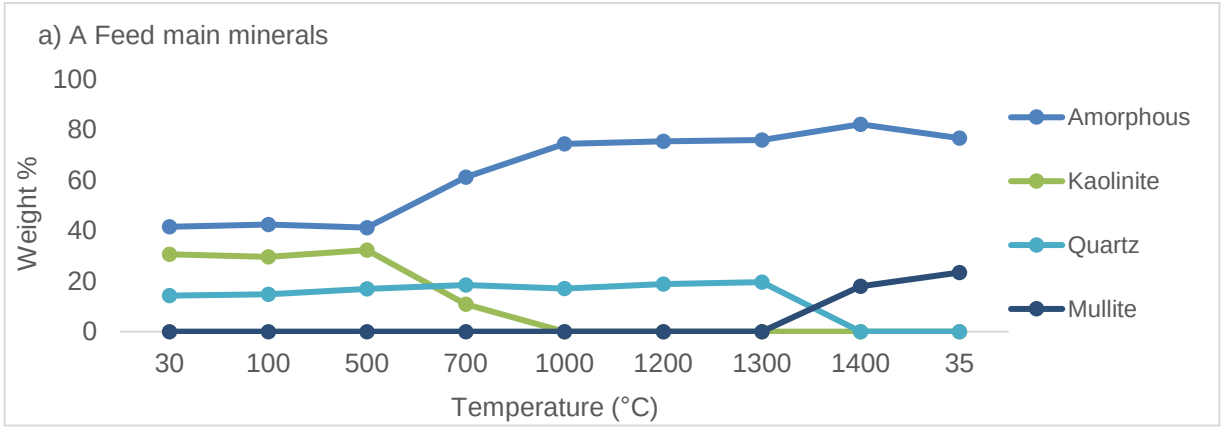

Figure 4-10(a) HT-XRD results for LTA of Feed A main minerals

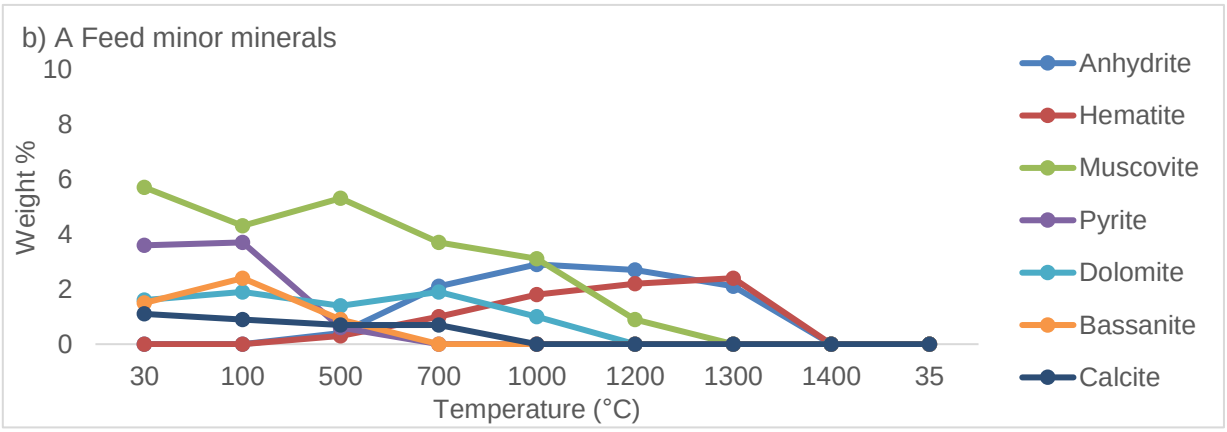

Figure 4-10(b) HT-XRD results for LTA of Feed A minor minerals

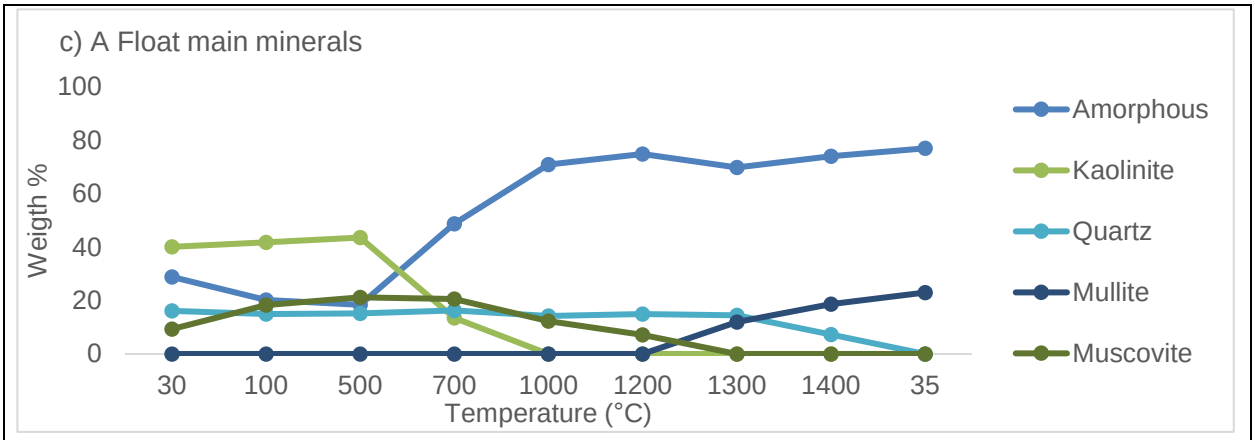

Figure 4-10(c) HT-XRD results for LTA of Float A main minerals

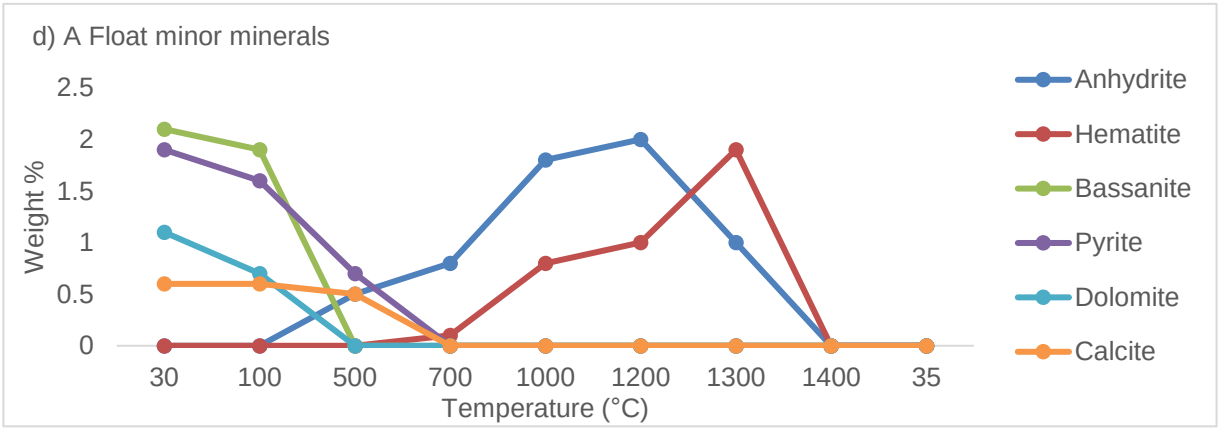

Figure 4-10(d) HT-XRD results for LTA of Float A minor minerals

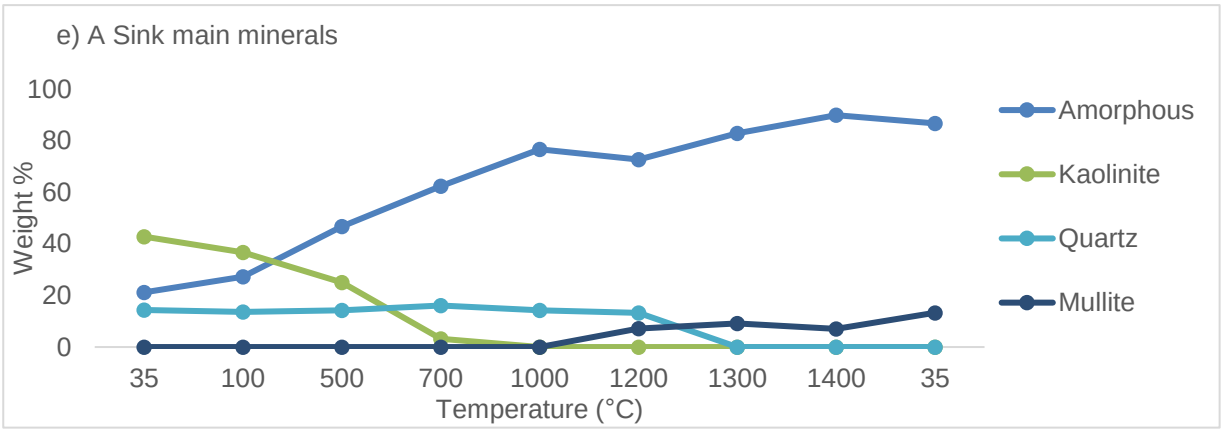

Figure 4-10(e) HT-XRD results for LTA of Sink A main minerals

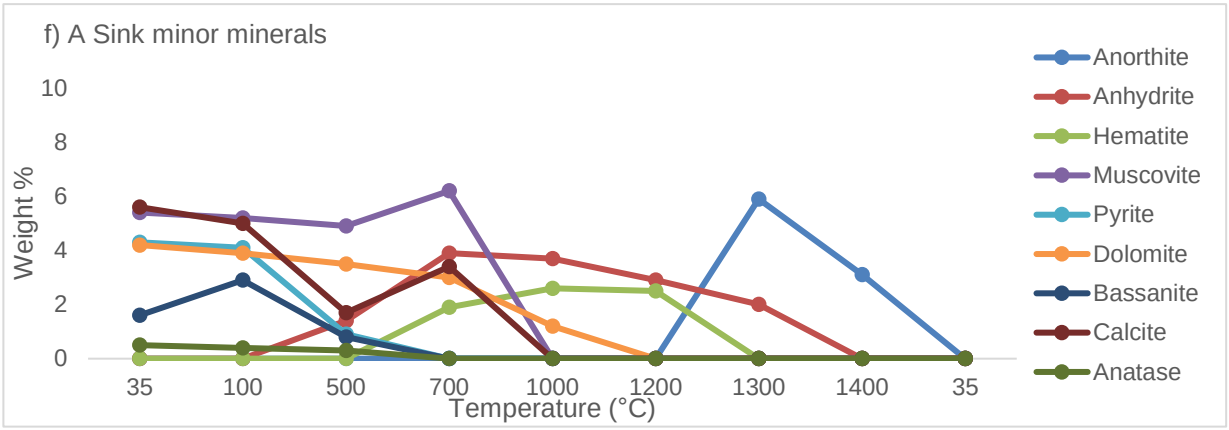

Figure 4-10(f) HT-XRD results for LTA of Sink A minor minerals

Figure 4-10 HT-XRD results for LTA of Feed A, Float A, and Sink A (%), divided into minor and major minerals.

the molten solutions at elevated temperatures during the combustion of the coal samples. During the HT-XRD experiments of LTA for Feed A, it is evident that quartz, which is an impure mineral, disappear at 1200°C and 1300°C, in the LTA samples of Sink A and Feed A respectively. Quartz, which could be pure submicron particles, is stable and persists in the LTA of Float A throughout the experiment. The relationship between the transformation of quartz at high temperatures and the mineral associations (reported in Table 4-2) can be summarised as follows; when impure quartz is associated with excluded kaolinite in the stone and carbominerites, transformation occurs due to metakaolinite and melt formation. However, when pure quartz grains are associated with included kaolinite, significantly less to almost no transformation of pure quartz will occur, as evident from the pure quartz grains which could be present in the LTA of Float A. The decrease in the quartz content above 1300°C coincides with the melting (or partial melting) of mineral matter at high temperatures.

A previous investigation, by Matjie (2008) was conducted on the mineral transformations in the LTA samples of South African coal with high ash fusion temperature and high proportions of SiO_2 and Al_2O_3, and its density separated fractions under oxidizing conditions, using a CSIRO dynamic HT-XRD equipment (Creelman *et al.*, 2013; Matjie, 2008). This author found that quartz, which could be an impure mineral associated with fluxing minerals and kaolinite, in the LTA sample of the feed coal reacted and completely disappeared at 1400°C to form the amorphous phase. These quartz grains in the LTA samples of the float and sink fractions decomposed and disappeared at 1300°C to form the amorphous phase. However, other researchers found that quartz contents in the low temperature radio-frequency ash samples, obtained from medium-volatile bituminous coal, have high calcium and iron proportions and a low ash fusion temperature.

The proportion of quartz decrease and form amorphous phase as the temperature increased from 1000°C to 1200°C when using HT-XRD analysis (French *et al.*, 2001). Other researchers found that when impure quartz transforms at an elevated temperature below the melting temperature of quartz, the structure of its polymorph opens and reacts with cations (Na^+, K^+ dissolved in water pores in the coal samples) and lowers the melting point of the quartz (Benson, 1987; Bryers, 1996; Raask, 1985; Ward, 1984; Ward & French, 2005). This may be due to the inversion of quartz which was also observed at temperatures of 575°C by previous authors (Vassileva & Vassilev, 2006). Another reason for this phenomenon may be due to the initial occurrence of impure quartz as part of the microscopic plant particles and thus associated with fluxing minerals and the reactive organic matter, i.e., the macerals (Creelman *et al.*, 2013).

Kaolinite is the dominant clay mineral, as observed from the XRD results in Figures 4-4 to 4–6. In the LTA of Feed A, kaolinite decomposed at 700°C, with traces still present at 1000°C in the LTA of Feed A and Float A. Dehydration of kaolinite in the coals that contain a high proportion of extraneous kaolinite is complete at around 1000°C. Initial decomposition of kaolinite occurs through dehydroxylation, when an OH group is released, at temperatures ranging from 450°C to 600°C to form an amorphous phase referred to as metakaolinite ($Al_2O_3 \cdot 2SiO_2$) (French *et al.*, 2001). Kaolinite in the LTA samples produced from other coals decomposes and disappear 500° C to 600°C to form amorphous metakaolinite (French *et al.*, 2001; Matjie, 2008). However, kaolinite in the LTA of the sink fractions decompose and disappear at 700°C to form the amorphous phase (Matjie, 2008). Upon the interaction of metakaolinite with fluxing cations (such as Na^+, K^+, Ca^+ and Fe as ferrous (Fe^{2+})) in the water pores in coal and transformed products (CaO, MgO, FeO) of dolomite, calcite and pyrite, new aluminosilicate phases form which subsequently fuse or melt at high temperatures associated with coal combustion (Creelman *et al.*, 2013; Matjie *et al.*, 2008; Ward, 2002; Ward, 2016). Decomposition and transformation of extraneous clay minerals at elevated temperatures, especially kaolinite, lead to the formation of mullite ($3Al_2O_3.2SiO_2$), tridymite (SiO_2) as well as Ca-Mg silicates (Vassileva & Vassilev, 2006).

Calcite decomposes at low temperatures, as observed in Figure 4-10. Free CaO is thus available to react with metakaolinite at low temperatures. Decomposition of dolomite occurs at 1000°C for the LTA of Feed A and Sink A, while dolomite entirely disappears below 1000° C in the LTA of Float A. This decomposition at 1000°C is as a result of the association of high amounts of dolomite and kaolinite in the carbominerites of Feed A and Sink A as observed in Table 4-2. The decomposition of dolomite at low temperatures in the LTA of Float A fraction can be explained by the lack of mineral associations in the float fraction.

Pyrite decomposes at 500°C in the LTA of Feed A, Float A, and Sink A where association with kaolinite is observed in the stone fragments and carbominerites of Feed A and Sink A. Trace amounts of excluded siderite ($FeCO_3$) are observed in Sink A. The reported decomposition temperature for pyrite (Matjie *et al.*, 2012a) is between 340°C and 530°C. At high temperatures, excluded pyrite will interact exothermically due to the reaction of oxygen with the sulphur, whereas the excluded siderite will expel CO_2 through an endothermic reaction. Both of these reactions will lead to the formation of an iron oxide residue (Matjie *et al.*, 2012a; Ward, 2002).

The HT-XRD results for LTA of Feed B, Float B, and Sink B can be observed in Figure 4-11. Significantly low levels of quartz are observed in the LTA of Feed B, and decomposition of quartz is observed at 1300°C and 1400°C for the LTA of Feed B and Sink B, respectively. The quartz diminishes at a significantly low temperature of 700°C in the LTA of Float B. The mineral associations for Feed B, based on QEMSCAN results (Rautenbach *et al.*, 2019), are reported in Table 4-3. Association of quartz with kaolinite is mainly observed in the stone fragments of Feed B and Sink B. The decomposition of quartz at high temperatures are due to these associations. Lower levels of quartz are also present in the ash sample as determined by XRD analysis. Polymorphic transformation of quartz to tridymite is observed at 1300°C for the LTA of Sink B. Although quartz is mainly stable up to 1300°C the decrease in quantities can be either due to the dissolution of quartz into the melt or as a result of solid-state reactions of quartz with liberated fluxing elements (Ca^{2+}, Mg^{2+}, and Fe^{2+}) (Vassileva & Vassilev, 2006).

Decomposition of kaolinite occurs at 700°C in the LTA of Feed B, Float B, and Sink B, which leads to the formation of metakaolinite. Calcite decomposes below 1000°C, while the decomposition of dolomite occurs at 1000°C in the LTA of Feed B and at 700°C in the LTA of Float B. Evidently, no traces of dolomite, bassanite or lime are detected for the LTA of Sink B, which correlates with the XRD and XRF results. This is due to the very low proportion of calcite in the LTA of Sink B. According to Vassilev *et al.,* (1995) the decomposition of calcite and dolomite in the high-rank coal occurs in the range of 680°C to 915°C. According to the mineral associations reported in Table 4-3, calcite is associated with kaolinite in the carbominerites and stone fragments present in Feed B and Sink B, while 100% of calcite is associated with included kaolinite within the float fraction, thus resulting in the decomposition at 700°C in the LTA of Float B.

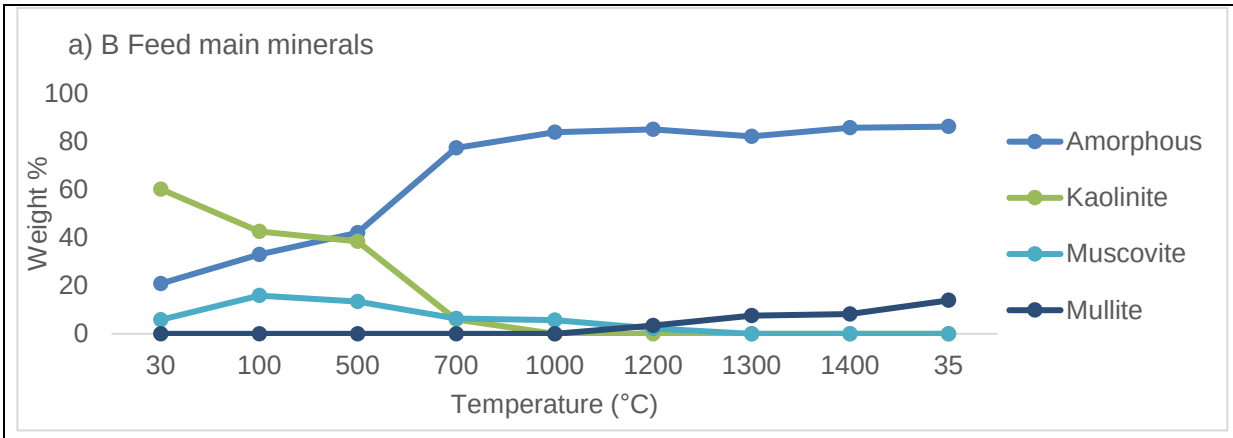

Figure 4-11(a) HT-XRD results for the LTA of Feed B main minerals

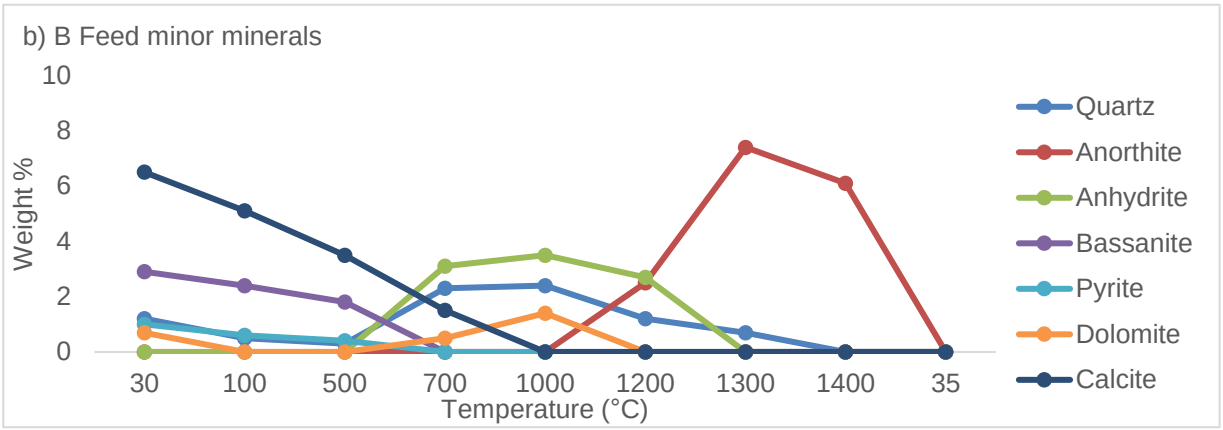

Figure 4-11(b) HT-XRD results for the LTA of Feed B minor minerals

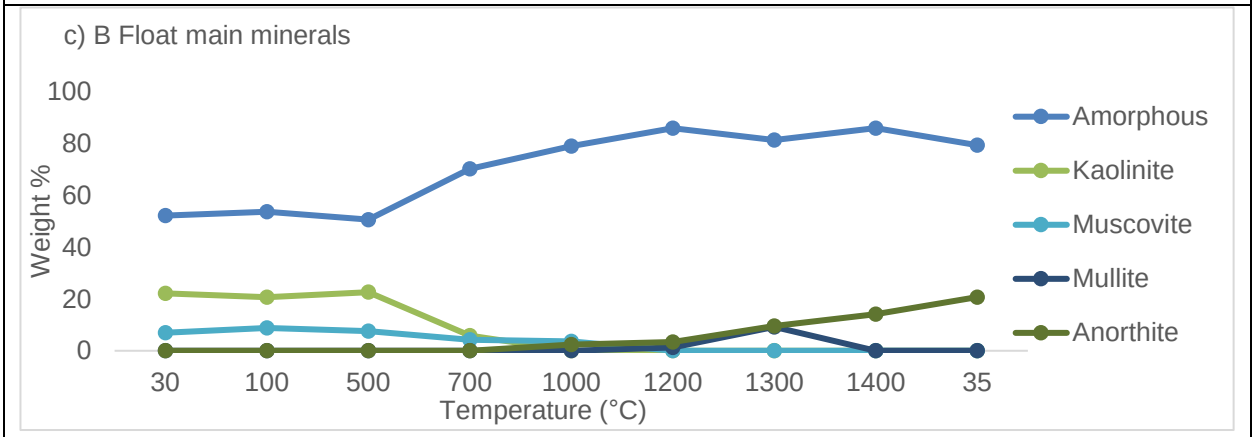

Figure 4-11(c) HT-XRD results for the LTA of Float B main minerals

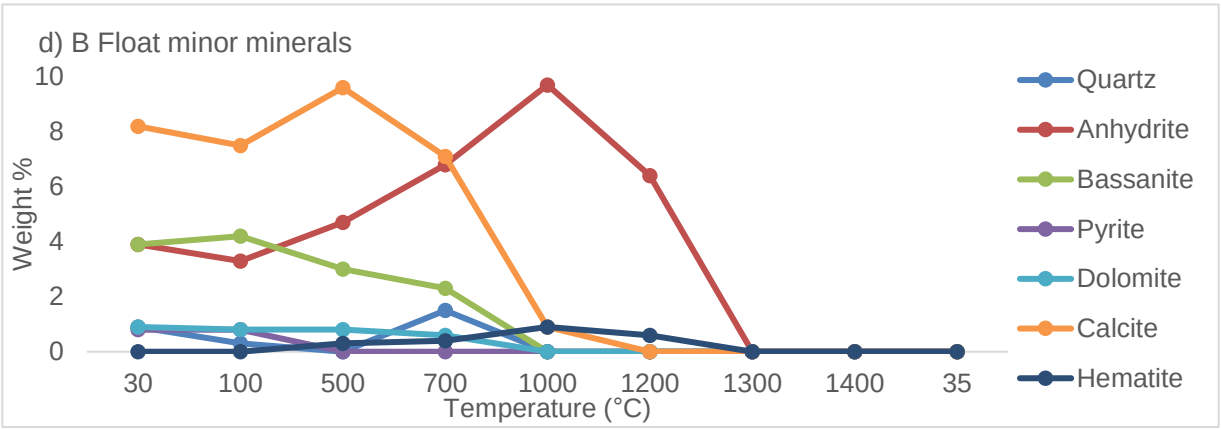

Figure 4-11(d) HT-XRD results for the LTA of Float B minor minerals

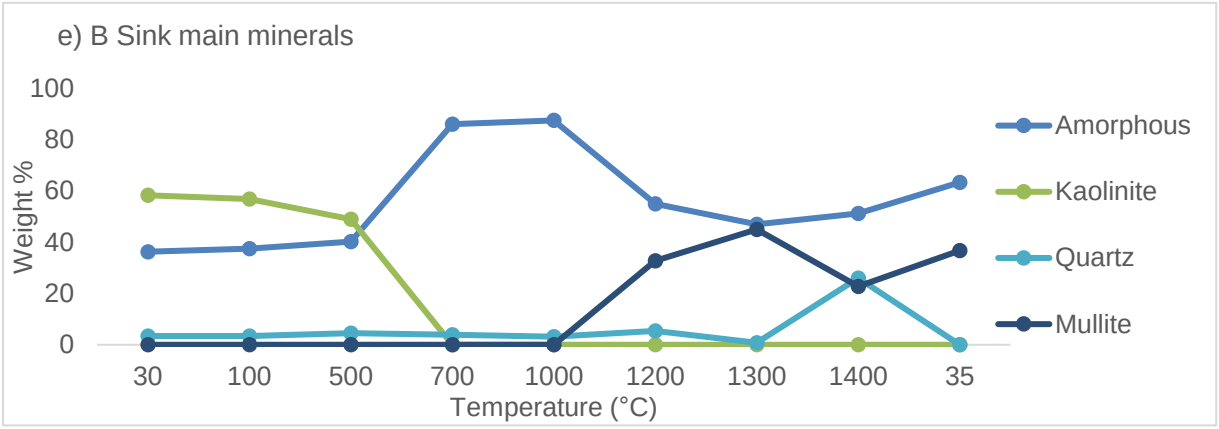

Figure 4-11(e) HT-XRD results for the LTA of Sink B main minerals

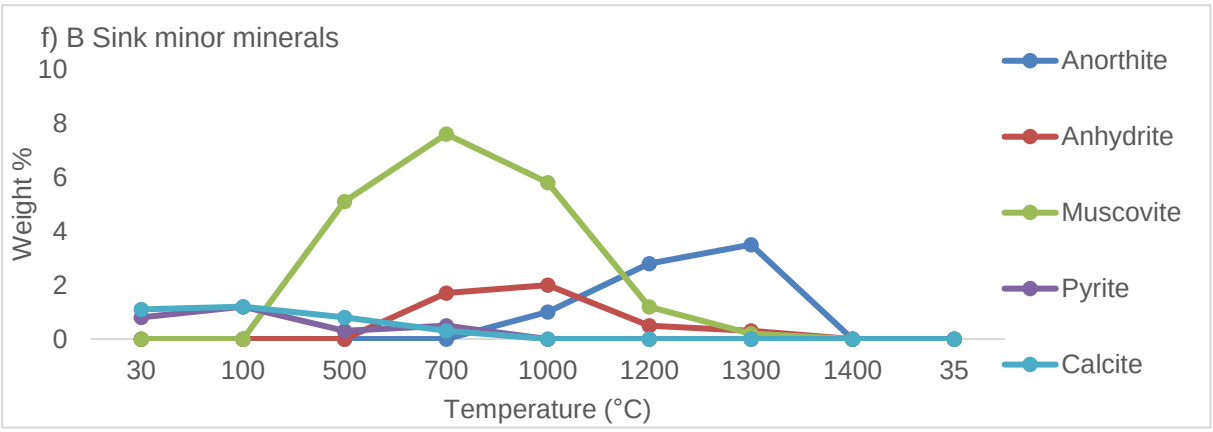

Figure 4-11(f) HT-XRD results for the LTA of Sink B minor minerals

Figure 4-11 HT-XRD results for the LTA of Feed B, Float B, and Sink B (%), divided into minor and major minerals.

Dolomite decomposition occurs at 1000°C in the LTA of Feed B due to association with kaolinite in the carbominerites, included minerals in this coal, as well as in the stone fragments. Other minerals that form due to the decomposition of carbonates include anhydrite ($CaSO_4$) at high temperatures and bassanite ($CaSO_4 \cdot ½H_2O$) at low temperatures ranging from 100°C and 400°C. In addition, included calcite which is coalesced or associated with either dolomite, pyrite or kaolinite within coal macerals (calcite + pyrite + dolomite + kaolinite + macerals) reacts differently at different temperatures to form transformed products of minerals and amorphous phase than extraneous calcite (discrete particle of calcite) during combustion and gasification (Matjie, 2008; Matjie *et al.*, 2011; Van Alphen, 2005).

Pyrite (FeS_2) is the principal Fe-bearing mineral that occurs in the LTA residues of all samples evaluated in this study. The mineral associations of pyrite in Feed B are mainly associated with cleat infillings, while 100% of pyrite in the Float B fraction is included, and 100% excluded pyrite is associated with cleat infillings.

Mineral transformations, determined by HT-XRD, in the LTA of Feed C, Float C, and Sink C can be observed in Figure 4-12. Quartz persists to high temperatures during HTXRD analysis and can be explained by the mineral associations reported in Table 4-4. Quartz is mainly associated with kaolinite in the stone fragments and carbominerites in Feed C and Float C. Association of quartz and included kaolinite is observed in the float fractions, thus explaining the decomposition of quartz at 1300°C as a result of the interaction between quartz and included kaolinite. The higher decomposition temperature of kaolinite in the LTA of Sink C can be related to the association of kaolinite with (>80%) stone minerals as reported in Table 4-4.

Pyrite associations in Feed C are mainly with carbominerite and included minerals in the feed fraction. 100% of the pyrite in the float fraction is associated with included minerals, and in Sink C. The excluded pyrite is associated with cleats and stone minerals as well as carbominerites. A decrease in the pyrite content is observed as the temperature increased up to 700°C, after which the pyrite decomposes.

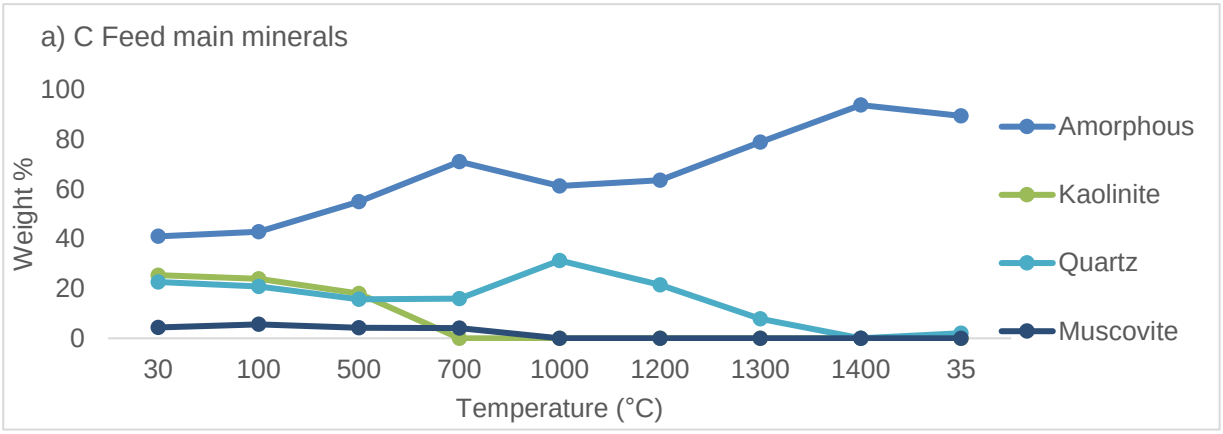

Figure 4-12(a) HT-XRD results for the LTA of Feed C main minerals

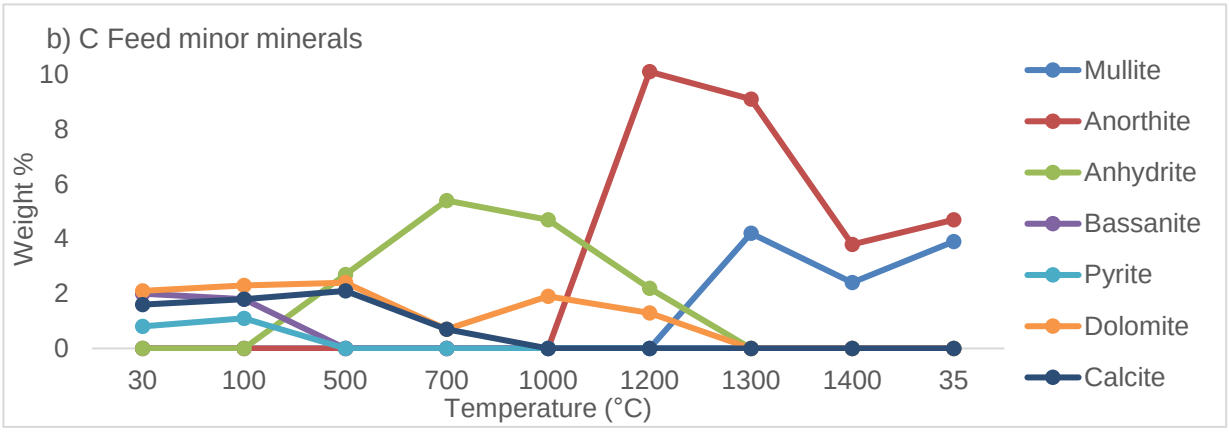

Figure 4-12(b) HT-XRD results for the LTA of Feed C minor minerals

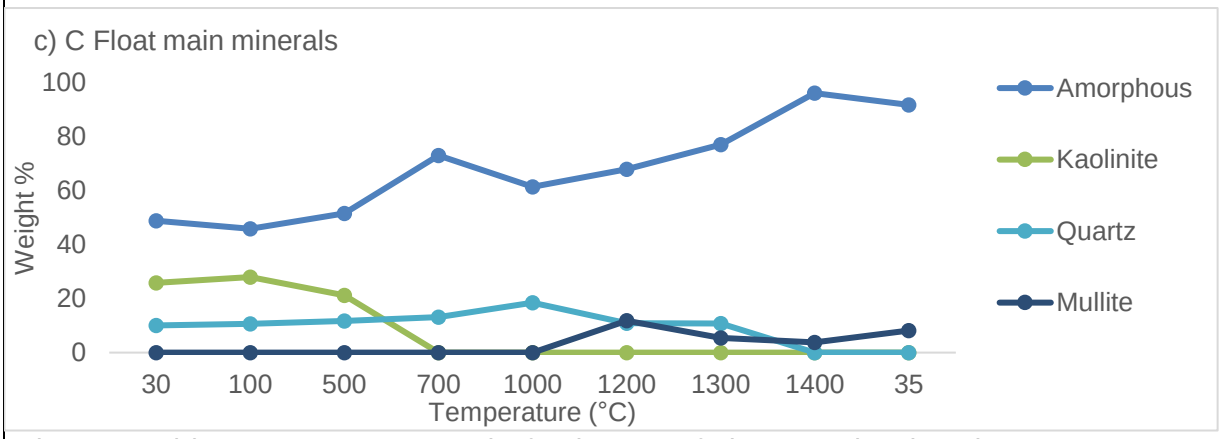

Figure 4-12(c) HT-XRD results for the LTA of Float C main minerals

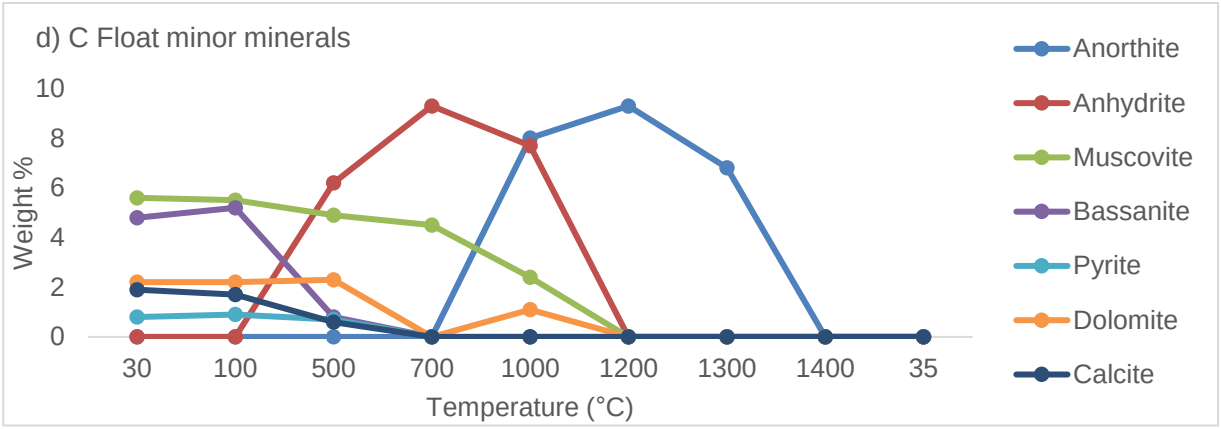

Figure 4-12(d) HT-XRD results for the LTA of Float C minor minerals

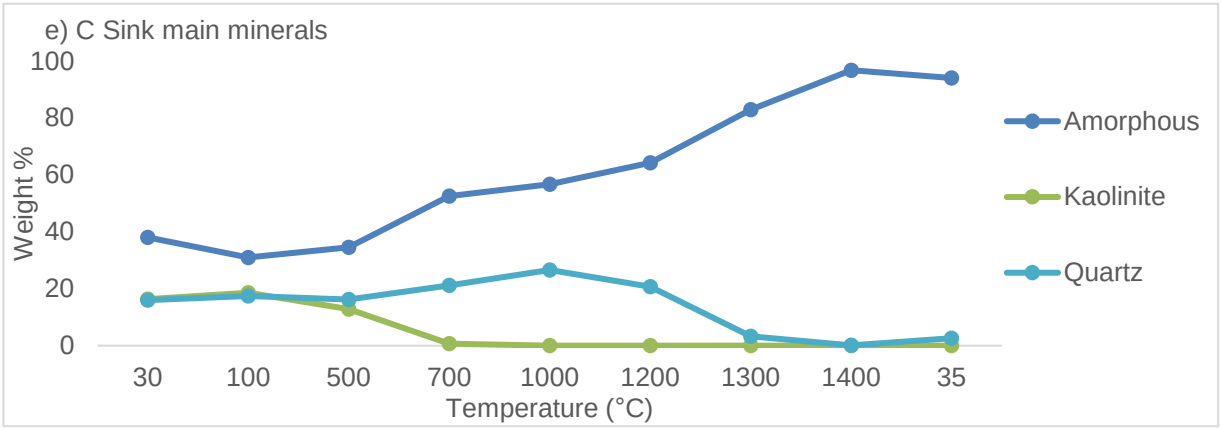

Figure 4-12(e) HT-XRD results for the LTA of Sink C main minerals

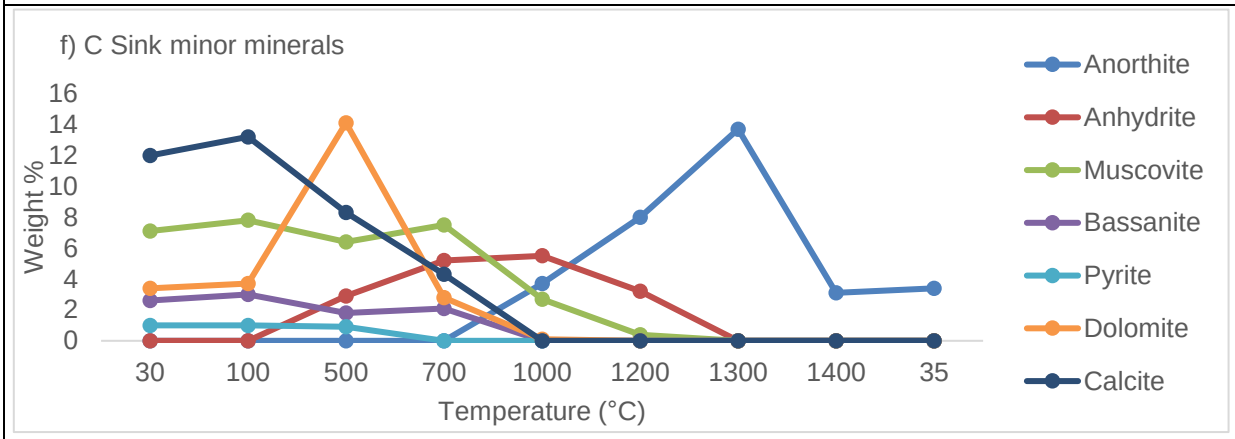

Figure 4-12(f) HT-XRD results for the LTA of Sink C minor minerals

Figure 4-12 HT-XRD results for the low-temperature ashes of Feed C, Float C and Sink C (%), divided into minor and major minerals.

The transformed product hematite (Fe_2O_3) of the excluded/liberated pyrite in the LTA samples of coals and their density separated fractions appears at temperatures ranging from 500°C and persists up to high temperatures of 1200°C to 1400°C, as expected.

Muscovite/Illite is present in the LTA residues of Feeds A, B, and C, from ambient temperature and persist up to temperatures ranging from 1000°C to 1300°C. According to the mineral associations, reported in Tables 4-2 to 4–4, illite is mainly associated with stone minerals, which explains the high decomposition temperatures of 1000°C to 1300°C. The clay minerals lose an OH-group from their lattice at low temperatures and will form mullite or spinel phases from approximately 950°C to 1050°C (Vassileva & Vassilev, 2006; Ward, 2016). K^+ or K_2O, will fuse and react with metakaolinite at approximately 1200°C to 1350°C, which in turn will lead to the formation of slag by lowering the ash fusion temperature (AFT) (Reifenstein *et al.*, 1999; Ward, 2002; Ward, 2016).

These mineralogical results for the LTA samples produced from the coals and density separated fractions are similar to those obtained for the LTA samples of other coals (French *et al.*, 2001; Matjie, 2008). The HT-XRD results for the LTA samples produced in this study reveal that anhydrite appears at 200°C and persists to high temperatures of 1200°C and 1300°C. The decomposition of anhydrite will augment the formation of a melt as well as the formation of calcium aluminum silicate minerals and calcium aluminosilicate amorphous materials. The presence of anhydrite correlates to the calcium content present in the LTA samples before HT-XRD tests.

Anorthite ($CaAl_2Si_2O_8$) crystallizes from the molten solution at 900°C and persists up to 1400°C. Anorthite can also be formed via solid-state reaction, where CaO (transformed product of excluded calcite/dolomite) reacts with mullite (transformed product of excluded kaolinite). It is interesting to note that no anorthite formation was observed for the LTA samples of Feed A or Float A, although traces of anorthite appears briefly at 1300°C in the LTA of Sink A. This is due to the low levels of CaO present in the LTA of Feed A and Float A, according to the XRF analysis. Another reason may be that the calcite and dolomite are not associated with kaolinite which is confirmed in Tables 4-2 to 4–4, where no associations between calcite, dolomite, and kaolinite were observed in Float A. Mullite crystallizes from the molten solution at high temperatures above 1000°C and persists throughout the experiment. Mullite is the main mineral phase present, with the amorphous phase, in the residue after cooling down to room temperature. Mullite forms as a result of 1) solid-state reactions at 800°C to 1400°C; 2) decomposition of clay minerals at 800°C to 1100°C, and 3) crystallisation from the melt phase at 1200° to 1600°C.

The amorphous phase increases as the mineral matter (i.e., crystalline material) in the LTA samples decompose with increasing temperatures. The significant difference between the LTA results and the HT-XRD on raw coal results were the amorphous content and can be observed in Figure 4-13. Carbon present in the raw coal sample will delay mineral transformations and cause reactions to occur at elevated temperatures than in the LTA samples.

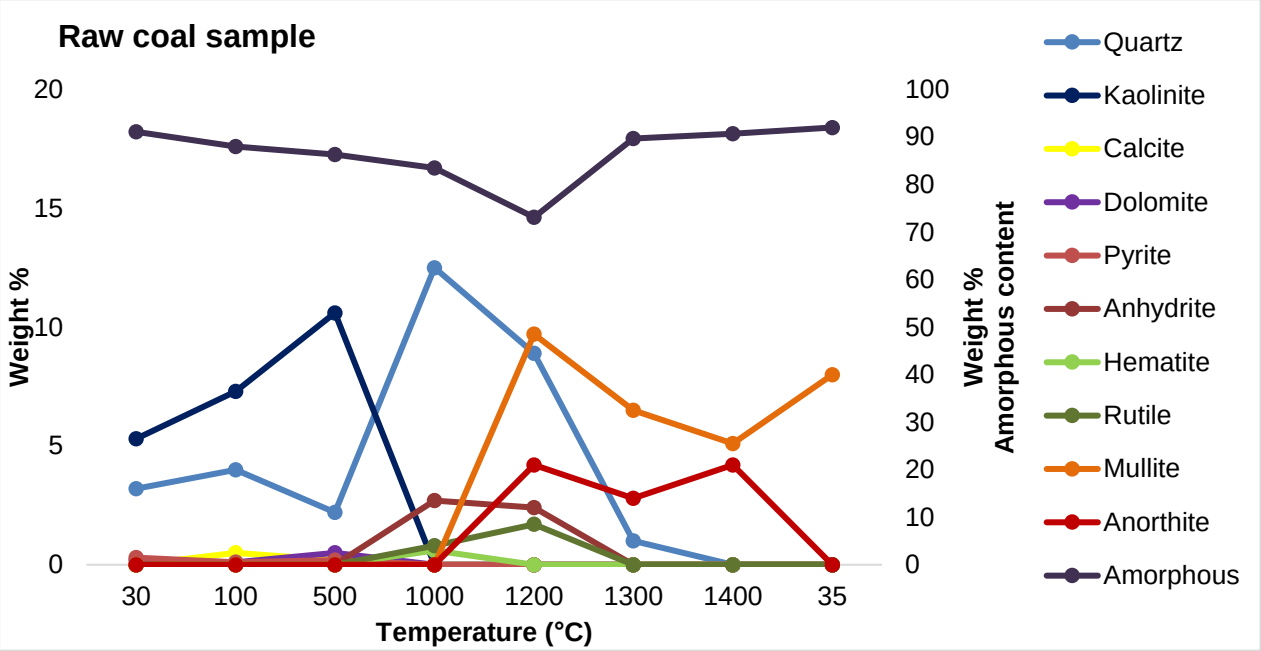

Figure 4-13 HT-XRD results for the raw coal sample (Feed A) (%).

4.4 Conclusions

Summary

Mineral matter associations, as well as the mode of occurrence in different coal samples, are of utmost importance as the mineral matter is the primary cause of slagging, sintering, and fouling of ash. The analytical results for the LTA samples obtained from

LTA plasma ashing of coals and their density separated fractions, have indicated that these groups of materials have different mineralogical and chemical properties. Three coal samples under investigation contain similar qualitative mineral compounds, although the differences between the quantitative mineral proportions as well as the mode of occurrence of these minerals and non-mineral inorganic elements within the various coal samples are unique. Low-

temperature ashing successfully oxidizes the organic matter, which leads to a comprehensive, investigation of the original and artifact minerals within the coal.

The excluded or extraneous minerals are mainly associated with stone fragments or cleats present in the feed coals, and their feed coals and their density separated fractions. The included minerals are mainly associated with organic material (macerals). Feed A consists of mainly included quartz and kaolinite, while the fluxing element-bearing minerals (calcite, dolomite, and pyrite) are mainly present as excluded minerals.

HT-XRD results indicate that the LTA sample of Feed A containing the included calcite and dolomite that are associated with kaolinite in the coal macerals decompose at a considerably low temperature of 300°C for calcite and 400°C for dolomite to form amorphous materials. This calcite transformation could be due the included calcite and dolomite that are associated with kaolinite in the coal macerals (Table 4-2). Furthermore, HT-XRD results show that the crystallisation of anorthite from the melt only occurs in the LTA residues of Sink A, Feed coal B, Float B, Sink B, Float C, Feed coal C and Sink C due to the reactions between CaO (transformed product of excluded calcite, organic calcium and included calcite associated with kaolinite) and metakaolinite (excluded and included kaolinite minerals coalesced with calcite). Mullite also crystallizes from the molten solutions of the LTA samples of Feed coal A, Float A, Sink A, Feed B, Float B, Sink B, Feed C, and Float C. Gehlenite crystallizes from the molten solutions of LTA residue of Feed B that contains 7% to 15% CaO. Mullite (transformed product of excluded kaolinite) could react with the transformed product of either excluded calcite or excluded dolomite to form anorthite via solid-state reactions.

The XRD analysis detected lower proportions of quartz (4%) in the LTA of Feed B in comparison with the LTA residues of Feeds A and C containing 25% quartz, while proportions of quartz mainly reported to the LTA residue of the sink fractions, thus occurs as excluded quartz particles. Kaolinite is mainly present in LTA of Feed B as discrete particles, or associated with excluded minerals (rock fragments), while the fluxing element-bearing minerals (calcite, dolomite, and pyrite) that are associated with kaolinite are present as included minerals in the float fractions and also in the excluded minerals present in the sink samples. Anorthite formation occurs at high temperatures (1200°C to 1300°C).

The significant differences in mode of occurrence of minerals are observed between Feed A and Feed B, whereas Feed C indicates similarities as well as variation with these samples. Feed C contains mainly included kaolinite and excluded quartz, while the fluxing-bearing minerals mainly report to the sink C fraction.

Conclusions

The LTA result for the feed coal and its density separated fractions, as well as the XRD analysis results of the LTA samples, have shown that these samples contain different contents of mineral matter, non-mineral inorganics and minerals. QEMSCAN results for the different feed coals indicate that these samples contain different proportions of mineral-maceral associations and minerals. Therefore, the mineral matter in the LTA samples of the Float (containing included minerals) and sink (containing mainly excluded minerals) fractions of the different feed coals evaluated in this study react differently during the HT-XRD experiments. QEMSCAN results show that:

- The mineral-maceral associations in the carbominerite, stone fragment and included particles in the Feed A may lead to the formation of slags during the combustion of this coal at elevated temperatures. Mullite and anorthite can crystallize from the molten solution during the cooling of it to room temperature. Also, amorphous aluminosilicate materials will be formed during the crystallisation of these slagging minerals
- While the mineral-maceral associations in the cleats in Feed A and Float A will not lead to slag formation of this sample. Mullite and anorthite can form at elevated temperatures of > 1100°C via the solid-state reactions.
- The mineral-maceral associations in the carbominerites and stone fragments present in Sink A or Feed A will cause slag formation at elevated temperatures.
- The mineral-maceral associations in Float B, cleats, and stone particles in Feed B and cleats in Sink B will not lead to a melt during the HT-XRD experiments.
- The mineral-maceral associations in the carbominerite and included minerals in Feed B, stones and carbominerites in Sink B will cause a melt in the HT- XRD analyser.
- The mineral-maceral associations in Feed C will be responsible for the formation of slag during the combustion of this sample in the HT-XRD analyser.

The HT-XRD and QEMSCAN results for the samples evaluated in this study are in good agreement. These coal samples will behave differently based on the mode of occurrence of mineral matter. Based on the HT-XRD results for the LTA samples of Feed A, Float A, and Sink A, Feed A is non-slagging material, and no minerals (anorthite, gehlenite, and mullite) that are associated with the slagging formation were detected during the combustion of feed coal A in the HT-XRD analyser. This implies that the high proportions of pyrite in the feed coal A is extraneous pyrite cleats and not associated with kaolinite. These excluded pyrite cleats contribute little or minimal, to the melt formation during the combustion of this coal.

Included minerals in the LTA sample of Feed B will form mainly anorthite that will end up in the ash, as well as, mullite at 1300°C. The excluded minerals in Feed B will form anorthite between 1200°C and 1300°C and mullite at 1200°C, which will persist until the cool down temperature.

Mullite as well as anorthite will form during the thermal treatment of the included minerals in Feed C, while the transformations and interactions of excluded fluxing minerals (calcite, pyrite, and dolomite) associated with kaolinite will lead to the formation of anorthite at 1000°C in the LTA of Feed C. Organically associated inorganic elements will form slag due to the association of the fluxing elements (CaO, MgO, FeO) with kaolinite in the coal sample.

This study aimed to better understand transformations and interactions of mineral matter in the coal feedstock and their density separated fractions at elevated temperatures without making any assumptions, using a dynamic HT-XRD analyser.

The authors would like to thank various crucial role players for their contributions and assistance with this study. Thanks are expressed to Sasol and South African Research Chairs Initiative of the DST and NRF (Coal Research Chair Grant Nos. 86880, UID85643, UID85632) for the financial contributions, Vincent Dube at SABS Secunda for the assistance with the density separation, Ben Ashton at Sasol R&T for guidance with the HT-XRD experiments, Shinelka Singh for QEMSCAN analysis, as well as all the relevant personnel at the University of New South Wales for XRF analysis on the LTA samples.

This work was supported by the National Research Foundation [86880,UID85632,UID85643];and Sasol South Africa.

Chapter References

Babcock & Company, W. 1923. Steam: its generation and use: Babcock & Wilcox Company.

Benson, S.A. 1987. Laboratory studies of ash deposit formation during the combustion of Western U.S. coals. The Pennsylvania State University.

Bryers, R.W. 1996. Fireside slagging, fouling, and high-temperature corrosion of heat-transfer surface due to impurities in steam-raising fuels. *Progress in Energy and Combustion Science*, 22(1):29-120.

Creelman, R.A., Ward, C.R., Schumacher, G. & Juniper, L. 2013. Relation between coal mineral matter and deposit mineralogy in pulverized fuel furnaces. *Energy Fuels*, 27:5714-5724.

Falcon, R.M.S. & Ham, A.J. 1988. The characteristics of Southern African coals. *Journal of Southern African Institution of Mineral and Metallurgy*, 88(5):145-161.

Falcon, R.M.S. & Snyman, C.P. 1986. An introduction to coal petrography: Atlas of petrographic constituents in the bituminous coals of Southern Africa. Johannesburg, RSA: The Geological Society of South Africa.

Frazer, F.W. & Belcher, C.B. 1973. Quantitative determination of the mineral-matter content of coal by a radiofrequency-oxidation technique. *Fuel*, 52(1):41-46.

French, D., Dale, L., Matulis, C., Saxby, J., Chatfield, P. & Hurst, H.J. 2001. Characterization of mineral transformations in PF combustion by dynamic high-temperature X-ray diffraction analysis. Paper presented at the Proceedings of the 18th Pittsburgh International Coal Conference, Newcastle, Australia.

Gluskoter, H.J. 1965. Electronic low temperature ashing of bituminous coal *Fuel*, 44:285-291.

Jeffrey, L.S. 2005. Characterization of the coal resources of South Africa. J*ournal of Southern African Institution of Mineral and Metallurgy*, 105(2):95-102.

Mahlaba, J.S., Kearsley, E.P. & Kruger, R.A. 2011. Physical, chemical and mineralogical characterisation of hydraulically disposed fine coal ash from SASOL Synfuels. *Fuel*, 90:2491-2500.

Matjie, R., Li, Z., Ward, C.R., Bunt, J. & Strydom, C. 2016. Determination of mineral matter and elemental composition of individual macerals in coals from Highveld mines. *Journal of the Southern African Institute of Mining and Metallurgy*, 116(2):169-180.

Matjie, R.H. 2008. Sintering and slagging of mineral matter in South African coals during the coal gasification process. University of Pretoria.

Matjie, R.H., French, D., Ward, C.R., Pistorius, P.C. & Li, Z. 2011. Behaviour of coal mineral matter in sintering and slagging of ash during the gasification process. *Fuel Processing Technology*, 92(8):1426-1433.

Matjie, R.H., Li, Z., Ward, C.R. & French, D. 2008. Chemical composition of glass and crystalline phases in coarse coal gasification ash. *Fuel*, 87(6):857-869.

Matjie, R.H., Li, Z., Ward, C.R., Kosasi, J., Bunt, J.R. & Strydom, C.A. 2015. Mineralogy of Furnace Deposits Produced by South African coals during Pulverized-Fuel Combustion tests. *Energy Fuels*, 29(12):8226-8238.

Matjie, R.H., Van Alphen, C. & Pistorius, P.C. 2006. Mineralogical characterisation of Secunda gasifier feedstock and coarse ash. *Minerals Engineering*, 19(3):256-261.

Matjie, R.H., Ward, C.R. & Li, Z. 2012a. Mineralogical Transformation in Coal Feedstocks during Carbon Conversion, based on Packed-Bed Combustor Tests: Part 1 Bulk Coal and Ash Studies. *Coal Combustion and Gasification products*, 4:45-54.

Matjie, R.H., Ward, C.R. & Li, Z. 2012b. Mineralogical transformations in coal feedstock during carbon conversion, Based in packed-bed combustor tests: Part 2. Behavior of individual particles. *Coal Combustion and Gasification products*, 4:55-67.

Miller, R.N., Yarzab, R.F. & Given, P.H. 1979. Determination of the mineral-matter contents of coals by low-temperature ashing. *Fuel*, 58(1):4-10.

Norrish, K. & Hutton, J. 1969. An accurate X-ray spectrographic method for the analysis of a wide range of geological samples. *Geochimica et cosmochimica acta*, 33(4):431-453.

Pinetown, K.L., Ward, C.R. & Van der Westhuizen, W.A. 2007. Quantitative evaluation of minerals in coal deposits in the Witbank and Highveld Coalfields, and the potential impact on acid mine drainage. *International Journal of Coal Geology*, 70:166-183.

Raask, E. 1985. The mode of occurrence and concentration of trace elements in coal. *Progress in Energy and Combustion Science*, 11(2):97-118.

Rautenbach, R., Strydom, C., Bunt, J., Matjie, R., Campbell, Q. & Van Alphen, C. 2019. Mineralogical, chemical, and petrographic properties of selected South African power stations' feed coals and their corresponding density separated fractions using float-sink and reflux classification methods. *International Journal of Coal Preparation and Utilization*, 39(8):421-446.

Reifenstein, A.P., Kahraman, H., Coin, C.D.A., Calos, N.J., Miller, G. & Uwins, P. 1999. Behaviour of selected minerals in an improved ash fusion test: quartz, potassium feldspar, sodium feldspar, kaolinite, illite, calcite, dolomite, siderite, pyrite and apatite. *Fuel*, 78(12):1449-1461.

Rietveld, H.M. 1969. A Profile refinement method for Nuclear and Magnetic structures. *Journal of Applied Crystallography* 2:65-71.

Snyman, C.P. 1998. Coal. *(In* Wilson, M.G.C. & Anhaeusser, C.R., *eds*. The Mineral Resources of South Africa. South Africa: Council of Geoscience. p. 136-205).

Taylor, J.C. 1991. Computer Programs for Standardless Quantitative Analysis of Minerals Using the Full Powder Diffraction Profile. *Powder Diffraction*, 6(1):2-9.

Van Alphen, C. 2005. Factors influencing fly ash formation and slag deposit formation (slagging) on combusting a South African pulverised fuel in a 200 MWe boiler. University of the Witwatersrand Johannesburg, South Africa.

Van Dyk, J., Benson, S., Laumb, M. & Waanders, B. 2009. Coal and coal ash characteristics to understand mineral transformations and slag formation. *Fuel*, 88(6):1057-1063.

Van Dyk, J.C., Melzer, S. & Sobiecki, A. 2006. Mineral matter transformation during Sasol-Lurgi fixed bed dry bottom gasification - utilization of HT-XRD and FactSage modelling. *Minerals Engineering*, 19(10):1126-1135.

Vassileva, C.G. & Vassilev, S.V. 2006. Behaviour of inorganic matter during heating of Bulgarian coals: 2. Subbituminous and bituminous coals. *Fuel Processing Technology*, 87(12):1095-1116.

Ward, C.R. 1984. Coal Geology and Coal Technology: Blackwell Scientific Publications; Illustrated edition edition (1984).

Ward, C.R. 2002. Analysis and significance of mineral matter in coal seams. *International Journal of Coal Geology*, 50(1-4):135-168.

Ward, C.R. 2016. Analysis, origin and significance of mineral matter in coal: An updated review. *International Journal of Coal Geology*, 165:1-27.

Ward, C.R. & French, D. 2005. Relation between coal and fly ash mineralogy, based on quantitative X-ray diffraction methods. *World Coal Ash (WOCA), April*, 11:15.

CHAPTER 5

THE TRANSFORMATION OF INCLUDED AND EXCLUDED MINERALS IN SOUTH AFRICAN COAL SAMPLES DURING LABORATORY COMBUSTION STUDIES

Rudelle Rautenbach, Ratale. H. Matjie, Christien. A. Strydom, John. R. Bunt, Chris van Alphen

This work will be submitted to the **Coal Combustion and Gasification Products** journal for publication.

Abstract

The main objective of this work was to relate the coalescence of included minerals and the fragmentation of excluded minerals, during combustion, to the slagging propensities of South African coal samples. By incorporating the behaviour of mineral matter under combustion conditions, into ash-deposition prediction methods, the heterogeneous nature of ash properties was considered, which were disregarded in previous traditional ash deposition predictions.

The mode of occurrence of mineral matter played a crucial role in the formation of high-temperature mineral phases under combustion conditions. The float and sink fractions of the three different South African coal samples provided different results when subjected to elevated temperatures.

Formations of high-temperature minerals, such as mullite and cristobalite, were mainly due to the transformation reactions of kaolinite and quartz at elevated temperatures respectively. However the formation of anorthite at elevated temperatures can be attributed to the interaction of fluxing minerals (calcite, dolomite, pyrite and siderite) that are associated with kaolinite in the coal sample. The presence of anorthite, mullite and alumina-silicate glasses at elevated temperatures can therefore be used as an indication of the slagging propensity of South African coal. Implementation of the results obtained from this study will be significant in thermochemical processes to minimise ash deposition, slagging and equipment erosion problems.

Keywords: included minerals, excluded minerals, anorthite, slag prediction

5.1 Introduction

Coal-fired power stations in South Africa generate more than 90% of the country's electricity by combusting pulverized coal (Jeffrey, 2005; Wagner *et al.*, 2018). Nevertheless, several problems exist that are related to ash deposition during combustion, which has a negative effect on boiler efficiency. There are, in general, three sequential processes related to ash deposition. The minerals are, firstly, transformed to high temperature minerals in ash particles; these ash particles are conveyed onto the heat transfer surfaces, after which the ash particles retained on these deposit surfaces attach to the walls of the boilers (Wang & Harb, 1997; Yan *et al.*, 2001). Ash-related operational problems during combustion include slagging, fouling, agglomeration as well as corrosion (Gupta *et al.*, 1998; Wen *et al.*, 2016; Wen *et al.*, 2015; Yan *et al.*, 2001). Slagging occurs at elevated temperatures in the radiative section, while fouling deposits are found in the convective heating section at lower temperatures (Rushdi *et al.*, 2005). There are various factors which contribute to slagging such as molten fly ash particles sticking to the surface, fly ash particles carried by the gas flow to the boiler walls as well as the low excess air environment resulting in a reduced atmosphere which consequently increases the number of materials with lower melting points.

The slag build-up may result in the formation of a molten phase due to the increase of the surface temperature. The surface of the slag deposit may also act as an efficient fly ash collector. Large slag deposits may break loose from the boiler wall and cause damages to the bottom of the furnace. These large slag deposits with hard minerals (anorthite, microcline (potassium feldspars), mullite, quartz and cristobalite) can abrade and erode plant equipment while the large slag deposits with soft minerals and aluminosilicate glasses will not wear away equipment during combustion. It furthermore reduces the heat transfer rate leading to dramatic fouling deposits due to the increase of the temperature within the convective pass. Fouling occurs when the ash deposits attach to convective heat exchange surfaces exposed to high temperatures such as reheaters, superheaters, and economisers (Bryers, 1996; Erickson *et al.*, 1995; Matjie *et al.*, 2011; Van Dyk *et al.*, 2009; Yan *et al.*, 2001).

Coal mineral matter can be characterised into three groups, included or inherent minerals that are closely associated with the organic matrix, excluded minerals which are present as discrete mineral particles or rock fragments and organically associated inorganic elements. Various mineral transformations, complex interactions and phase changes occur in the mineral matter of coal during coal utilisation processes. These interactions of minerals at elevated temperatures are the main cause of ash deposition problems such as slagging and fouling. The mineral

associations (modes of occurrence of minerals in coal samples) are essential for the investigation of ash deposition problems during coal utilisation (Matjie, 2008; Van Alphen, 2005; Ward, 2002).

Comprehensive studies on the mineral matter in coal have been conducted due to the significance of coal mineralogy during combustion. These previous studies, however, focused on the mineral matter as a whole and neglected the impact of the transformation of included and excluded minerals separately (Wen *et al.*, 2016). In order to comprehend and manage the slag tendencies of coals during combustion, thorough investigation and characterisation of the transformation of the included minerals in the float fraction, excluded minerals in the sink fraction, as well as the organically associated inorganic elements in the float fraction, should be conducted. The previous modelling of the behaviour of included minerals was based on two extremes; either no-coalescence or full-coalescence (Wigley *et al.*, 1997). Yan *et al.,* (2001), demonstrated the implication of the coalescence of included mineral matter during the deposition of ash particles by including a partial coalescence scheme in order to predict ash deposition. These authors concluded that during combustion, the ash chemistry, as well as the particle size, are mainly influenced by the coalescence and transformation of included mineral matter. According to Ward (2002), extensive knowledge regarding the correlation between the characteristics of the mineral matter in the parent coal and the formation of high-temperature minerals during coal utilisation is of importance in order to fully comprehend the mineral interactions taking place during coal utilisation (Ward, 2002).

The objective of this study was to explore the behaviour of included minerals in the float fraction (<1.5 g/cm^3), excluded minerals in the sink fraction (>1.9 g/cm^3) and organically bound inorganic elements in the float fraction (<1.5 g/cm^3) during coal utilisation in order to incorporate the mineral associations and mode of occurrence of minerals in the coal with slag prediction methods. By incorporating the behaviour of both included and excluded minerals under combustion conditions, the heterogeneous nature of ash properties is considered, which were disregarded in previous traditional ash deposition predictions. It is expected that included fluxing minerals (calcite, dolomite, and pyrite) that are associated with included kaolinite coalesce and form the molten solutions of calcium/magnesium/iron aluminosilicate during gasification and combustion of the coal. The high-temperature crystalline phases present in ash are primarily formed through the thermal decomposition of minerals, i.e. the decomposition of kaolinite and calcite will lead to the formation of mullite and lime, respectively (Hlatshwayo *et al.*, 2009; Matjie *et al.*, 2005; Matjie *et al.*, 2011; Matjie *et al.*, 2008; Unsworth *et al.*, 1988; Van Alphen, 2005). Mullite is the transformed product of excluded kaolinite associated with calcite/dolomite, which reacts with calcium oxide (transformed product of either excluded calcite or excluded dolomite) to form gehlenite

(intermediate phase). It is also assumed that the excluded kaolinite transform to mullite during the coal combustion at elevated temperatures, while excluded calcite or dolomite transformed to CaO or MgO at elevated temperatures and report to the ash content (Hlatshwayo *et al.*, 2009; Matjie, 2008; Van Alphen, 2005; Yan *et al.*, 2001).

Anorthite is hard Ca-rich mineral ($CaAl_2Si_2O_8$) and forms as a result of the reaction between CaO (transformed product of either included dolomite or calcite associated with included kaolinite) and metakaolinite (transformed of included kaolinite) at elevated temperatures (Hlatshwayo *et al.*, 2009; Unsworth *et al.*, 1988). It is reported that the ash deposition mechanism can be explained by following the formation of anorthite during coal utilisation (Unsworth *et al.*, 1988). CaO (transformed product of excluded calcite and dolomite) react with metakaolinite (transformed product of excluded kaolinite) to form gehlenite and anorthite via the solid state reactions. While the remnant particles of metakaolinite transform to mullite (Hlatshwayo *et al.*, 2009; Matjie, 2008; Van Alphen, 2005; Yan *et al.*, 2001).

5.1.1 The proposed slag prediction method

Several attempts to predict slagging behaviour of coals have been studied and are described in literature (Erickson *et al.*, 1995; Lawrence *et al.*, 2008; Lee & Lockwood, 1999; Ma *et al.*, 2007; Rushdi *et al.*, 2005; Wang & Harb, 1997), however, these prediction methods of the slagging and fouling propensities of coal contain various limitations. By using the ash chemistry of the coal as a prediction method of the behaviour during combustion, it is assumed that the inorganic material behaves homogeneously and approach equilibrium, which is not the case. While predictions based merely on the ash properties tend to exclude the mineral interactions at various temperatures during combustion (Bryers, 1996; Russell *et al.*, 2002).

Some of the empirical slag prediction indices were used in order to determine the slagging propensities of the three coals, and their density separated fractions under investigation. The empirical indices used were based on XRF analysis results which are the sum of the total elemental composition of the coal ash sample. The empirical indices reported in Table 5-1 did not predict slag behaviour, or only low slagging propensity, for South African coal samples, except for the iron to calcium ratio indices. These predictions were not accurate because slag and clinker formations do occur in South African boilers as a result of the mineral contents and their mode of occurrences (especially within the included minerals represented by the <1.5 g/cm^3 coal float fractions) in the South African coals. These empirical indices take the total acidic and the total basic elemental oxides present in both included and excluded minerals into the equation when calculating the slagging propensities.

Table 5-1 Prediction of the slagging propensities of the coal samples and their density separated coal fractions based on the XRF analysis results, as reported by (Rautenbach *et al.*, 2019b)

	Feed A	Float A	Sink A	Feed B	Float B	Sink B	Feed C	Float C	Sink C	Slag propensity
Slagging factor (F_s)	0.42 *low slag*	0.13 *low slag*	0.82 *low slag*	0.09 *low slag*	0.17 *low slag*	0.04 *low slag*	0.13 *low slag*	0.12 *low slag*	0.36 *low slag*	2.0 – 2.6 *(high slag)* > 2.6 *(severe slag)*
Base – Acid Ratio (B/A_R)	0.20 *low slag*	0.14 *low slag*	0.17 *low slag*	0.17 *low slag*	0.28 *low slag*	0.07 *low slag*	0.18 *low slag*	0.20 *low slag*	0.19 *low slag*	0.4 – 0.7 *(high slag)*
Silica percentage (Si_R)	76.2 *low slag*	83.5 *low slag*	80.3 *low slag*	77.9 *low slag*	65.7 *low slag*	89.7 *low slag*	79.2 *low slag*	75.4 *low slag*	79.7 *low slag*	50 – 65 *(severe slag)*
Silica to alumina ratio (Si/Al_R)	1.76 *medium slag*	1.90 *medium slag*	1.85 *medium slag*	1.29 *medium slag*	1.29 *medium slag*	1.31 *medium slag*	1.98 *medium slag*	1.58 *medium slag*	2.49 *medium slag*	
Iron to calcium ratio (Fe/Ca_R)	0.37 *high slag*	0.58 *high slag*	2.03 high slag	0.50 *high slag*	0.16 *high slag*	1.04 *low slag*	0.49 *high slag*	0.30 *high slag*	0.34 *high slag*	0.3 – 3.0 *(High/severe slag)*

F_s **= B/A_R x %S;** B/A_R **= $(Fe_2O_3+CaO+ MgO+Na_2O+ K_2O)/(SiO_2+ Al_2O_3+TiO_2)$;**

Si_R **= $(SiO_2$ x 100)/$(SiO_2+Fe_2O_3+CaO+ MgO)$;** Si/Al_R **= SiO_2 / Al_2O_3;** Fe/Ca_R **= $(Fe_2O_3$ / CaO);**

>1.9 g/cm^3 Sink fraction; <1.5 g/cm^3 float fraction

Alternative methods for the prediction of slagging behaviour for South African coal samples need to be investigated. These methods must incorporate the transformation of mineral matter, i.e. included minerals, excluded minerals and organically bound inorganic elements, as well as the mode of occurrence of mineral matter in the coals. This article will focus on the behaviour of included minerals in the <1.5 g/cm^3 float fraction and excluded minerals in the >1.9 g/cm^3 sink fraction under combustion conditions in order to relate coalescence of included minerals and the fragmentation and transformation of excluded minerals to slag formation of South African coal samples.

5.2 Experimental procedures

Feed coal to combustion, as well as the respective fly ash and coarse ash samples, were collected from three different power stations in South Africa using ISO 1988:1975 and ISO 13909-4:2016. The three coarse feed coal samples were submitted for density separation at the South African Bureau of Standards (SABS) laboratories in Mpumalanga, Secunda. A Samuel Osborne LTD jaw crusher was used for crushing the feed coal, and their respective density separated fraction to -500 µm +38 µm. The sample preparation is described in Rautenbach *et al*., (2019a). The density separation yielded two fractions, a float fraction <1.5 g/cm^3 and a sink fraction of >1.9 g/cm^3. Rautenbach *et al.,* (2019a) determined that the density separation successfully separated maceral-rich fractions (float fractions) with mineral-rich fractions (sink fractions). The float fractions contain high concentrations of macerals, fixed carbon, and volatile matter, while a decrease in the mineral matter present in the floats was observed after float-sink separation. The sink fractions consist of high proportions of siltstone, mudstone, sandstone, and pyrite, which relate to the high proportions of quartz and kaolinite concentrations present in the sink fractions (Rautenbach *et al.*, 2019a; Rautenbach *et al.*, 2019b). Proximate and ultimate analyses results of these feed, float, and sink samples, as well as the percentage yield of the fractions after density separation, are reported in Table 5-2, as described by (Rautenbach, *et al.*, 2019a)

Table 5-2 Proximate and ultimate analyses results for the feed coals, float and sink fractions with % yield after density separation (Rautenbach *et al.,* 2019a)

		Feed A	Float A	Sink A	Feed B	Float B	Sink B	Feed C	Float C	Sink C
Proximate analysis (wt %, db[a])	Ash	36.6	8.0	64.1	34.0	12.9	69.6	26.2	10.9	61.7
	VM[b]	22.2	33.9	16.7	21.3	29.3	16.5	22.9	28.7	17.4
	FC[c]	41.1	58.1	19.2	44.7	57.8	13.9	50.9	60.4	20.9
Ultimate analysis (wt %)	C	79.6	82.2	67.1	76.6	78.3	51.9	79.5	78.2	62.9
	H	4.7	5.3	4.8	4	4.5	4.7	3.9	4.3	3.5
	N	1.7	1.9	1.6	1.9	2	1.5	1.9	2.1	1.7
	S	2.1	0.9	4.8	0.5	0.6	0.6	0.7	0.6	1.9
	O[d]	13.9	10.7	26.5	17.4	15.2	41.8	14.6	15.4	32
% yield of fractions after density separation			13	24		12	16		22	5

[a] Dry basis; [b] Volatile matter; [c] Fixed Carbon; [d] By difference.

Ash samples were prepared from the feed coal as well as their density separated fractions by initially ashing the samples at 1000°C in a rotary kiln followed by subsequent heating up to 1100°C, 1200°C and 1300°C, respectively in a muffle furnace. The horizontal rotary kiln furnace was equipped with a lined steel reactor tube which was open at both ends in order to introduce air and emit volatile gaseous products. Approximately 5 kg of coal was introduced into the rotary kiln, which was then heated up to 1000°C at 10°C/min and then kept at 1000°C for three hours. The ash was recovered and divided into four sets of sample for higher temperature processing at 1100°C, 1200°C and 1300°C, respectively, in a muffle furnace. The ash was placed in clay trays inside the muffle furnace, which was connected to a fish pond pump to provide an oxidising environment. The furnace was heated up at a rate of 10°C/min and kept at the specific temperature for three hours before allowing to cool down inside the furnace chamber.

Contamination of chrome-bearing steel occurred during the ashing of coal in the rotary kiln and was evident from the analyses conducted on these samples. These steel or rust particles did not interact with minerals present in the coal samples during the burning of coals at elevated temperatures under air. The formation of slag phases at high temperatures as a result of the interaction between kaolinite and fluxing element-bearing minerals were not influenced by the presence of the chrome bearing steel and will thus not influence the XRD results. The prepared ash samples, as well as the collected samples from the power stations (fly ash and coarse ash), were characterised using X-ray diffraction (XRD), X-ray fluorescence (XRF) and QEMSCAN analyses.

XRD analysis was conducted using a NWU PANalytical X'Pert Pro instrument with an X'Celerator detector and a Co X-ray tube. The samples were spiked with a Si standard in order to determine the amorphous content and were consequently micronised using a McCrone micronising mill. X'Pert Highscore Plus software (Speakman, 2012) was used together with the International Centre for Diffraction Data (ICDD) program in order to determine the crystalline phases and the amorphous content present in the ash samples. The refined Rietveld method was used to quantify the crystalline and amorphous phases contained in the ash samples (Rietveld, 1969). XRD analysis results of the feed coals and their density separation fractions before ashing are displayed in Table 5-3, as reported by (Rautenbach *et al.*, 2019b)

Table 5-3 XRD analysis results (%) for the feed, float and sink fractions as reported by Rautenbach *et al.*, (2019a).

	Feed A	Float A	Sink A	Feed B	Float B	Sink B	Feed C	Float C	Sink C
Quartz	7.5	6.3	10	1	0.5	4.5	7.1	3	16.8
Kaolinite	18	11.7	27.7	20.2	8.8	59.6	18.7	9	26.3
Calcite	2.1	0.4	1.1	3.2	3.4	3.9	1.5	0.3	5.4
Pyrite	0.3	0	3	0.9		0.5	1.6		1.3
Muscovite	0.1	1.3		4	0.8	0.2	4.1		
Illite	1.2	0.6		3.5			1.6		
Microcline		0.8			0.8				
Portlandite			0.1			0.2			0.1
Goyazite		0.3			0.1			0.1	0.1
Dolomite	9.5	0.5	5.1	0.5	0.2	0.2	0.7	1	2
Anatase	0.2	0.6	0.2	0.2	0.3		0.2	0.1	0.5
Rutile				0.1		0.1			
Gypsum	0.8								
Fluorapatite	0.2	0.4			0.4			0.3	
Graphite	0.4						2.8		
Mineral matter	**39.9**	**22.9**	**47.2**	**33.6**	**15.3**	**69.2**	**35.5**	**13.8**	**52.5**
Amorphous (aluminosilicate glasses)	59.6	77	52.9	66.3	84.6	30.8	61.6	86	47.5

The elemental concentrations were determined by XRF analysis using an NWU PANalytical Axios MAX XRF instrument. An Rh X-ray tube was used to irradiate the pressed ash samples while a Super Q database was used in order to determine the elemental concentrations (Norrish & Hutton, 1969). Table 5-4 displays the XRF analysis results of the ash samples of the feed coals and their density separation fractions before ashing, as reported by Rautenbach *et al.,* (2019b).

Table 5-4 XRF analysis results for the ash samples (%) of feed, float and sink fractions as reported by Rautenbach *et al.,* (2019b)

	Feed A	Float A	Sink A	Feed B	Float B	Sink B	Feed C	Float C	Sink C
SiO_2	50.7	53.4	54.2	46.5	41.3	51.6	54.3	47.3	58.8
Al_2O_3	28.8	28.1	29.4	36.1	31.9	39.4	27.4	29.9	23.6
Fe_2O_3	3.4	3.7	8.4	4.0	2.8	2.8	4.0	3.2	3.6
TiO_2	2.1	5.0	1.5	2.1	4.0	2.3	1.8	4.3	1.6
P_2O_5	1.5	1.7	0.2	0.2	0.5	0.1	0.7	1.2	0.2
CaO	9.0	6.3	4.1	8.1	17.8	2.7	8.2	10.7	10.5
MgO	3.4	0.6	0.8	1.1	1.0	0.4	2.1	1.5	0.9
Na_2O	0.5			0.6			0.3	0.1	
K_2O	0.7	1.2	1.0	0.9	0.2	0.5	0.8	0.8	0.6
SO_3			0.5	0.3	0.4	0.2	0.5	0.8	0.2

The prepared ash samples of sample A and C at 1300°C, as well as the ash collected from the power stations, were subjected to QEMSCAN analysis by the Sustainability Division Research, Testing, and Development at Eskom, South Africa. Sample preparation for QEMSCAN analysis entailed the mixing of the ash samples with molten carnauba wax in a 30 mm mould. The solid wax samples were polished in order to expose the mineral particles in the samples. Digital images of the ash samples were created by a scanning electron microscope (SEM) equipped with Energy Dispersive X-ray (EDX) as well as Backscatter Electron signals (BSE). Field Emission Gun (FEG) based QEMSCAN 650 was used to determine various characteristics, including the modal proportions of all the minerals as well as the density distribution of the ash particles. The schematic representation of the experimental procedure can be observed in Figure 5-1.

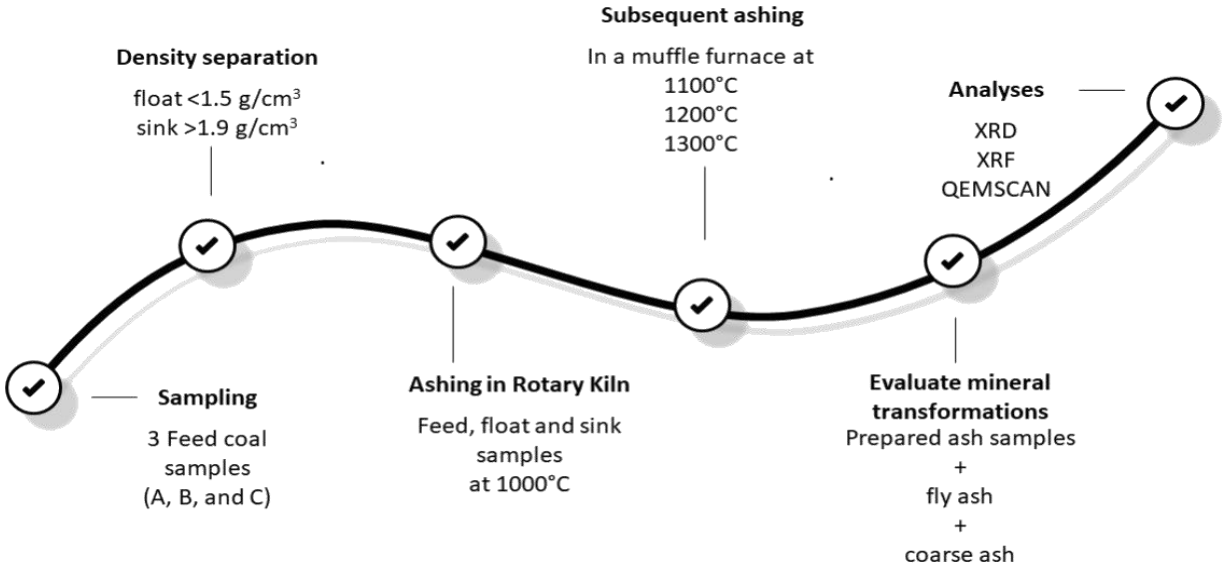

Figure 5-1 Schematic representation of the experimental procedure for preparing ash samples from the feed coals A, B, and C, and their density separated fractions and subsequent analyses.

5.3 Results and Discussion

5.3.1 Mineralogy of fly ash and coarse ash samples from the power stations

The XRD results of the ash samples (coarse ash and fly ash) from the power stations can be observed in Table 5-5. These ash samples were collected from the power stations in order to compare the mineralogy with the prepared ash samples. The ash samples contain predominantly amorphous (glassy) content in the range of 57% to 65%. Mullite ($Al_6Si_2O_{13}$) was the primary high-temperature mineral phase present in the ash samples with 16% and 19% in the coarse ash and fly ash of sample A, 14.5% and 16% in the coarse ash and fly ash of sample B, and 23% and 29% in the coarse ash and fly ash of sample C, respectively.

The formation of mullite occurs as a result of the transformation of predominantly excluded kaolinite ($Al_2Si_2O_5(OH)_4$) as well as other clay minerals such as illite ($K_{1.5}Al_4(Si_{6.5}Al_{1.5})O_{20}(OH)_4$) to metakaolinite at elevated temperatures (Matjie *et al.*, 2012; O'Gorman & Walker Jr, 1973; Ward, 2002). Mullite can also crystallise from the molten solution, which is formed due to reactions of kaolinite associated with fluxing minerals (calcite, dolomite, and pyrite) at high temperatures. The reactive silica derived from the transformation of kaolinite will lead to the formation of cristobalite (SiO_2), which is a high-temperature mineral that may also be derived from quartz at elevated temperatures (Matjie *et al.*, 2008; Matjie *et al.*, 2012; Reifenstein *et al.*, 1999). The low proportions of quartz reported for the fly ash and coarse ash of sample C (3% and 4%, respectively) are the

result of the mineral associations between quartz, kaolinite and fluxing minerals. This association of quartz with kaolinite and fluxing minerals may result in the molten solution and a subsequent crystallisation of mullite from this molten solution (Matjie *et al.*, 2011; Van Alphen, 2005). The power station ash of sample B contains the highest amount of quartz (14.7% and 15.6%) while the quartz content for sample A is between 8.5% and 9.5% for the fly and coarse ash. This variance of the quartz content in the ash samples is an indication of the differences in the mode of occurrence of mineral matter in coal. Minor concentrations of sillimanite (Al_2SiO_5), which can also be mullite (1 part SiO_2: 1 part Al_2O_3) are present in all the ash samples from the power stations. Significantly low levels of anorthite are observed in these ash samples. Anorthite is a calcium feldspar ($CaAl_2Si_2O_8$) that forms during coal utilisation either through crystallisation from the melt or due to solid-state reactions that occur between the minerals, mainly Ca-bearing minerals (Matjie *et al.*, 2005; Matjie *et al.*, 2011; Matjie *et al.*, 2008; Unsworth *et al.*, 1988).

From the study by Unsworth *et al.,* (1988), it is concluded that the abundance of crystalline Ca-aluminosilicates in the ash deposits would enhance the melting characteristics of the corresponding phases. Van Alphen (2005) also proposed that there is a definite association between anorthite formation and slagging properties of ash deposits due to the low quantities of anorthite present in the fly ash of South African coal. Trace amounts of anhydrite ($CaSO_4$) are present in the ash samples (B and C), possibly due to the interaction of SO_2 and CaO at elevated temperatures within the reactor (Matjie *et al.*, 2012; Van Alphen, 2005). The minor proportions of rutile present in the ash samples indicate the association of Ti with excluded minerals, as reported by (Rautenbach *et al.*, 2019a).

Table 5-5 XRD results of the fly ash and the coarse ash samples taken from the three different power stations (w/w %).

		Anhydrite	Rutile	Mullite	Quartz	Sillimanite	Anorthite	Cristobalite	Calcite	Amorphous
A	Coarse ash	0.00	0.10	16.68	9.72	5.42	0.51	0.31	0.31	66.94
	Fly ash	0.00	0.10	19.90	8.63	5.28	0.10	0.10	0.41	65.48
B	Coarse ash	0.00	0.51	14.80	15.92	4.69	1.63	0.92	0.82	60.71
	Fly ash	0.10	0.10	16.41	14.98	5.40	0.10	0.00	0.20	62.69
C	Coarse Ash	0.31	0.41	23.34	4.28	8.26	1.73	0.51	0.20	60.96
	Fly Ash	0.10	0.20	29.27	2.74	8.54	0.30	0.10	0.00	58.74

5.3.2 X-ray fluorescence analysis results of the fly ash and coarse ash samples

The XRF analysis results of the coarse and fly ash samples, from the power stations, are displayed in Table 5-6. These ash samples consist of similar elemental compositions and are characterised as silica-rich ash due to the abundance of SiO_2 (ranging from 45% to 55%) in all the ash samples. Lower proportions of Al_2O_3, ranging from 24% to 37%, in comparison with the SiO_2 content, are also present in all the ash samples. Minor proportions of CaO (< 15%) and Fe_2O_3 (< 11%) are present in the ash samples from the power stations, while the rest of the components reported in Table 6 are present in trace amounts (< 1%).

Table 5-6 XRF results (%) of the fly ash and coarse ash from the three different power stations.

	SiO_2	Al_2O_3	Fe_2O_3	CaO	TiO_2	MgO	K_2O	SO_3
A Coarse Ash	54.62	26.14	10.99	4.04	1.30	0.85	0.79	0.32
A Fly Ash	54.87	28.69	8.22	3.82	1.42	0.91	0.80	0.13
B Coarse Ash	51.16	24.14	4.79	13.18	1.39	2.33	0.73	0.10
B Fly Ash	51.88	26.81	3.62	11.20	1.52	2.18	0.73	0.03
C Coarse Ash	45.25	34.65	4.24	11.29	1.77	0.97	0.52	0.05
C Fly Ash	45.20	36.58	3.59	9.44	1.94	1.00	0.64	0.06

5.3.3 Mineralogy of the ash samples prepared under laboratory combustion conditions

The XRD results of the prepared ash samples, including the feed, float and sink fractions, at various temperatures (1000°C, 1100°C, 1200°C and 1300°C) are compared to their corresponding coarse ash and fly ash samples from the power station. The XRD results for sample A, sample B, and sample C are reported in Table 5-7, Table 5-8, and Table 5-9, respectively. As determined by Rautenbach *et al.,* (2019b) the float fractions represent maceral-rich included minerals, while the sink fractions consist mainly of mineral-rich extraneous minerals. The high amorphous (glassy) content in the ash samples is evident from the XRD results reported in Tables 5-7 to 5-9. The amorphous content in the fly ash and coarse ash samples (A, B, and C) range from 57% to 65%. The ash prepared at 1000°C from the feed, float and sink samples (A, B, and C) contain the highest amount of amorphous material which decreases with an increase in temperature (from 1000°C to 1300°C) due to the formation of high-temperature mineral phases. This trend is observed for all the prepared ash samples, i.e., the feed, float, and sink fractions of samples A, B, and C.

The amorphous phase consists primarily of a mixture of SiO_2 and Al_2O_3 due to the thermal decomposition of clay minerals. Elemental exchange occurs swiftly within the amorphous phase, where either quicklime (CaO), wustite (FeO) and periclase (MgO) derived from the transformations of calcite, dolomite and pyrite at elevated temperatures can react metakaolinite or to form high-temperature hard minerals such as anorthite (Creelman *et al.*, 2013).

The mullite content in Feed A (Table 5-7) due to the transformation of excluded kaolinite increases with an increase in temperature from 1% at a 1000°C to 17% at 1300°C, while a decrease in the quartz and sillimanite content is observed, with only 1% quartz, and 0.6% sillimanite remaining in the ash sample of Feed A prepared at 1300°C. Calcite decomposes with an increase in temperature and is depleted at 1200°C, while anorthite formation is observed up to 1200°C (40%) after which it forms part of the melt upon further heating to 1300°C in Feed A. Cristobalite (SiO_2), is a product of the transformation of quartz and reactive silica derived from the transformation of kaolinite at high temperatures (Creelman *et al.*, 2013). Cristobalite formation can also occur once the alumina in the melt is depleted due to the crystallisation of mullite (Creelman *et al.*, 2013). The cristobalite content increased from 0.5% to 12% (in Feed A) with an increase in temperature; this coincides with the transformation of excluded quartz and excluded kaolinite, as observed in Table 5-7.

The included mineral transformations, represented in Float A differs from the feed sample and is reported in Table 5-7. The mullite content fluctuates with the temperature increase up to 1200°C (15% mullite), after which it transforms as part of the melt upon further heating of Float A to 1300°C. The included quartz content (Float A), decreases from 6% at 1000°C to 0% at 1300°C, while crystallised sillimanite concentrations increase slightly from 1000°C to 1100°C, after which it forms part of the melt at 1200°C. A significant increase in the anorthite content is observed at 1200°C (19.6%) due to the transformation of included minerals (calcite or dolomite associated with kaolinite in the macerals); however, a decrease to only 3.6% occurs upon further heating up to 1300°C. It was determined by Matjie *et al.,* (2008) and Matjie (2008) that anorthite will melt at 1400°C. Cristobalite content in Float A increases considerably from 2.3% at 1200°C up to 17% at 1300°C. As expected, the remaining minerals such as calcite transformation and illite decompose to form the melt at high temperatures and are not present in the ash sample of Float A prepared at 1300°C.

The mullite, quartz, and sillimanite present in Sink A, transformed and decompose at similar temperatures as in Float A, as described above. Significant differences between the included mineral transformations in Float A and extraneous mineral transformations, Sink A, relates to the anorthite, cristobalite, and rutile (TiO_2) formations. An increase is observed for the anorthite

content in Sink A, from 1000°C to 1200°C, followed by a slight decrease to 11% at 1300°C. The transformation of extraneous minerals (Sink A) cause higher anorthite formation at 1300°C compared to Feed A and Float A ash samples. Cristobalite content is significantly low in Sink A compared to Float A, while rutile is present in Sink A at 1300°C (7%) with trace amounts (< 1%) present in Feed A and Float A ash samples. The high quantities of anorthite in the ash samples are due to the slagging of minerals at elevated temperatures.

Table 5-7 XRD results (%) of the ash samples of sample A prepared at various temperatures.

		Anhydrite	Rutile	Mullite	Quartz	Sillimanite	Anorthite	Cristobalite	Calcite	Aluminosilicate glass
	A Coarse ash	0.00	0.10	16.68	9.72	5.42	0.51	0.31	0.31	66.94
	A Fly ash	0.00	0.10	19.90	8.63	5.28	0.10	0.10	0.41	65.48
Feed A	1000°C	0.43	0.00	1.16	13.33	8.84	0.29	0.58	1.45	73.91
	1100°C	0.00	0.00	13.75	5.66	2.70	10.38	1.48	0.13	65.90
	1200°C	0.00	0.29	14.45	1.75	0.44	15.77	2.63	0.00	64.67
	1300°C	0.00	0.00	17.62	0.86	0.69	1.21	12.95	0.00	66.67
Float A	1000°C	0.00	0.00	11.79	6.27	4.48	0.60	0.75	1.04	75.07
	1100°C	0.00	0.14	8.09	2.46	7.37	13.01	1.73	0.00	67.20
	1200°C	0.00	0.00	15.87	1.71	0.00	20.48	2.39	0.00	59.56
	1300°C	0.00	0.00	0.00	0.00	3.10	3.88	18.60	0.00	74.42
Sink A	1000°C	1.82	0.00	0.33	9.78	0.33	0.00	0.33	4.48	82.92
	1100°C	0.00	0.00	7.73	5.98	9.84	2.46	1.41	0.00	72.58
	1200°C	0.00	0.95	4.73	0.38	5.29	17.20	3.40	0.00	68.05
	1300°C	0.00	7.73	0.00	0.00	2.58	11.80	2.36	0.00	75.54

The main differences between the power station fly ash and coarse ash (sample A) with the ash prepared under laboratory combustion conditions (Feed A, Float A, and Sink A) are summarised

below. Firstly, the quartz transforms completely at elevated temperatures within the prepared ash samples, although it is present in the fly ash and coarse ash sampled from the power station from Limpopo province. Secondly, the mullite concentrations in Feed A, at high temperatures, are in the same proximity as the mullite concentration in the fly ash and the coarse ash. However, this is not observed for the mullite concentration in the Float A and Sink A ash samples. Thirdly, anorthite formation is more prominent in the prepared ash samples than in the fly ash and coarse ash due to the association of kaolinite with fluxing minerals and also due to the different combustion conditions used in the power stations and laboratory. The higher quantities of anorthite observed are due to the crystallisation of anorthite from the melt phase as well as solid-state reactions between minerals that initiate anorthite formation. During the formation of fly ash and coarse ash, these reactions responsible for the anorthite formation did not take place as low anorthite formation is expected at temperatures above 1600°C where the power stations operate (Matjie *et al.*, 2005; Van Alphen, 2005). Cristobalite is also prominent at high temperatures in the prepared ash samples, although only trace amounts of cristobalite are present in the fly ash and coarse ash. These trace amounts of cristobalite in the power stations ash samples are also expected as no cristobalite formation is expected at temperatures of 1600°C (Matjie *et al.*, 2005; Van Alphen, 2005). Sillimanite formation occurs in the prepared ash samples above 1000°C and persists to high temperatures; it is also observed in the fly ash and coarse ash samples.

The XRD results of the fly ash, coarse ash as well as the prepared ash of Feed B, Float B, and Sink B are presented in Table 5-8. A decrease in the mullite content in Feed B is observed with an increase in temperature up to 1300°C. Significantly low concentration of mullite is observed in Float B, while Sink B contains predominantly mullite, which increases from 9% at 1000°C to 22% at 1300°C. Consequently, the crystallisation of mullite from the molten solution occurs due to the transformation and interaction of excluded dolomite and calcite associated with included kaolinite. Quartz is present in small quantities (< 4%) within Feed B, Float B, and Sink B, although the fly ash and coarse ash contains approximately 15% quartz. With an increase in the temperature the quartz content, in Feed B, Float B, and Sink B, decreases entirely due to the transformation and reaction with kaolinite in order to form cristobalite and anorthite. Cristobalite formation occurs at high temperatures and persists in low quantities at 1300°C in Feed B, Float B, and Sink B.

Anorthite formation occurs at elevated temperatures in the ash samples of Feed B, Float B and Sink B (approximately 5% at high temperatures), while only trace amount <1.6% is expected in the power station ash samples. This absence of anorthite in the fly ash correlates with previous studies (Matjie *et al.*, 2005; Moitsheki *et al.*, 2010; Nguyentranlam & Galvin, 2004; Unsworth *et al.*, 1988; Van Alphen, 2005; Van Dyk *et al.*, 2009). The presence of anorthite, mullite, and

aluminosilicate glass phases in the ash samples are the result of the severe slagging of mineral matter at high temperatures above 1200°C.

Several differences are observed when the ash samples of Feed B, Float B and Sink B, prepared under laboratory combustion conditions, are compared to the fly ash and coarse ash sampled at the power stations, as expected. The main reason, therefore, is the difference in the experimental conditions as well as the mode of occurrence of mineral matter in the various fractions (feed, float, and sink). The mullite proportion in Sink B is similar to the mullite content in the fly ash and coarse ash, while the quartz content in the prepared ash samples (Feed B, Float B, and Sink B) is significantly lower than the quartz content in the fly ash and coarse ash. Sillimanite (similar to mullite with 1 part SiO_2 and 1 part Al_2O_3) is present in all the ash samples. While anorthite formation occurs predominantly within the prepared ash samples (Feed B, Float B, and Sink B) with a trace amount of anorthite present in the coarse ash sample (sample B) from the power station under the different operating conditions.

Table 5-8 XRD results (%) on the ash samples of sample B prepared at various temperatures.

		Anhydrite	Rutile	Mullite	Quartz	Sillimanite	Anorthite	Cristo-balite	Calcite	Alumino-silicate glasses
	B Coarse ash	0.00	0.51	14.80	15.92	4.69	1.63	0.92	0.82	60.71
	B Fly ash	0.10	0.10	16.41	14.98	5.40	0.10	0.00	0.20	62.69
Feed B	1000°C	1.46	0.00	16.99	1.94	3.88	0.16	0.49	4.53	70.55
	1100°C	0.00	0.50	13.46	0.66	4.98	14.29	1.66	0.33	64.12
	1200°C	0.00	1.05	17.63	0.17	4.89	15.71	2.27	0.87	57.42
	1300°C	0.00	10.40	4.16	0.00	5.20	13.51	3.53	1.04	62.16
Float B	1000°C	0.60	0.40	0.80	0.20	0.20	2.19	1.19	6.56	87.87
	1100°C	0.00	0.66	1.77	0.00	3.54	10.40	1.11	0.00	82.52
	1200°C	1.14	0.00	1.14	0.23	3.41	15.91	1.82	0.23	76.14
	1300°C	0.00	0.00	0.90	0.30	2.70	6.01	2.10	2.10	85.89
Sink B	1000°C	0.81	0.00	9.18	4.03	0.00	0.00	0.48	4.03	81.48
	1100°C	0.00	0.00	20.17	1.66	5.52	13.67	0.83	0.00	58.15
	1200°C	0.00	0.00	26.20	1.42	3.26	15.72	0.85	0.00	52.55
	1300°C	0.00	0.00	24.35	0.00	4.06	14.76	1.85	0.00	54.98

The comparison between the mineralogy of the fly ash and coarse ash produced from the power stations as well as the laboratory prepared ash of Feed C, Float C and Sink C is reported in Table 5-9. Feed C contains the highest proportion of mullite at 1100°C (13%), after which it transforms into an amorphous phase upon a further increase in temperature. However, only a trace amount of mullite is observed in the prepared ash samples of Float C and Sink C. An increase in the rutile concentration, within the included mineral fraction (Float C), is observed at 1200°C after which it forms part of the amorphous phase with a further increase in temperature. High proportions of quartz are observed at 1000°C for all of the laboratory prepared ash samples, after which the quartz transforms at increased temperatures to form part of the glassy amorphous phase and cristobalite. Quartz is primarily present in Sample C as excluded minerals. Sillimanite is present in all the samples at high temperatures, although in low proportions. Cristobalite occurs at high temperatures and persists throughout the ashing experiment up to 1300°C.

Significantly high proportions of anorthite are present at elevated temperature (1200°C and 1300°C) in the ash sample of Feed C. Anorthite is the predominant high-temperature mineral phase that forms as a result of the transformation of included minerals (Float C) at temperatures of 1100°C and above. Low quantities of anorthite formation occur in the ash of Sink C initially; however, at 1300°C, approximately 8% of the crystalline material is anorthite due to the interactions of excluded minerals. The formation of anorthite, associated with excluded mineral transformations, coincides with the decrease in excluded-quartz content at elevated temperatures.

Table 5-9 XRD results (%) on the ash samples of Sample C prepared at various temperatures

		Anhydrite	Rutile	Mullite	Quartz	Sillimanite	Anorthite	Cristobalite	Calcite	Amorphous
	C Coarse Ash	0.31	0.41	23.34	4.28	8.26	1.73	0.51	0.20	60.96
	C Fly Ash	0.10	0.20	29.27	2.74	8.54	0.30	0.10	0.00	58.74
Feed C	1000°C	1.13	0.00	13.11	13.27	0.00	0.00	0.32	4.21	67.96
	1100°C	0.34	0.00	14.02	7.77	4.56	1.86	1.35	0.84	69.26
	1200°C	0.00	0.97	3.31	3.51	3.90	16.57	3.70	0.39	67.64
	1300°C	0.00	0.00	0.00	0.00	2.44	26.00	2.67	1.11	67.78
Float C	1000°C	0.17	0.34	0.00	6.29	0.00	6.97	1.02	3.57	81.63
	1100°C	0.34	1.17	1.68	1.34	4.02	17.59	1.84	0.34	71.69
	1200°C	0.35	9.79	0.52	0.17	2.97	15.03	3.15	1.92	66.08
	1300°C	0.00	2.64	0.00	0.00	5.87	11.14	2.64	0.88	76.83
Sink C	1000°C	2.49	1.40	0.00	22.27	0.31	0.16	0.31	3.27	69.78
	1100°C	2.56	0.00	2.08	15.84	1.60	2.08	1.44	0.64	73.76
	1200°C	0.20	0.20	0.00	4.78	1.59	3.59	1.99	1.00	86.65
	1300°C	0.00	0.20	0.00	0.00	0.00	16.34	1.57	6.10	75.79

The mullite content in the prepared ash of Feed C, at 1000°C and 1100°C, is the highest, compared to the ash samples of Float C and Sink C, and thus in better relation to the mullite content in the fly ash and coarse ash. Higher quantities of quartz are present in the prepared ash than in the fly ash and coarse ash from the power station plant. This is due to the temperatures that reach up to 1600°C in the power station boilers. Interestingly the opposite is observed in the laboratory ash samples of Sample A and Sample B. Considerably low levels of mullite are observed for the prepared ash samples, as expected anorthite is the predominant crystalline phase present, in the prepared ash samples, at elevated temperatures. High proportions of

anorthite, mullite, and aluminosilicate glass phase in the ash samples are due to severe slagging of mineral matter at elevated temperatures.

5.3.4 X-ray fluorescence analysis results of the ash samples prepared under laboratory combustion conditions

The XRF results of the coarse ash and fly ash samples from the respective power stations are compared to the prepared ash samples of the feed, float and sink fractions, under laboratory (Hlatshwayo *et al.*, 2009; Matjie, 2008; Matjie *et al.*, 2012; Van Dyk *et al.*, 2009) combustion conditions, in Table 5-10 to 5-12. According to the results in Table 5-10, the elemental composition of the fly ash, coarse ash, and the prepared ash samples are very similar. These similarities are expected due to the low proportion of inorganic elements that volatilise during thermochemical processes. The ash samples consist of predominantly SiO_2, followed by Al_2O_3, Fe_2O_3, and CaO in smaller amounts. The remaining elemental oxides are only present in trace amounts. These results correlate with XRF results of South African coals reported in the literature (Hlatshwayo *et al.*, 2009; Matjie, 2008; Matjie *et al.*, 2012; Van Dyk *et al.*, 2009).

Table 5-10 XRF results on the ash samples prepared at various temperatures (%)

		Sample A						
		SiO_2	**Al_2O_3**	**Fe_2O_3**	**CaO**	**TiO_2**	**MgO**	**SO_3**
A	Coarse ash	55.59	26.60	11.18	4.11	1.32	0.87	0.33
	Fly ash	55.96	29.25	8.39	3.89	1.45	0.93	0.14
Feed A	1000°C	49.77	25.82	17.62	4.22	1.36	0.84	0.36
	1100°C	50.30	26.24	16.82	4.23	1.38	0.85	0.18
	1200°C	50.45	26.22	16.68	4.29	1.39	0.85	0.12
	1300°C	49.98	25.85	17.57	4.23	1.40	0.86	0.11
Float A	1000°C	43.57	22.02	27.15	3.94	2.21	0.63	0.49
	1100°C	45.24	22.93	24.79	4.13	2.29	0.61	nd
	1200°C	44.35	22.31	26.46	4.01	2.27	0.60	nd
	1300°C	44.80	24.69	23.23	4.64	2.10	0.54	nd
Sink A	1000°C	39.35	20.18	27.76	7.85	1.26	1.75	1.85
	1100°C	40.52	20.73	27.55	8.13	1.28	1.77	0.02
	1200°C	40.72	21.15	26.80	8.16	1.38	1.79	nd
	1300°C	40.71	20.72	27.57	7.99	1.29	1.73	nd

Table 5-10 (continue) XRF results on the ash samples prepared at various temperatures (%)

		Sample B						
		SiO_2	Al_2O_3	Fe_2O_3	CaO	TiO_2	MgO	SO_3
B	Coarse	53.64	25.32	5.02	13.82	1.46	0.10	0.63
	Fly	54.20	28.01	3.78	11.70	1.58	0.03	0.69
Feed B	1000°C	41.04	30.92	13.25	11.07	2.05	1.36	0.31
	1100°C	42.08	31.99	12.20	11.25	2.11	0.05	0.31
	1200°C	42.20	31.86	12.19	11.31	2.13	nd	0.30
	1300°C	41.97	31.48	13.01	11.16	2.06	nd	0.33
Float B	1000°C	28.59	21.12	30.56	15.78	2.55	0.89	0.50
	1100°C	30.21	22.07	28.20	16.38	2.66	nd	0.49
	1200°C	29.59	21.84	29.04	16.36	2.66	nd	0.51
	1300°C	31.52	21.89	26.96	16.54	2.58	nd	0.51
Sink B	1000°C	46.64	35.05	11.53	3.77	2.06	0.79	0.16
	1100°C	47.22	35.30	11.41	3.79	2.11	0.01	0.16
	1200°C	47.45	35.55	10.92	3.79	2.13	nd	0.16
	1300°C	46.89	35.91	10.68	4.35	1.96	nd	0.20

Table 5-10 (continue) XRF results on the ash samples prepared at various temperatures (%)								
		Sample C						
		SiO_2	Al_2O_3	Fe_2O_3	CaO	TiO_2	MgO	SO_3
C	Coarse	46.00	35.22	4.31	11.47	0.98	1.80	0.21
	Fly	46.12	37.33	3.67	9.63	1.02	1.98	0.25
Feed C	1000°C	45.60	20.88	18.73	10.72	1.90	1.44	0.72
	1100°C	46.16	21.43	17.36	10.89	1.93	1.51	0.72
	1200°C	46.59	21.98	15.93	11.33	1.94	1.49	0.74
	1300°C	46.54	21.72	16.57	11.10	1.85	1.52	0.70
Float C	1000°C	41.73	26.52	13.73	11.54	2.20	2.98	1.30
	1100°C	42.83	27.70	11.22	11.83	2.24	2.90	1.29
	1200°C	42.98	27.91	10.83	11.81	2.24	2.93	1.31
	1300°C	44.49	27.94	11.07	11.31	1.77	2.31	1.12
Sink C	1000°C	50.04	15.14	15.47	15.81	2.15	1.04	0.34
	1100°C	50.07	14.99	15.48	15.95	2.17	0.98	0.36
	1200°C	48.80	14.81	16.94	15.91	2.16	1.02	0.36
	1300°C	50.20	16.44	13.95	15.89	2.15	1.02	0.34

5.3.5 Mineralogy of ash samples prepared at 1300°C derived from QEMSCAN analysis

The ash prepared at 1300°C in the muffle furnace of Feed A, Float A, Sink A, as well as Feed C, Float C and Sink C, were submitted for QEMSCAN analysis in order to determine and compare the mineralogical compositions. These QEMSCAN results of the ash samples are reported in Table 5-11. The false-colour images, derived from QEMSCAN analysis, of the ash prepared at 1300°C for sample A (feed, float, and sink) and sample C (feed, float, and sink) are displayed in Table 5-12.

The QEMSCAN results are normalised in order to eliminate the chrome bearing steel contamination, which occurred during the ashing process in the rotary kiln. However, the aim is to identify and characterise the formation of slag phases at high temperatures, which occur due to mineral associations between kaolinite and fluxing minerals. The presence of chrome bearing steel will not influence the formation of high-temperature mineral phases.

Table 5-11 Modal proportions (%) of minerals in the ash prepared at 1300°C of Feed A, Float A, Sink A, Feed C, Float C, and Sink C, derived from QEMSCAN analysis.

	Feed A 1300°C	Float A 1300°C	Sink A 1300°C	Feed C 1300°C	Float C 1300°C	Sink C 1300°C
Ash:Iron Oxide (Sulphur)	0.15	0.65	0.53	0.53	0.17	0.40
Ash:Calcium/CaMg oxide	0.15	0.22	0.27	0.36	0.17	0.26
Fouling:(Sulphates, salts)	0.00	0.43	0.27	1.42	0.17	0.13
Microcline	0.15	0.43	0.00	0.00	0.00	0.00
Muscovite/Illite	0.92	0.22	0.00	0.00	0.00	0.00
Mullite	0.15	0.86	0.27	0.36	0.17	0.13
Kaolinite	39.02	7.11	1.33	1.07	2.26	0.26
Quartz	26.42	26.94	12.00	9.07	7.81	5.95
Slag (Ca,Mg,Al,Si) Iron	2.15	23.06	21.60	13.52	6.77	20.11
Slag:Anorthite(Composition)	0.92	0.00	2.40	3.02	3.82	1.85
Slag:Aluminosilicate(Ca,Mg,Fe)	23.66	14.66	12.00	11.92	24.83	12.43
Slag:Silica(Ca,Mg,Fe)	6.30	25.43	49.33	58.72	53.82	58.47

Slagging ash phases, determined by QEMSCAN, consist of varying proportions of the fluxing elements (Ca, Mg, Fe) bearing aluminosilicate phases. Four slagging phases are identified in the ash samples prepared at 1300°C, as reported in Table 5-11. The silica-slag phase (slag: silica(Ca, Mg, Al)) that contains varying amounts of fluxing elements (Ca, Mg, Fe) is the dominant slag phase in all of the ash samples, except for Feed A. This silica-slag phase, consists of a higher quantity Si than Al in the slag. Similar proportions of this silica-rich slag phase are present in Feed C, Float C and Sink C (53% to 58%), however, significantly lower proportions are present in Sample A, mainly Feed A (6%).

Fluxing element bearing aluminosilicate (Ca, Fe, Mg) slag phase (slag: aluminosilicate(Ca, Fe, Mg)) can be characterised as a typical slag phase with similar proportions of Al and Si, while the proportions of the fluxing elements may vary. This slag phase is dominant in Feed A, which coincides with the significantly high proportion of aluminosilicate (meta-kaolinite) present in Feed A at 1300°C, as well as the low proportion of the silica-slag phase. Relatively higher proportions of the aluminosilicate-slag phase are also present in Float C in comparison with Feed C and Sink C.

The third slag phase identified in the ash samples at 1300°C is a slag phase (slag: anorthite (composition) with a similar composition as anorthite ($CaAl_2Si_2O_8$). This slag ash phase is only present in small proportions, with 2.4% in Sink A and > 1% in Feed A and Float A. Sink C contains the lowest concentration (1.9%), with Feed C and Float C consisting of approximately 3% of the anorthite-slag phase.

The (Ca, Mg, Al, Si)-Iron slag phase represents a thin coating of silica-rich deposits on heat transfer surfaces. Only 2% of this slag phase formed in Feed A, while 21% to 23% of the (Ca, Mg, Al, Si)-Fe slag formation occur in Float A and Sink A. Float C forms less of the (Ca, Mg, Al, Si)-Fe slag (6%) when compared to Feed C (13%) and Sink C (20%). It is evident from QEMSCAN results that the slag phases are mainly due to fume deposits that form on the heat transfer surfaces. However, the slag phase that forms in Feed A at 1300°C is predominantly coarse fly ash with minimal deposition of slag on the surface.

Table 5-12 False color QEMSCAN images for (a) Feed A, (b) Float A, (c) Sink A, (d) Feed C, (e) Float C, and (f) Sink C.

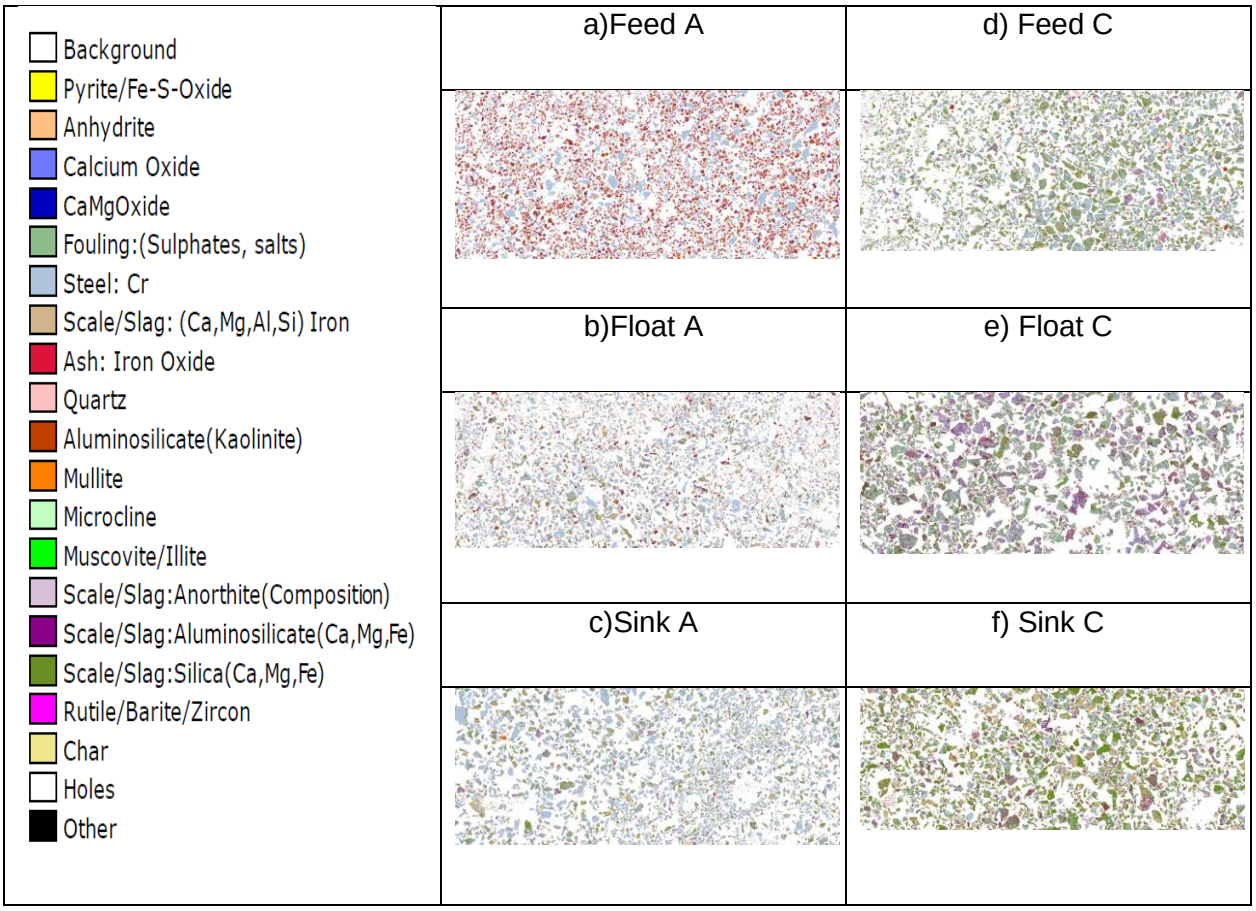

The foremost minerals and slag phases present in the ash samples are observed in the false-colour images in Table 5-12. Significant differences between the two feed samples (Feed A and Feed C) are evident from these images.

5.3.6 Comparison of expected slag behaviour

According to Van Alphen (2005), the fly ash phases responsible for slag formation is mainly Ca-Mg aluminosilicate glass derived from the transformation of kaolinite associated with calcite and dolomite, Fe-Ca-Mg aluminosilicate glasses derived from the transformation of kaolinite associated with dolomite calcite and pyrite and kaolinite associated with pyrite. The kaolinite(carbonate) phase represents the association of kaolinite with calcite and dolomite (i.e., Al-Si-O with minor proportions Ca and Mg). The kaolinite(pyrite, carbonate) fly ash phase refers to the interaction of kaolinite with pyrite, calcite, and dolomite, while the kaolinite(pyrite) phase refers to the association of kaolinite and pyrite.

The XRD, XRF, and QEMSCAN analysis results are used to calculate the expected slag formation for each technique, respectively. These calculations are based on the association of kaolinite with fluxing minerals containing Fe, Ca and Mg, which results in slag formation under combustion conditions (Unsworth *et al.*, 1988; Van Alphen, 2005). The calculated slag formation for each analytical technique (XRD, XRF, and QEMSCAN modal proportions) and the measured slag, determined by QEMSCAN analysis, are compared in Figure 5-2.

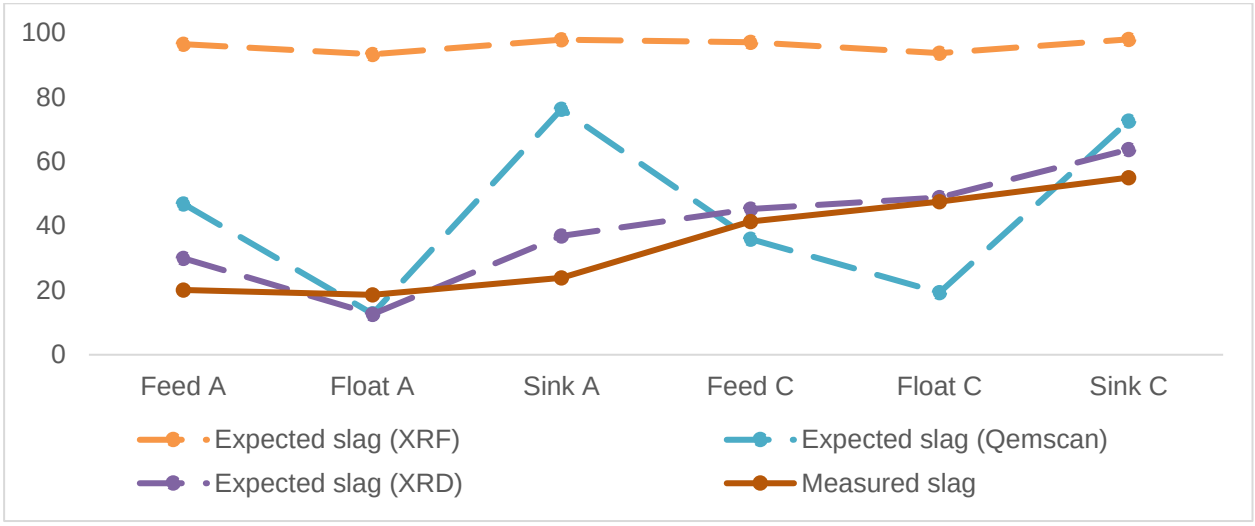

Figure 5-2 Comparison of the slag models derived from XRD, XRF, and QEMSCAN results.

The expected slag formation, calculated using XRF analyses results, is significantly high, due to the incorporation of the total inorganic elements concentrations contained in the ash, thus not differentiating between crystalline material and the amorphous content. The expected slag formation, calculated from XRD analyses results, are relatively similar (± 10%) to the measured slag. These similarities emphasise the relationship between crystalline material (i.e., the formation of anorthite and mullite) with slag formation. It is interesting to note that, for Float A and Feed C, the slagging propensity calculations, based on XRD and QEMSCAN analyses, are comparable with the measured slag.

5.4 Conclusions

This paper aims to incorporate the heterogeneous nature of coal ash with slag prediction methods by investigating the transformation of included and excluded minerals, as well as the organically bound inorganic elements under laboratory combustion experiment conditions. Current ash-deposition prediction methods that incorporate the mineralogy of coal are based on assumptions with regards to the transformation of included minerals (mineral associations in the carbon matrix) and excluded minerals (mineral associations in rock fragments) during coal conversion processes. This work focused on expanding the knowledge of the transformation of included minerals in the <1.5 g/cm^3 float fraction and the excluded minerals in the >1.9 g/cm^3 sink fraction without making any assumptions.

The behaviour of included and excluded minerals in three South African coal samples with different mineral associations and mineral modes of occurrences were investigated under laboratory combustion conditions.

With regards to sample A, the included mineral transformations resulted in the formation of higher proportions mullite and cristobalite when compared to the transformations of excluded minerals. Anorthite formation occurred as a result of both included and excluded mineral transformations. Included kaolinite coalesced and reacted at lower temperatures to form metakaolinite which then reacted with available calcium oxide form the melt and anorthite subsequently crystallise from this melt. Upon further heating (1300°C) the crystalline material in the ash of the float fraction forms part of the amorphous phase, which is responsible for lowering the ash fusion temperature. Excluded minerals (calcite, dolomite and kaolinite) transformations lead to the formation of anorthite at temperatures of 1200°C and above via the solid-state reactions. This anorthite was stable and melted at high temperatures of >1300°C.

The differences in the mode of occurrence of minerals (between Sample A and Sample B) can be used to explain the formation of different high-temperature minerals. Significant mullite

formation occurred in sample B as a result of the transformation of excluded kaolinite. While small proportions of mullite particles formed during the interaction of included calcite/dolomite/pyrite associated with kaolinite contained in the float fraction from Sample B. Both included and excluded minerals lead to the formation of anorthite via solid-state and crystallisation reactions. The anorthite in the ash sample of the float fraction transforms to the calcium aluminosilicate glass (amorphous material) at elevated temperatures ranging from 1300°C to 1400°C. As expected, the anorthite in the sink fraction persists due to low temperature of this rock fragment.

Sample C exhibited different mineral interactions and transformations under laboratory conditions when compared to sample A and B. Mullite formation occurs when kaolinite transforms in both included and excluded minerals. Anorthite crystallised from the molten solution at elevated temperatures of 1300°C.

The presence of anorthite at high temperatures can be used as an indication of slag deposition due to mineral matter interactions. Based on this statement, the included minerals in sample A will not lead to slag formation, while the transformation of the excluded minerals will lead to medium slagging behaviour. Sample B will exhibit severe slag deposition due to the interactions of the excluded minerals, while low slagging behaviour can be expected from the transformation of included minerals. The transformation of both included and excluded minerals, in Sample C, will lead to medium slag formation

Acknowledgements

The work presented in this paper is based on the research financially supported by the South African Research Chairs Initiative of the Department of Science and Technology (DST) and National Research Foundation (NRF) of South Africa (Coal Research Chair Grant Nos. 86880, UID85643, UID85632). Any opinion, finding or conclusion or recommendation expressed in this material is that of the author(s) and the NRF does not accept any liability in this regard.

The authors would also like to acknowledge Vincent Dube at SABS Secunda, Belinda Venter at North West University, Xolisa Goso and his team at Mintek as well as Shinelka Singh at Eskom for their assistance with various aspects of coal preparation and analytical techniques applied in this study.

Chapter References

Bryers, R.W. 1996. Fireside slagging, fouling, and high-temperature corrosion of heat-transfer surface due to impurities in steam-raising fuels. *Progress in Energy and Combustion Science*, 22(1):29-120.

Creelman, R.A., Ward, C.R., Schumacher, G. & Juniper, L. 2013. Relation between coal mineral matter and deposit mineralogy in pulverized fuel furnaces. *Energy Fuels*, 27:5714-5724.

Erickson, T.A., Allan, S.E., McCollor, D.P., Hurley, J.P., Srinivasachar, S., Kang, S.G., Baker, J.E., Morgan, M.E., Johnson, S.A. & Borio, R. 1995. Modelling of fouling and slagging in coal-fired utility boilers. *Fuel Processing Technology*, 44(1-3):155-171.

Gupta, R., Wall, T., Kajigaya, I., Miyamae, S. & Tsumita, Y. 1998. Computer-controlled scanning electron microscopy of minerals in coal—implications for ash deposition. *Progress in Energy and Combustion Science*, 24(6):523-543.

Hlatshwayo, T.B., Matjie, R.H., Li, Z. & Ward, C.R. 2009. Mineralogical Characterization of Sasol Feed Coals and Corresponding Gasification Ash Constituents. *Energy & Fuels*, 23(6):2867-2873.

Jeffrey, L.S. 2005. Characterization of the coal resources of South Africa. *Journal of Southern African Institution of Mineral and Metallurgy*, 105(2):95-102.

Lawrence, A., Kumar, R., Nandakumar, K. & Narayanan, K. 2008. A Novel tool for assessing slagging propensity of coals in PF boilers. *Fuel*, 87:947-950.

Lee, F. & Lockwood, F. 1999. Modelling ash deposition in pulverized coal-fired applications. *Progress in Energy and Combustion Science*, 25(2):117-132.

Ma, Z., Iman, F., Lu, P., Sears, R., Kong, L., Rokanuzzaman, A., McCollor, D.P. & Benson, S.A. 2007. A comprehensive slagging and fouling prediction tool for coal-fired boilers and its validation/application. *Fuel Processing Technology*, 88(11-12):1035-1043.

Matjie, R., Ginster, M., Van Alphen, C. & Sobiecki, A. 2005. Detailed characterisation of Sasol ashes. (*In*. Proceedings organised by.

Matjie, R.H. 2008. Sintering and slagging of mineral matter in South African coals during the coal gasification process. University of Pretoria.

Matjie, R.H., French, D., Ward, C.R., Pistorius, P.C. & Li, Z. 2011. Behaviour of coal mineral matter in sintering and slagging of ash during the gasification process. *Fuel Processing Technology*, 92(8):1426-1433.

Matjie, R.H., Li, Z., Ward, C.R. & French, D. 2008. Chemical composition of glass and crystalline phases in coarse coal gasification ash. *Fuel*, 87(6):857-869.

Matjie, R.H., Ward, C.R. & Li, Z. 2012. Mineralogical Transformation in Coal Feedstocks during Carbon Conversion, based on Packed-Bed Combustor Tests: Part 1 Bulk Coal and Ash Studies. *Coal Combustion and Gasification products*, 4:45-54.

Moitsheki, L.J., Matjie, R.H., Baran, A., Mooketsi, O.I. & Schobert, H.H. 2010. Chemical and mineralogical characterization of a South African bituminous coal and its ash, and effect on pH of ash transport water. *Minerals Engineering*, 23(3):258-261.

Nguyentranlam, G. & Galvin, K.P. 2004. Applications of the Reflux Classifier in solid-liquid operations. *International Journal of Mineral Processing*, 73:83-89.

Norrish, K. & Hutton, J. 1969. An accurate X-ray spectrographic method for the analysis of a wide range of geological samples. *Geochimica et cosmochimica acta*, 33(4):431-453.

O'Gorman, J.V. & Walker Jr, P.L. 1973. Thermal behaviour of mineral fractions separated from selected American coals. *Fuel*, 52(1):71-79.

Rautenbach, R., Matjie, R.H., Strydom, C.A., Bunt, J.R., Ward, C.R., French, D. & Van Alphen, C. 2019a. Evaluation of mineral matter transformations in low-temperature ashes of South African coal feedstock samples and their density separated cuts using high-temperature X-ray diffraction. *International Journal of Coal Preparation and Utilization*:1-28.

Rautenbach, R., Strydom, C., Bunt, J., Matjie, R., Campbell, Q. & Van Alphen, C. 2019b. Mineralogical, chemical, and petrographic properties of selected South African power stations' feed coals and their corresponding density separated fractions using float-sink and reflux classification methods. *International Journal of Coal Preparation and Utilization*, 39(8):421-446.

Reifenstein, A.P., Kahraman, H., Coin, C.D.A., Calos, N.J., Miller, G. & Uwins, P. 1999. Behaviour of selected minerals in an improved ash fusion test: quartz, potassium feldspar, sodium feldspar, kaolinite, illite, calcite, dolomite, siderite, pyrite and apatite. *Fuel*, 78(12):1449-1461.

Rietveld, H.M. 1969. A Profile refinement method for Nuclear and Magnetic structures. *Journal of Applied Crystallography* 2:65-71.

Rushdi, A., Gupta, R., Sharma, A. & Holcombe, D. 2005. Mechanistic prediction of ash deposition in a pilot-scale test facility. *Fuel*, 84(10):1246-1258.

Russell, N.V., Mendez, L.B., Wigley, F. & Williamson, J. 2002. Ash deposition of a Spanish anthracite: effects of included and excluded mineral matter. *Fuel*, 81:657-663.

Unsworth, J.F., Barratt, D.J., Park, D. & Titchener, K.J. 1988. Ash formation during pulverized coal combustion: 2. The significance of crystalline anorthite in boiler deposits. *Fuel*, 67(5):632-641.

Van Alphen, C. 2005. Factors influencing fly ash formation and slag deposit formation (slagging) on combusting a South African pulverised fuel in a 200 MWe boiler. University of the Witwatersrand Johannesburg, South Africa.

Van Dyk, J., Benson, S., Laumb, M. & Waanders, B. 2009. Coal and coal ash characteristics to understand mineral transformations and slag formation. *Fuel*, 88(6):1057-1063.

Wagner, J., Malumbazo, N. & Falcon, R.M.S. 2018. Southern African Coals and Carbons: Definitions and Applications of Organic Petrology: Cape Town : Struik Nature.

Wang, H. & Harb, J.N. 1997. Modeling of ash deposition in large-scale combustion facilities burning pulverized coal. *Progress in energy and combustion science*, 23(3):267-282.

Ward, C.R. 2002. Analysis and significance of mineral matter in coal seams. *International Journal of Coal Geology*, 50(1-4):135-168.

Wen, C., Gao, X. & Xu, M. 2016. A CCSEM study on the transformation of included and excluded minerals during coal devolatilization and char combustion. *Fuel*, 172:96-104.

Wen, C., Xu, M., Zhou, K., Yu, D., Zhan, Z. & Mo, X. 2015. The melting potential of various ash components generated from coal combustion: Indicated by the circularity of individual particles using CCSEM technology. *Fuel Processing Technology*, 133:128-136.

Wigley, F., Williamson, J. & Gibb, W.H. 1997. The distribution of mineral matter in pulverised coal particles in relation to burnout behaviour. *Fuel*, 76(13):1283-1288.

Yan, L., Gupta, R. & Wall, T. 2001. The implication of mineral coalescence behaviour on ash formation and ash deposition during pulverised coal combustion. *Fuel*, 80(9):1333-1340.

CHAPTER 6

CONCLUDING SUMMARY

The hypothesis was stated in Chapter 1:

"During the combustion of coal various changes in the mineral matter may be observed at different temperatures. Included minerals within the macerals may interact to form minerals in the molten solution through crystallisation. Excluded minerals may interact to form high-temperature products during solid-solid state reactions as well as crystallisation. Organically associated inorganic elements within the macerals may interact with each other to form artefact minerals and fine ash particles at low temperatures. Submicron minerals infilling cleat fractures in the vitrinite may transform at elevated temperatures to fly ash particles".

6.1 Summary

The focus of this study was to investigate the transformation of mineral matter, i.e. included and excluded minerals, of South African coal under laboratory combustion conditions. Characterisation results of the chemical, mineralogical and petrographical properties, as well as the thermal behaviour of the included minerals in the float fraction and excluded minerals in the sink fraction, are limited for these specific South African coal samples. The main objectives stipulated were to qualitatively and quantitatively evaluate the mineral associations that are responsible for ash-deposition problems such as slagging and fouling during coal utilisation in the thermochemical processes. The mode of occurrence of minerals, mineral associations (included and excluded minerals), as well as the inorganic elements associated with the organic (macerals) matrix, were the main focus of this study (Matjie, 2008).

The incorporation of reflux classification on the coal samples was a novel approach in order to effectively beneficiate South African feed coals to produce mineral-rich and maceral-rich fractions. Reflux classification successfully eliminated any liberated excluded mineral particles still present in the pulverised float fraction after float-sink density separation. It was evident from the chemical, mineralogical and petrography results that the mineral occurrences and associations were significantly different in the three South African coal samples evaluated in this study (Rautenbach *et al.*, 2019b).

The main reason for slagging and fouling formation are reportedly due the interactions between included kaolinite, included fluxing minerals (calcite, dolomite, and pyrite) and the inorganic elements associated with the macerals. By integrating the various analytical techniques used in

this study, the concentrations and mode of occurrence of the submicron included kaolinite, the included fluxing element-bearing minerals and the inorganic elements linked to the macerals were successfully determined.

Incorporating the analyses results of the feed coal, float and sink fractions into existing slag prediction indices, significantly low or no slag formation was predicted for South African coals. This outcome emphasised the limitations of these slag prediction indices and the importance of developing an alternative method to predict slag behaviour for South African coal samples, based on mineral matter transformations.

Low-temperature oxygen plasma ashing was successful in oxidising the organic matter in the feed coal, float and sink fractions in order to isolate the mineral matter for characterisation. The LTA samples were subjected to high-temperature X-ray diffraction, where the transformations and reactions of minerals, at elevated temperatures, were conclusively determined without making any assumptions. The characterisation results of the LTA samples indicate the difference in the proportions of included minerals, excluded minerals and non-mineral inorganic elements in the feed coals as well as in the density separated fractions. Consequently, during high-temperature X-ray diffraction, different mineral reactions and high-temperature mineral phases were observed for the various LTA samples.

Mineral distributions within the LTA of the respective feed, float and sink fractions were determined by QEMSCAN analysis. The quartz and kaolinite particles in coal sample A are predominantly present as included minerals, while the fluxing minerals are associated with excluded minerals and included minerals. The opposite was observed for coal sample B, where the fluxing element-bearing minerals (calcite, dolomite, pyrite, siderite) containing Ca^{2+}, Mg^{2+}, Fe^{2+} are closely associated with the included minerals while the remaining kaolinite and quartz particles are primarily present as excluded minerals. The mineral distributions in the LTA of sample C are totally different in comparison with samples A, and B. Fluxing element-bearing minerals (containing calcite, dolomite, pyrite or siderite) are closely associated with excluded minerals, while the kaolinite particles are mainly present as submicron included kaolinite particles, and the quartz particles are equally present as included and excluded minerals (Rautenbach *et al.*, 2019b).

The mineral-maceral associations within the carbominerites, cleats, stone fragments and included minerals were detected by QEMSCAN analysis in order to relate the associations of minerals with slagging propensity. The results indicate that slagging would occur during the combustion of Feed A, mainly as a result of the mineral associations within the included minerals, carbominerites and stone fragments. No slag formation was predicted as a result of included minerals present

in the float fraction (<1.5 g/cm^3) due to the mineral associations within the cleats. The same principle was observed for Float B (included minerals) where the mineral associations will not cause slag formation. However, the mineral associations in the carbominerites and stone fragments will cause slagging behaviour (in Feed B and Sink B).

Severe slagging propensity was observed for sample C (within the feed, float and sink fractions) where the mineral associations will lead to the formation of slag during combustion. It was also concluded that the non-mineral fluxing inorganic elements or included fluxing minerals associated with included kaolinite in the organic matter (coal macerals) would cause slag behaviour. The excluded fluxing minerals that are associated with excluded kaolinite in the sink fractions or rock fragments would also cause slag formation.

In order to comprehensively incorporate the heterogeneous nature of coal ash and slag prediction methods, the transformation of included and excluded minerals were evaluated in the laboratory under combustion conditions. The results of the combustion experiments are in good agreement with the mineral associations determined by QEMSCAN as well as with the results from the HT-XRD analysis. The presence of anorthite at elevated temperatures were used as an indication of slag formation tendencies.

The findings from QEMSCAN and HT-XRD analyses indicated that due to mineral associations, the included minerals in coal sample A will not lead to slag formation, while the stone fragments associated with excluded minerals (excluded kaolinite associated with excluded calcite, dolomite, pyrite or siderite) in the rock fragments in the sink sample will cause slag behaviour. This was confirmed by the combustion experiments, where anorthite formation was observed, either due to the solid-state reaction or as a result of crystallisation from the molten solution at temperatures up to 1300°C. Anorthite will, however, melt at temperatures above 1300°C to form part of the aluminosilicate glasses (Matjie *et al.*, 2005; Van Alphen, 2005). The anorthite formation occurred as a result of the association of either excluded or included calcite, dolomite, pyrite or siderite particles with either excluded kaolinite particles or included kaolinite particles. The presence of anorthite at elevated temperatures can be used as an indication of slag formation (Rautenbach *et al.*, 2019a).

It was concluded that sample B would exhibit slagging tendencies due to the transformation of included as well as excluded fluxing mineral particles associated with kaolinite particles, which were confirmed by the formation of anorthite in Float B and Sink B during combustion conditions. Lower slagging propensities could, however, be expected as a result of the transformation of included minerals compared to the excluded minerals.

The mineral associations within sample C indicated that during combustion, the transformation minerals would lead to slag formation. During the combustion experiments, the reactions and transformation of excluded minerals formed a molten solution where the anorthite crystallised from with a further increase or decrease in temperature.

The significance of this study is that previous research about the behaviour and transformation of mineral matter during coal utilisation were mainly based on assumptions, where this study successfully quantified the mineral associations in coal. The results of this investigation ultimately indicated the correlation between the occurrences of minerals, the association within included and excluded mineral as well as the relation to slagging behaviour.

6.2 Further research and recommendations

To further extend the knowledge of South African coal samples and their behaviour during coal utilisation comprehensive evaluation and characterisation of the middling fraction (i.e. between 1.5 g/cm^3 and 1.9 g/cm^3) must be conducted.

Integration of additional experimental techniques, such as combustion in the laboratory drop-tube furnace using the operating conditions in the existing commercial power station plants, will enhance the understanding of mineral behaviour at combustion conditions comparable with industry.

Proper blending of the various fractions during the feedstock preparation should be explored in order to minimise slagging in combustion boilers due to a decrease in the mode of occurrence of mineral matter that is responsible for the slag formation.

Chapter References

Matjie, R., Ginster, M., Van Alphen, C. & Sobiecki, A. 2005. Detailed characterisation of Sasol ashes. (*In*. Proceedings organised by.

Matjie, R.H. 2008. Sintering and slagging of mineral matter in South African coals during the coal gasification process. University of Pretoria.

Rautenbach, R., Matjie, R.H., Strydom, C.A., Bunt, J.R., Ward, C.R., French, D. & Van Alphen, C. 2019a. Evaluation of mineral matter transformations in low-temperature ashes of South African coal feedstock samples and their density separated cuts using high-temperature X-ray diffraction. *International Journal of Coal Preparation and Utilization*:1-28.

Rautenbach, R., Strydom, C., Bunt, J., Matjie, R., Campbell, Q. & Van Alphen, C. 2019b. Mineralogical, chemical, and petrographic properties of selected South African power stations' feed coals and their corresponding density separated fractions using float-sink and reflux classification methods. *International Journal of Coal Preparation and Utilization*, 39(8):421-446.

Van Alphen, C. 2005. Factors influencing fly ash formation and slag deposit formation (slagging) on combusting a South African pulverised fuel in a 200 MWe boiler. University of the Witwatersrand Johannesburg, South Africa.

ANNEXURE A

FACTSAGE MODELLING

FACTSAGE™ Thermo-Equilibrium modeling was used as a predictive tool for slag formation as well as the identification of possible mineral phases which can be expected to form at high temperatures during coal combustion. The FACTSAGE™ results are compared to the actual experimental data obtained from the quantitative HT-XRD analyzer in order to examine the transformation and the mode of occurrence of mineral matter and how they relate to slag formation during coal combustion.

A.1 FACTSAGE™ Thermo-Equilibrium modeling

FACTSAGE™ is a software package composed of FACT-win, formerly known as F*A*C*T, and ChemSage, formerly known as SOLGASMIX. FACTSAGE™ 7.1 was used in this study mainly as a prediction tool with regards to slag formation and mineral transformation. Further information on this thermochemical software is available at www.factsage.com. There are various modules within FACTSAGE™, but for this study, the “Equilib” module was used. This “Equilib” module runs on the basis of the Gibbs energy minimization algorithm. The concentrations of specific chemical species are calculated when compounds react in order to reach a chemical equilibrium state (Bale *et al.*, 2016; Van Dyk *et al.*, 2006). The model simulating combustion conditions up to 1400°C at 1 atm pressure was used in this study in order to compare the results with the HT-XRD experiments. The elemental concentrations of the prepared LTA’s were used as the input data while the databases used for the equilibrium calculations included FToxide, FactPS, FTsalt, and Factmisc.

A.2 FACTSAGE™ modeling

FACTSAGE™ 7.1, (a thermodynamic-equilibrium modeling program), was used to predict likely mineral matter transformations as well as slag formation of the LTA samples. The predicted slag formation temperatures are summarized in Table A-1. Slag-liquid formation temperature as predicted by FACTSAGE™ is compared to the temperature where slag occurred during HT-XRD. The formation of anorthite and mullite phases during HT-XRD was used as an indication of slag formation and thus the temperatures correlating with the formation of these minerals were used in Table A-1.

Table A-1 Slag-liquid formation temperature as predicted by FACTSAGE™ modeling compared with HT-XRD results

Sample	FACTSAGE (°C)	HT-XRD (°C)
Feed A	1100	1400
Float A	1300	1300
Sink A	1200	1200
Feed B	1300	1200
Float B	1400	1000
Sink B	1300	1000
Feed C	1400	1200
Float C	1400	1000
Sink C	1200	1000

Slag formation, according to FACTSAGE™ modeling, will occur at higher temperatures for the float fractions (from 1300°C to 1400°C) when compared to the sink fractions (from 1200°C to 1300°C). The formation of mullite and anorthite were observed at higher temperatures in the feed samples during HT-XRD when compared to the float and the sink fractions. It was evident that slag formation occurred at lower temperatures, as determined by HT-XRD, as compared with the FACTSAGE predictions, except for sample A feed. This is due to the FACTSAGE calculations that incorporate only equilibrium phase reactions and thus do not include crystallization of mullite from the melt. As the temperature increased, the quantity of slag increased with a concomitant decrease in mineral content until the only slag was present at 1400°C.

The phases reported and predicted by FACTSAGE™ modeling in Figure A-1 are based on the reactions occurring at an equilibrium state. Figure A-1 indicates the modeling results of minerals in the LTA residues of a) Feed A; b) Float A; c) Sink A; d) Feed B; e) Float B; f) Sink B; g) Feed C; h) Float C; i) Sink C. Fe-bearing minerals, Fe_2O_3 and $Al_2Fe_2O_6$ were predicted for the mineral matter of sample A, feed and sink fractions, but not for samples B and C. The XRF analysis (Table 6) indicated that significantly high proportion of Fe_2O_3 was present in the LTA of Feed A (7.3%), while lower proportions were reported for the LTA of Feed B and Feed C (3.1% and 3.0% respectively). The differences in the proportion of Fe-bearing minerals present, according to FACTSAGE™, were thus expected since the XRF data for the LTA of the feed coals were used as input data for the modeling. According to the FACTSAGE™ simulation the main minerals that were predicted in the LTA of samples A, B and C are quartz, sillimanite (Al_2SiO_5), anorthite and anhydrite. Cordierite ($2MgO{\cdot}2Al_2O_3{\cdot}5SiO_2$) was predicted in the LTA residues of Sink A, Float B

and sample C (feed, float, and sink). The main difference between the samples are the concentrations of the fluxing elements (Ca, Mg and Fe as Ferrous (Fe^{2+})) of fluxing minerals. From the modeling predictions, it can be summarized that the fluxing elements present in the LTA residue of sample A are mainly associated with excluded minerals whereas the fluxing elements in the LTA of sample B are mainly associated with included minerals. However the fluxing elements within sample C reported to both the sink and the float samples, thus could be present in the sample as both included and excluded minerals.

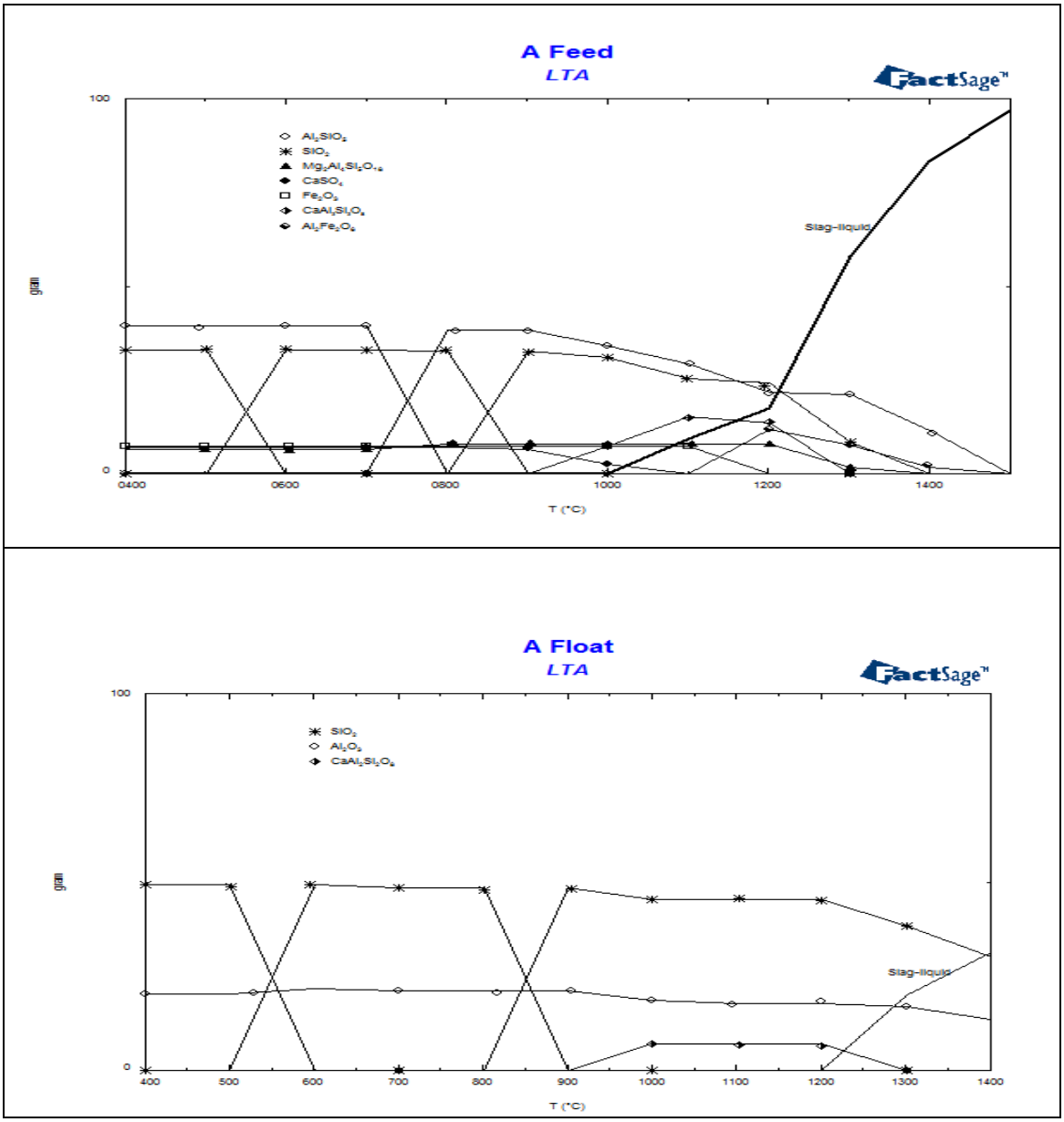
A Feed
LTA
FactSage™
100
0
gfw
Al_2SiO_5
SiO_2
$Mg_2Al_4Si_5O_{18}$
$CaSO_4$
Fe_2O_3
$CaAl_2Si_2O_8$
$Al_2Fe_4O_9$
Slag-liquid
0400
0600
0800
1000
1200
1400
T (°C)
A Float
LTA
FactSage™
100
0
gfw
SiO_2
Al_2O_3
$CaAl_2Si_2O_8$
Slag-liquid
400
500
600
700
800
900
1000
1100
1200
1300
1400
T (°C)

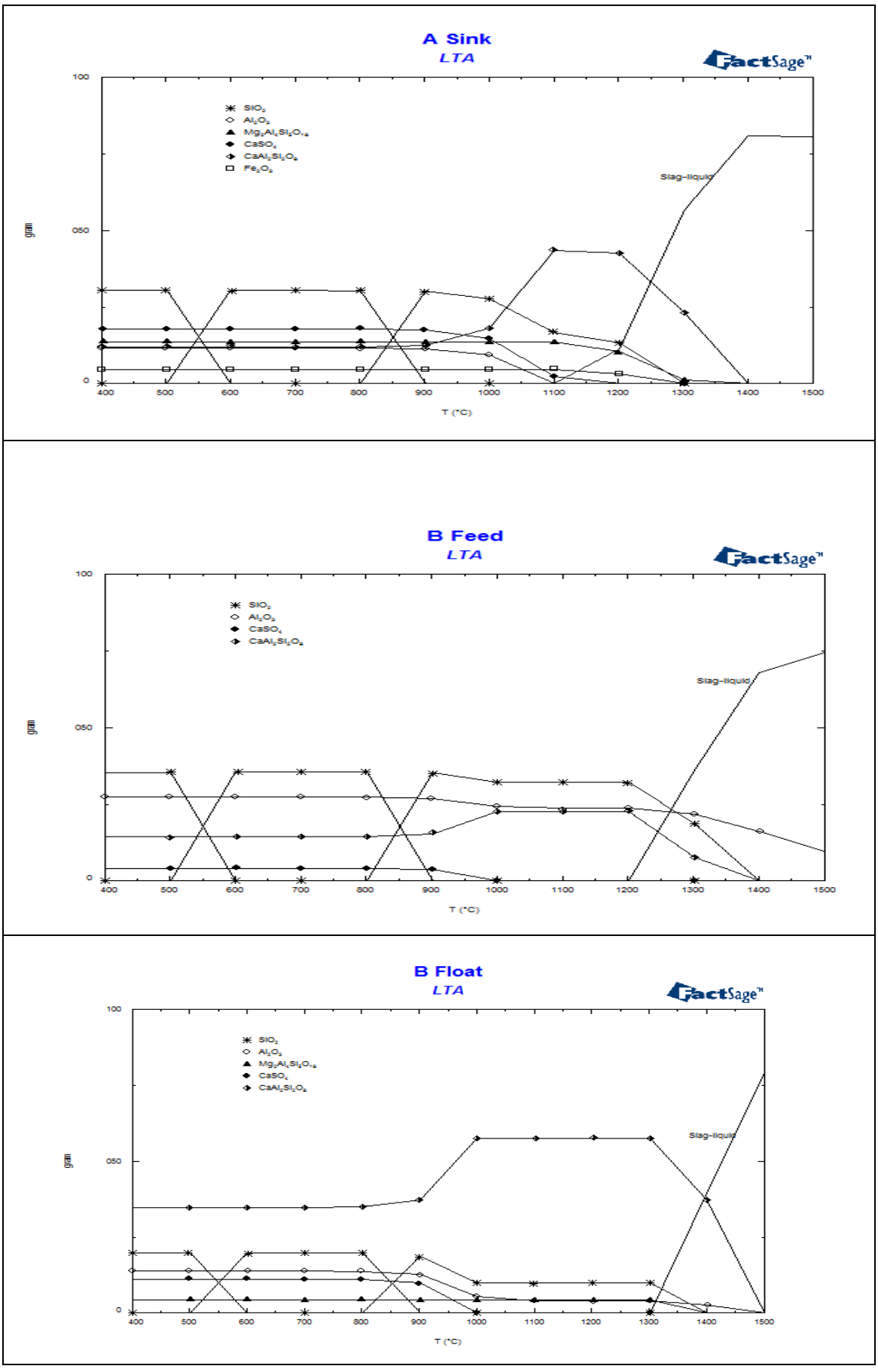
A Sink
LTA
FactSage
100
050
0
gram
SiO2
Al2O3
Mg2Al4Si5O18
CaSO4
CaAl2Si2O8
Fe2O3
Slag-liquid
400
500
600
700
800
900
1000
1100
1200
1300
1400
1500
T (°C)
B Feed
LTA
FactSage
100
050
0
gram
SiO2
Al2O3
CaSO4
CaAl2Si2O8
Slag-liquid
400
500
600
700
800
900
1000
1100
1200
1300
1400
1500
T (°C)
B Float
LTA
FactSage
100
050
0
gram
SiO2
Al2O3
Mg2Al4Si5O18
CaSO4
CaAl2Si2O8
Slag-liquid
400
500
600
700
800
900
1000
1100
1200
1300
1400
1500
T (°C)

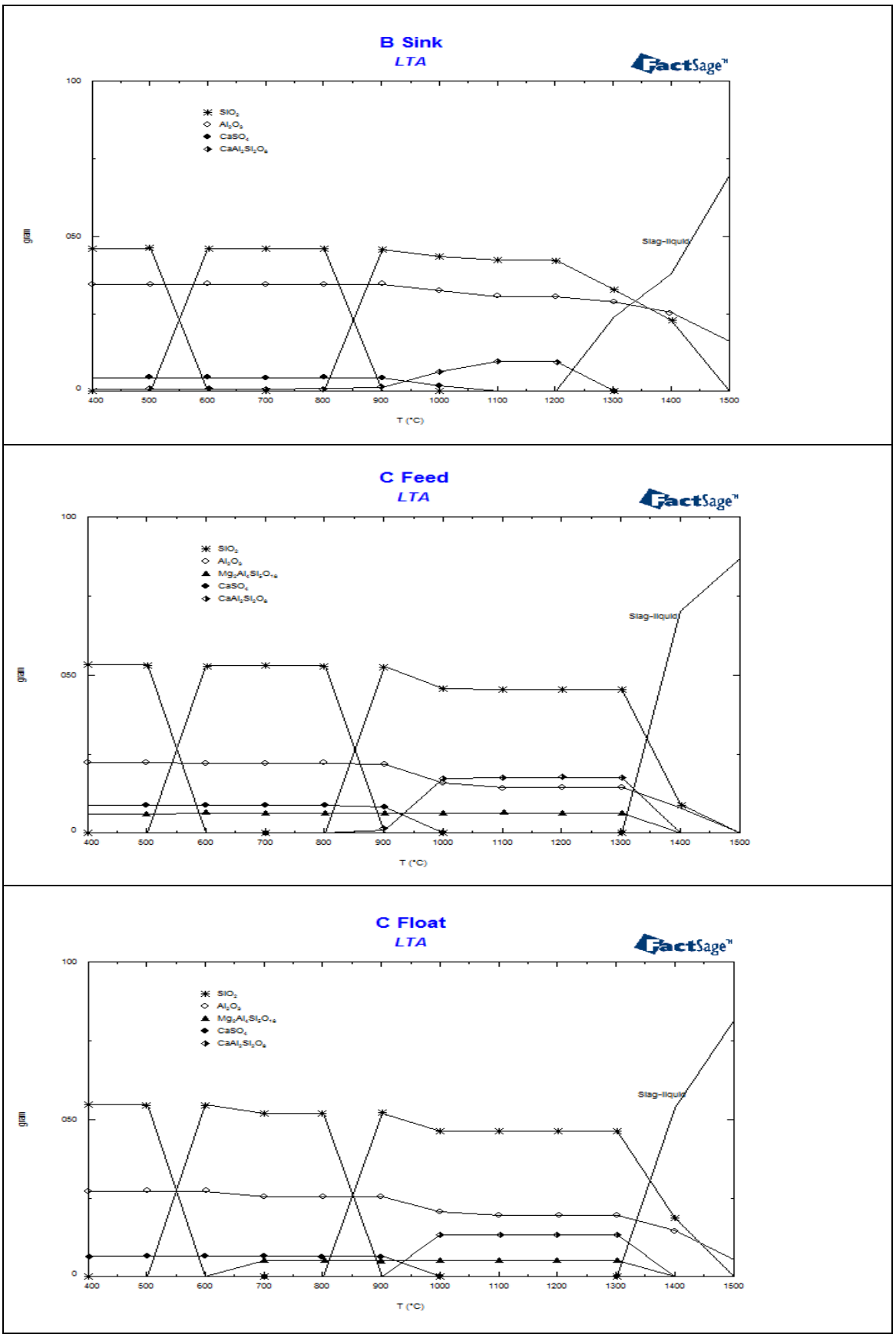
B Sink
LTA
FactSage™
100
050
0
gfan
SiO2
Al2O3
CaSO4
CaAl2Si2O8
Slag-liquid
400
500
600
700
800
900
1000
1100
1200
1300
1400
1500
T (°C)
C Feed
LTA
FactSage™
100
050
0
gfan
SiO2
Al2O3
Mg2Al4Si5O18
CaSO4
CaAl2Si2O8
Slag-liquid
400
500
600
700
800
900
1000
1100
1200
1300
1400
1500
T (°C)
C Float
LTA
FactSage™
100
050
0
gfan
SiO2
Al2O3
Mg2Al4Si5O18
CaSO4
CaAl2Si2O8
Slag-liquid
400
500
600
700
800
900
1000
1100
1200
1300
1400
1500
T (°C)

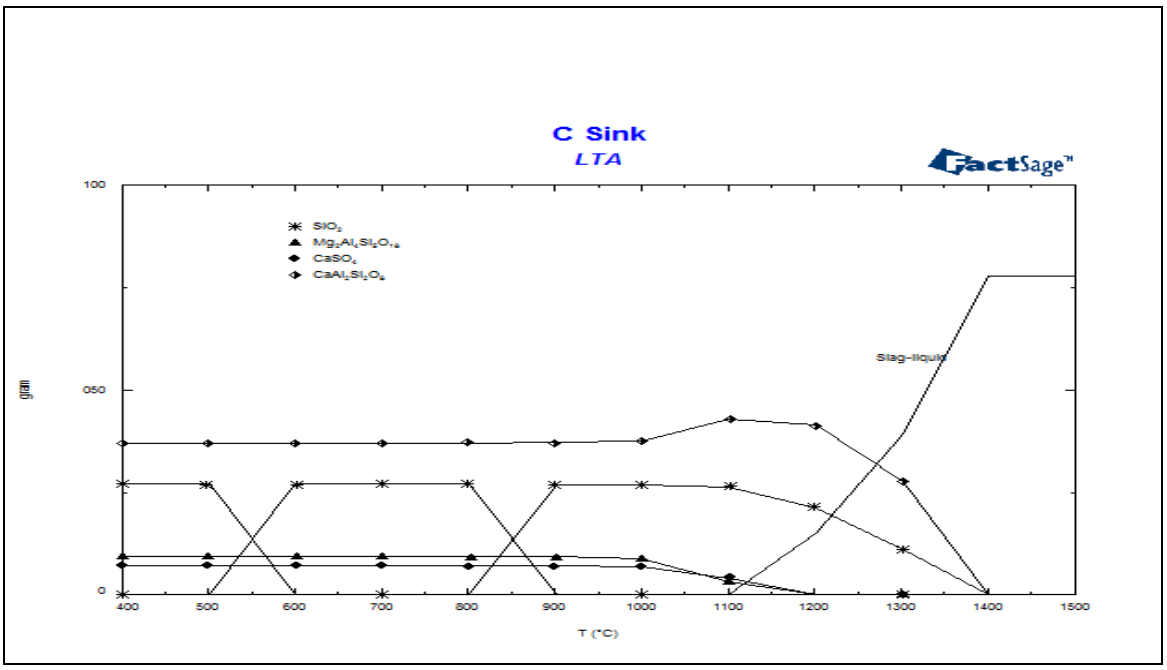

Figure *A-1* **Modeling results of mineral matter in the LTA residues of a) Feed A; b) Float A; c) Sink A; d) Feed B; e) Float B; f) Sink B; g) Feed C; h) Float C; i) Sink C**

A.3 Comparison of FACTSAGE™ and HT-XRD results (minerals formed during a slag/melt formation)

The high-temperature mineral phases predicted in the molten solution by FACTSAGE™ modeling and the slagging minerals formed during HT-XRD are compared in Table A-2. HT-XRD results indicated that mullite and anorthite crystallized from the molten solutions of the LTA samples at elevated temperatures of 1000°C and persisted up to 1400°C. The crystallization of anorthite from the molten solutions of LTA samples was heavily dependent on the proportion of CaO contained in these LTA samples and the associations of calcite and kaolinite. The crystallization of mullite from the melt depends on the proportion of aluminum silicate dissolved in this melt. Whilst the FACTSAGE™ modeling predicted equilibrium phases such as anorthite and cordierite at higher temperatures (1200°C to 1300°C) and not crystallized phases in the LTA samples. The FACTSAGE™ modeling did not predict cordierite and anorthite at 1400°C in other LTA of coals and their density separated fractions excluding Float B which contained anorthite. No mullite formation was predicted by FACTSAGE™ modeling, thus only equilibrium sillimanite phases were predicted. Fe-minerals were also predicted for the LTA residues of Sample A, due to equilibrium reactions. The HT-XRD and FACTSAGE™ results for the LTA residues of coals and their density separated fractions obtained in this study confirmed that the modes of occurrence of minerals in the feed coals and mineral matter associations play significant roles in the formation of the molten solutions during thermo-chemical processes.

Table A-2 Comparison between high-temperature mineral phases as observed from HT-XRD and predicted by FACTSAGE™.

	1200°C		1300°C		1400°C	
	HT-XRD	FACTSAGE™	HT-XRD	FACTSAGE™	HT-XRD	FACTSAGE™
A Feed	Quartz	Quartz Sillimanite Cordierite Anorthite	Quartz	Quartz Sillimanite Cordierite	Mullite	Sillimanite
A Float	Quartz	Quartz Anorthite	Quartz Mullite	Quartz	Quartz Mullite	Quartz
A Sink	Quartz Mullite	Quartz Cordierite Anorthite	Mullite Anorthite	Anorthite	Mullite Anorthite	N.D
B Feed	Quartz Mullite Anorthite	Quartz Anorthite	Quartz Mullite Anorthite	Quartz Anorthite	Mullite Anorthite	N.D
B Float	Mullite Anorthite	Quartz Cordierite Anorthite	Mullite Anorthite	Quartz Cordierite Anorthite	Anorthite	Anorthite
B Sink	Quartz Mullite Anorthite	Quartz Anorthite	Quartz Mullite Anorthite	Quartz	Quartz Mullite	Quartz
C Feed	Quartz Anorthite	Quartz Cordierite Anorthite	Quartz Mullite Anorthite	Quartz Cordierite Anorthite	Mullite Anorthite	Quartz
C Float	Quartz Mullite Anorthite	Quartz Cordierite Anorthite	Quartz Mullite Anorthite	Quartz Cordierite Anorthite	Mullite	Quartz
C Sink	Quartz Anorthite	Quartz Anorthite	Quartz Anorthite	Quartz Anorthite	Quartz Anorthite	N.D
N.D: No phase detected						

A.4 Conclusion

Anorthite formation occurred at high temperatures (1200°C to 1300°C) and according to FACTSAGE™ modeling higher levels of anorthite was predicted in LTA of the float fractions which correlates with the high proportion of Ca in these samples. The FACTSAGE™ model did not predict mullite in the LTA residues of the feed coals and their density separated fractions but predicted sillimanite and cordierite in other LTA samples of the feed coals and density separated fractions. According to the FACTSAGE™ results, the quartz content was stable up to high temperatures as quartz is a thermal inactive mineral. From these results it was evident that FACTSAGE™ modeling does not recognize crystallization of mineral phases at high temperatures and only calculate the reactions at equilibrium.

Chapter References

Bale, C.W., Belisle, E., Chartrand, P., Decterov, S.A., Eriksson, G., Gheribi, A.E., Hack, K., Jung, I.-H., Y.-B., K., Melancon, J., Pelton, A.D., Petersen, S., Robelin, C., Sangster, J., Spencer, P. & Van Ende, M.-A. 2016. FactSage thermochemical software and databases, 2010-2016. *CALPHAD: Computer Coupling of Phase Diagrams and Thermochemistry*, 54:35-53.

Van Dyk, J.C., Melzer, S. & Sobiecki, A. 2006. Mineral matter transformation during Sasol-Lurgi fixed bed dry bottom gasification - utilization of HT-XRD and FactSage modelling. *Minerals Engineering*, 19(10):1126-1135.